TAMPERE UNIVERSITY OF TECHNOLOGY
Department of Electrical Engineering

AAPO AAPRO
MODELING DYNAMICS OF PHOTOVOLTAIC INVERTER WITH LCL-TYPE GRID FILTER

Master of Science Thesis

Examiner: Professor Teuvo Suntio
Examiner and topic approved by the Faculty Council of the Faculty of Computing and Electrical Engineering on 13th August 2014

TIIVISTELMÄ

Aurinkosähkögeneraattori on teholähteenä haastava, koska sen sähköiset ominaisuudet riippuvat sen toimintapisteestä. Generaattori voi käyttäytyä joko tasavirta-tai tasajännitelähteen tavoin. Toimintapisteen vaihtelu vaikuttaa siihen liitetyn systeemin dynamiikkaan, koska generaattorin vaihtuva dynaaminen resistanssi (eli lähtöimpedanssi) aiheuttaa rajoitteita invertterin säätösuunnitteluun. Tämän vuoksi on tärkeää, että lähteen vaikutus sisällytetään johdettavan mallin dynamiikkaan, jotta invertterin käyttäytymistä pystytään ennustamaan tarkasti.

Tässä diplomityössä johdettiin kattava piensignaalimalli kolmivaiheisesta VSI-pohjaisesta aurinkosähköinvertteristä LCL-tyypin verkkosuotimella. Malli ottaa huomioon myös ristikkäisvaikutukset ja parasiittiset elementit kuten tehohäviöt keloissa, kondensaattoreissa ja kytkimissä. Täten mallia voidaan käyttää sellaisen järjestelmän analyysissä, jossa ristikkäisvaikutukset ovat erityisen suuret, esimerkiksi silloin, kun käytetään suuria passiivikomponentteja suuritehoisissa sovelluksissa. Analyyttinen malli johdettiin synkronisessa koordinaatistossa (eli dq-tasossa), jossa invertterin tasapainotila linearisointia varten voitiin ratkaista. Lisäksi epäideaalisen kuorman ja lähteen vaikutukset otettiin huomioon mallia johdettaessa, sillä nämä tekijät vaikuttavat invertterin dynamiikkaan merkittävästi.

Kehitetyn piensignaalimallin on todettu ennustavan tarkasti säädön suunnittelussa tärkeät siirtofunktiot. Lisäksi takaisinkytketyn järjestelmän malli mahdollistaa tulo-ja lähtöimpedanssien tarkan ennustamisen, joka on tärkeää analysoitaessa impedanssi-pohjaista stabiilisuutta verkkoonkytketyssä aurinkosähköinvertterissä.

Mallin oikeellisuus varmennettiin taajuusvastemittauksilla, jotka suoritettiin pienitehoisella prototyypillä. Piensignaalimalli käyttää kaskadisäätöä reguloimaan DC-puolen jännitettä ja verkkovirtoja, sekä vaihelukittua silmukkaa (phase-locked loop, PLL) verkkosynkronointiin. Mitatut siirtofunktiot vastaavat tarkasti ennustuksia.

ABSTRACT

Photovoltaic generator is a unique power source with both constant-current and constant-voltage-like characteristics depending on the operating point. The operating point affects system's dynamic response, because the generator has a varying dynamic resistance, which causes design constraints, e.g., to the control system design. Therefore, it is necessary to include the source-effect to the full-order dynamic model to predict inverter behavior accurately in its application area.

A full-order small-signal model of the three-phase VSI-based photovoltaic inverter with an LCL-type output filter was derived in this thesis, which does not neglect cross-coupling effects or parasitic elements such as ohmic losses in inductors, capacitors and switches. Therefore, the model is also suitable for analysis in cases where strong cross-coupling between the d and q-channels is expected, e.g., when output filter components have large values at high power levels. The model was derived in the synchronous reference frame (i.e., in dq-domain), where the steady-state operating point required for linearization can be solved. Additionally, the effect of non-ideal source and load impedances were included in the model as they have a significant effect on inverter dynamics.

The model is shown to give accurate predictions on the control-related transfer functions, which are essential in deterministic control design. Moreover, the closed-loop model allows the full-order output and input impedances to be accurately predicted which is important when analyzing the impedance-based stability of grid-connected PV inverter.

The small-signal model has been verified by extracting frequency responses from a scaled-down prototype. The model uses a cascaded control scheme to regulate DC-link voltage and output currents as well as phase-locked-loop as the grid synchronization method. Furthermore, more sophisticated control systems, e.g., feedforward, space-vector modulation with DC-link voltage sensing etc. can be included in the model. The measured transfer functions were found out to correlate very closely with the predictions.

PREFACE

This Master's Thesis was done for the Department of Electrical Engineering during year 2014. The topic was suggested by Professor Teuvo Suntio, who was also the examiner of the thesis. The prototype converter was designed and assembled in co-operation with M.Sc. Jukka Viinamäki and M.Sc. Juha Jokipii.

I want to express my gratitude especially to Ph.D. Tuomas Messo for all the help with theory behind the work and guidance through difficult subjects and measurements. Also I want to thank Prof. Teuvo Suntio for interesting topic and guidance during the whole process. Finally I want to thank all the team involved in my thesis work, M.Sc. Juha Jokipii, M.Sc. Jukka Viinamäki, B.Sc. Jyri Kivimäki, B.Sc. Matti Marjanen and B.Sc. Julius Schnabel for inspiring and great working environment.

Tampere 11.11.2014

Aapo Aapro

CONTENTS

TERMS AND SYMBOLS

GREEK ALPHABET

α	Real component in stationary reference frame
β	Imaginary component in stationary reference frame
Δ	Characteristic polynomial
φ	Angle of a space vector
Θ	Steady-state phase angle of the grid voltage
ω_{grid}	Grid fundamental angular frequency
ω_{p}	Controller pole angular frequency
ω_{s}	See ω_{grid}.
ω_{z}	Controller zero angular frequency

LATIN ALPHABET

$\mathbf{A}$	System matrix
$\mathbf{B}$	Input matrix
$\mathbf{C}$	Output matrix
C_{d}	Output-filter capacitance
C_{in}	Input-filter capacitance
C_{pv}	Parasitic capacitance of a PV cell
d	Direct component of a space-vector transformed variable
d	Duty ratio
d'	Complement of the duty ratio
$\mathbf{D}$	Input-output matrix
$d_{\mathrm{i(i=a,b,c)}}$	Duty ratio of upper switch of an inverter phase leg
$\underline{d}$	Space-vector of a duty ratio
$\underline{d}^s$	Space-vector of duty ratio in synchronous reference frame
d_{d}	Direct component of duty ratio
d_{q}	Quadrature component of duty ratio
D_{d}	Steady-state value of duty ratio's direct component
D_{q}	Steady-state value of duty ratio's quadrature component
G_{a}	Gain of the pulse width modulator
$G_{\mathrm{cc(d,q)}}$	D- and q-channel current controller transfer function
G_{cv}	Input voltage controller transfer function
$G_{\mathrm{ci-d}}$	D-channel open-loop (ol.) control-to-input transfer function
$G_{\mathrm{ci-q}}$	Q-channel ol. control-to-input transfer function
$G_{\mathrm{cL-d}}$	D-channel ol. control-to-inductor-current transfer function
$G_{\mathrm{cL-dq}}$	D-channel to q-channel ol. control-to-inductor-current transfer function
$G_{\mathrm{cL-q}}$	Q-channel ol. control-to-inductor-current transfer function
$G_{\mathrm{cL-qd}}$	Q-channel to d-channel ol. control-to-inductor-current transfer function
$G_{\mathrm{crL-dq}}$	D-channel to q-channel cross-coupling transfer function at open loop
$G_{\mathrm{crL-qd}}$	Q-channel to d-channel cross-coupling transfer function at open loop
$\mathbf{G_H}$	Matrix containing transfer functions of a current-to-current converter
$G_{\mathrm{io-d}}$	D-channel ol. input-to-output transfer function

$G_{\mathrm{io-q}}$	Q-channel ol. input-to-output transfer function
i_{C}	Output-filter capacitor current
i_{d}	Diode current
i_{Cin}	Input capacitor current of the converter
i_{in}	Input current of the converter
i_{o}	Output current of the converter
$\underline{i}_{\mathrm{L}}$	Space-vector of three-phase inductor currents
$\underline{i}_{\mathrm{L}}^{s}$	Space-vector of inductor currents in synchronous frame
$\underline{i}_{\mathrm{Li(i=a,b,c)}}$	Inductor current of phase i
i_{L1d}	Inverter-side inductor current d-component
I_{L1d}	Inverter-side inductor current d-component steady-state value
i_{L1q}	Inverter-side inductor current q-component
I_{L1q}	Inverter-side inductor current q-component steady-state value
i_{L2d}	Grid-side inductor current d-component
I_{L2d}	Grid-side inductor current d-component steady-state value
i_{L2q}	Grid-side inductor current q-component
I_{L2q}	Grid-side inductor current q-component steady-state value
i_{inS}	Input current of a non-ideal source
$\mathbf{I}$	Identity matrix
K_{vc}	Input voltage controller gain
K_{cc}	Output current controller gain
L	Inductance
L_{in}	Input voltage control loop
L_{out}	Output current control loop
q	Quadrature component of a space-vector transformed variable
s	Laplace variable
T_{s}	Switching period
T_{oi}	Output-to-input transfer function
$T_{\mathrm{oi-\infty}}$	Ideal output-to-input transfer function
$\mathbf{U}$	Vector containing Laplace transformed input variables
$\mathbf{u}$	Vector containing input variables
u_{oL}	Voltage of non-ideal load
$\mathbf{x}$	Vector containing state variables
$\langle x \rangle$	Average value of variable x
$\hat{x}$	AC-perturbation around a steady-state operation point
$\dot{x}$	Time derivative of variable x
$\underline{\mathbf{x}}$	Space-vector
$\underline{\mathbf{x}}^{*}$	Complex-conjugate of a space-vector
$\mathbf{Y}$	Vector containing Laplace transformed output variables
$\mathbf{y}$	Vector containing output variables
$Y_{\mathrm{o-d}}$	D-component of inverter output admittance
$Y_{\mathrm{o-q}}$	Q-component of inverter output admittance
$Y_{\mathrm{o-sci}}$	Short-circuit output admittance
$Y_{\mathrm{o-\infty}}$	Ideal output admittance
Y_{S}	Output admittance of a non-ideal source

$Z_{\text{in}-\text{oco}}$	Open-circuit input impedance
$Z_{\text{in}-\infty}$	Ideal input impedance
Z_{in}	Input impedance
Z_{G}	Load impedance

ABBREVIATIONS

AC	Alternating current
CC	Constant current
CF	Current-fed
CV	Constant voltage
CO_2	Carbon-dioxide
DC	Direct current
MPP	Maximum power point
MPPT	Maximum power point tracking
OC	Open-circuit
PCC	Point of common coupling
PLL	Phase-locked loop
PVG	Photovoltaic generator
PWM	Pulse-width modulation
RHP	Right-half plane
SC	Short-circuit
VSI	Voltage-sourced inverter

1. INTRODUCTION

The utilization of renewable energy resources will play a significant role in the near future. Globally, approximately 87% of the total energy produced is generated by fossil fuels and majority (i.e., 38%) comes from oil [1]. Only 7% is produced by renewable resources. Since the amount of fossil fuels in the world is decreasing, research in renewable energy resources must increase. Photovoltaic (PV) applications are one of the most studied topics in the field of renewable energy, and also the most promising alternative for fossil fuels.

PV generators are connected to the utility grid using PV inverters. Inverters have to be designed such that they supply as high quality power as possible into the utility grids. Since the number of the inverters and PV systems connected to utility grids is increasing, the stability and reliability of the connected power electronic systems have to be considered in more detail. In order to design reliable and stable PV systems, accurate behavior of the PV generator has to be known thoroughly. PV generators are often considered as a pure voltage sources. However, in reality they act as an operating point dependent current source [2], which will be discussed later in detail.

In order to provide undistorted currents to the utility grid, different type of grid-filters are used. Often a simple L-type filter may not attenuate current harmonics sufficiently without compromising size or performance. Therefore, a three-phase grid-connected PV inverter with LCL-type grid-filter is treated in this thesis. In addition, LCL-filters are also gaining popularity in industry due to their good filtering performance.

This thesis presents a full-order small-signal model for a grid-connected PV inverter with a cascaded control scheme, where the PV generator is modeled as a current source. The purpose of this thesis is to derive a model, which can be further used to analyze the effect of an LCL-filter on dynamic performance of the inverter. Chapter 2 shortly presents the basic operation of a PV generator and features related to its operation. In Chapter 3, a small-signal model of a two-level CF-VSI is derived in synchronous reference frame, which can be used to analyze the dynamic behavior of the aforementioned inverter. Chapter 4 presents measurements from a scaled-down prototype inverter with an LCL-filter in order to verify the derived inverter model. The conclusions are drawn in Chapter 5.

2. PHOTOVOLTAIC GENERATOR

According to [2], a PV generator is a non-linear current source with both constant-current-like and constant-voltage-like properties depending on the operating point. The PV generator is often treated as a voltage source although it is basically a current source. As a consequence, the dynamic behavior of the interfacing converters is usually not properly revealed and leads to different dynamical model of the inverter.

Generally a PV generator can be presented using a one-diode equivalent model as depicted in Fig. 2.1, which contains a photocurrent source i_{ph} as well as the parasitic elements of the PV cell and where i_{pv} and u_{pv} are the output current and the output voltage of the PV generator, respectively.
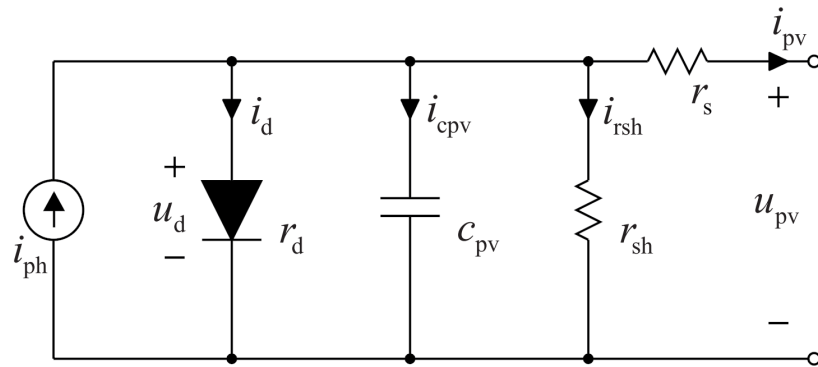
Figure 2.1: Simplified one diode model for PV cell.

The shunt resistance r_{sh} and the series resistance r_{s} represent various non-idealities in a real PV cell. The PV generator also contains parasitic capacitance c_{pv} and the current through the capacitance is denoted as i_{cpv}. Usually the value of the parasitic capasitance is small compared to the input capacitance of the interfacing inverter and, thus, it may be neglected. A commonly used equation for the current-voltage characteristics is presented in (2.1) as

$$i_{\mathrm{pv}} = i_{\mathrm{ph}} - i_{\mathrm{o}} \left[e^{\frac{u_{\mathrm{pv}} + r_{\mathrm{s}} i_{\mathrm{pv}}}{AkT/q}} - 1 \right] + \frac{u_{\mathrm{pv}} + r_{\mathrm{s}} i_{\mathrm{pv}}}{r_{\mathrm{sh}}}, \tag{2.1}$$

where A is diode ideality factor, k Boltzmann constant, q elementary charge and T

the temperature of the PV cell.

It is known that the PV generator has constant-current (CCR) and constant-voltage (CVR) regions as depicted in Fig. 2.2, which also illustrates the behavior of operating-point-dependent dynamic resistance r_{pv} as well as dynamic capacitance c_{pv}. The PV generator resembles a current source at the voltages below the maximum power point (MPP) voltage since the current produced by the PV generator is practically constant and the generator has high output impedance. Moreover, the generator behaves as a voltage source at the voltages above the MPP voltage due to nearly constant voltage and low output impedance. The point where the maximum power is extracted from the PV generator is called MPP. Control system of the interfacing converter regulates its input voltage equal to MPP for maximum power extraction.
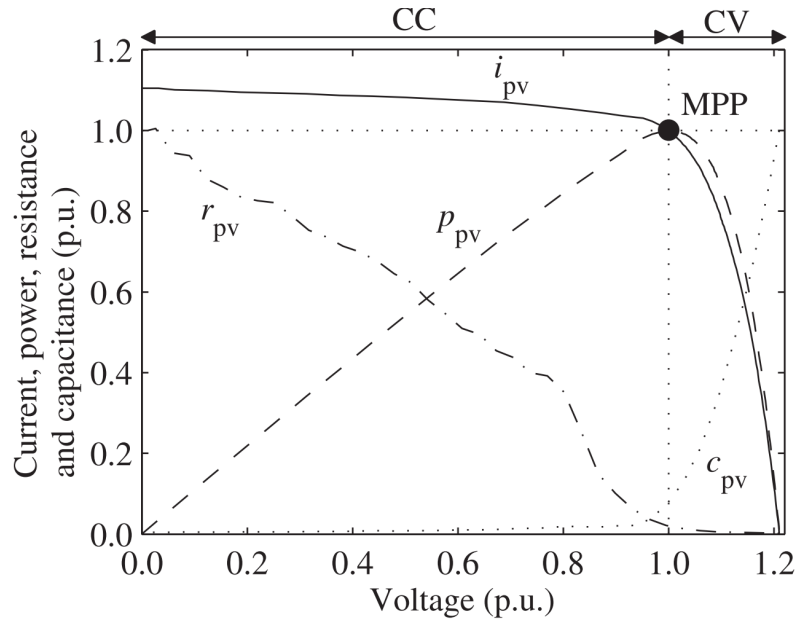
Figure 2.2: Voltage-current curve of a PV generator.

Moreover, non-linear behavior of the dynamic resistance and capacitance is evident. The dynamic resistance is highest in the CCR and the dynamic capacitance is highest in the CVR. Especially, the dynamic resistance affects the system dynamics and, thus causes design constrains, which are discussed later in this thesis.

The dynamic behavior of the PV generator is determined mostly by its dynamic resistance r_{pv} which also represents the low-frequency value of the impedance. The dynamic resistance can be given by

$$r_{pv} = r_d \parallel r_{sh} + r_s, \tag{2.2}$$

where r_d is the dynamic resistance of the diode, thus yielding a non-linear resistance. The dynamic capacitance can be expressed by

$$c_\mathrm{pv} \approx \frac{1}{2\pi r_\mathrm{pv} f_{\text{- 3db}}}, \qquad (2.3)$$

where $f_{\text{- 3db}}$ is the cut-off frequency of the impedance magnitude curve. According to [2], Eq. (2.3) models the c_pv with sufficient accuracy in CCR, whereas in CVR it slightly underestimates c_pv. As is shown in [2], the impedance of the PV generator behaves as an RC-circuit between frequencies of 1 kHz to 100 kHz, hence, the source impedance Z_S can be given according to Fig. 2.2 by

$$Z_\mathrm{S} = r_\mathrm{s} + r_\mathrm{d} \parallel r_\mathrm{sh} \parallel \frac{1}{sc_\mathrm{pv}}. \qquad (2.4)$$

Eq. (2.4) can be simplified by considering $r_\mathrm{s} \approx 0$, thus yielding

$$Z_\mathrm{S} \approx r_\mathrm{d} \parallel r_\mathrm{sh} \parallel \frac{1}{sc_\mathrm{pv}} \approx r_\mathrm{pv} \parallel \frac{1}{sc_\mathrm{pv}}, \qquad (2.5)$$

which at low frequencies can be reduced to

$$Z_\mathrm{S} \approx r_\mathrm{pv}. \qquad (2.6)$$

The output impedance of a PV generator can be approximated as in (2.6) since the input capacitance of the interfacing converter is much greater than c_pv. [2]

3. SMALL-SIGNAL MODELING OF A VSI-BASED PV INVERTER

This chapter presents a small-signal model for a three-phase VSI-based PV inverter with LCL-type grid-filter in Laplace-domain. This modeling technique, first introduced by Middlebrook in the 70's, is accurate up to the half of the switching frequency. Some studies also suggest z-domain modeling as nowadays the use of digital controllers is rapidly increasing [3], however, it is not used in this thesis. There are multiple studies, where the inverter and the filter are insufficiently modeled as the cross-couplings (due to the modeling technique) and the parasitic elements may not be included in the model as e.g. in [4–8]. Also there are publications analyzing only the time-domain behavior such as [4, 5, 9], which may not reveal the special dynamic characteristics found in frequency-domain analysis.

Often a simple L-type filter may not attenuate the switching ripple currents sufficiently. High power applications require higher value for inductance when using L-type filter and the dynamic response of the system may deteriorate. An LCL-filter enables a wide range of power levels with relatively small values for inductances and capacitance to achieve the same filtering performance as with only a L-type filter [10–12]. However, it is worth noting that an LCL-type filter causes also design constraints because of the resonant phenomenon and more complicated dynamic response requirements. High resonant peaking can be attenuated by passive or active damping methods [13, 14]. Passive damping is performed by adding a resistor in series with the output filter capacitor, whereas the active damping is performed with linear or nonlinear control methods to provide sufficient damping for the resonance. [14]

The inverter analyzed, in this thesis, is a two-level three-phase inverter based on the conventional VSI-topology, depicted in Fig. 3.1. The inverter is connected to the grid with an LCL-type grid-filter. According to the topology, the magnitude of the input voltage u_{in} has to be 2-or $\sqrt{3}$ -times greater than the magnitude of the grid phase voltages in order to achieve undistorted grid currents.
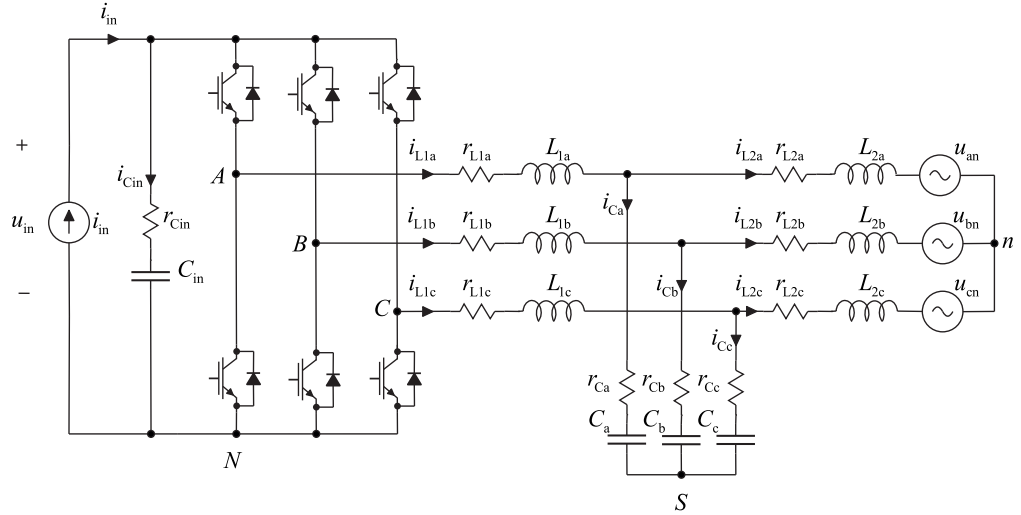
Figure 3.1: Three-phase grid-connected PV inverter with LCL-type grid filter fed from a current source.

As presented in Fig. 3.1, the system inputs are the input current i_{in} and the output phase voltages $u_{\text{(a,b,c)n}}$. According to the control engineering principles, the inputs of a dynamic system cannot be controlled, thus, they act as disturbance elements. Here the system outputs are the input voltage u_{in} and the output phase currents $i_{\text{L2(a,b,c)}}$. Generally, the system outputs are also the controlled variables, however, in this thesis the inverter-side inductor (i.e., the boost-inductor) currents $i_{\text{L1(a,b,c)}}$ are selected also as the controlled outputs. This selection is discussed later in detail.

3.1   Average model

Small-signal modeling begins by deriving equations according to circuit theory for inductor voltages and capacitor currents over one switching cycle. Equations can be obtained from Fig. 3.1, where r_{eq} denotes the sum of the switch on-time resistance r_{sw} and the inductor ESR value r_{L} as well as $r_{\text{C(a,b,c)}}$ which corresponds to the ESR and the damping resistor of the grid capacitor. Equations for aforementioned inverter can be presented by

$$\langle u_{\text{L1a}} \rangle = d_{\text{A}} \langle u_{\text{in}} \rangle - (r_{\text{eq}} + r_{\text{Ca}}) \langle i_{\text{L1a}} \rangle - \langle u_{\text{Ca}} \rangle - r_{\text{Ca}} \langle i_{\text{Ca}} \rangle - \langle u_{\text{SN}} \rangle, \tag{3.1}$$

$$\langle u_{\text{L2a}} \rangle = -(r_{\text{L2a}} + r_{\text{Ca}}) \langle i_{\text{L2a}} \rangle + r_{\text{Ca}} \langle i_{\text{L1a}} \rangle - \langle u_{\text{an}} \rangle + \langle u_{\text{Sn}} \rangle + \langle u_{\text{Ca}} \rangle, \tag{3.2}$$

$$\langle u_{\text{L1b}} \rangle = d_{\text{B}} \langle u_{\text{in}} \rangle - (r_{\text{eq}} + r_{\text{Cb}}) \langle i_{\text{L1b}} \rangle - \langle u_{\text{Cb}} \rangle - r_{\text{Cb}} \langle i_{\text{Cb}} \rangle - \langle u_{\text{SN}} \rangle, \tag{3.3}$$

$$\langle u_{\text{L2b}} \rangle = -(r_{\text{L2b}} + r_{\text{Cb}})\langle i_{\text{L2b}} \rangle + r_{\text{Cb}}\langle i_{\text{L1b}} \rangle - \langle u_{\text{bn}} \rangle + \langle u_{\text{Sn}} \rangle + \langle u_{\text{Cb}} \rangle, \tag{3.4}$$

$$\langle u_{\text{L1c}} \rangle = d_{\text{C}}\langle u_{\text{in}} \rangle - (r_{\text{eq}} + r_{\text{Cc}})\langle i_{\text{L1c}} \rangle - \langle u_{\text{Cc}} \rangle - r_{\text{Cc}}\langle i_{\text{Cc}} \rangle - \langle u_{\text{SN}} \rangle, \tag{3.5}$$

$$\langle u_{\text{L2c}} \rangle = -(r_{\text{L2c}} + r_{\text{Cc}})\langle i_{\text{L2c}} \rangle + r_{\text{Cc}}\langle i_{\text{L1c}} \rangle - \langle u_{\text{cn}} \rangle + \langle u_{\text{Sn}} \rangle + \langle u_{\text{Cc}} \rangle, \tag{3.6}$$

$$\langle i_{\text{Ca}} \rangle = \langle i_{\text{L1a}} \rangle - \langle i_{\text{L2a}} \rangle, \tag{3.7}$$

$$\langle i_{\text{Cb}} \rangle = \langle i_{\text{L1b}} \rangle - \langle i_{\text{L2b}} \rangle, \tag{3.8}$$

$$\langle i_{\text{Cc}} \rangle = \langle i_{\text{L1c}} \rangle - \langle i_{\text{L2c}} \rangle, \tag{3.9}$$

$$\langle u_{\text{in}} \rangle = \langle u_{\text{Cin}} \rangle + r_{\text{c}}\langle i_{\text{Cin}} \rangle, \tag{3.10}$$

$$\langle i_{\text{Cin}} \rangle = \langle i_{\text{in}} \rangle - d_{\text{A}}\langle i_{\text{L1a}} \rangle - d_{\text{B}}\langle i_{\text{L1b}} \rangle - d_{\text{C}}\langle i_{\text{L1c}} \rangle, \tag{3.11}$$

$$\langle i_{\text{oa}} \rangle = \langle i_{\text{L2a}} \rangle, \tag{3.12}$$

$$\langle i_{\text{ob}} \rangle = \langle i_{\text{L2b}} \rangle, \tag{3.13}$$

$$\langle i_{\text{oc}} \rangle = \langle i_{\text{L2c}} \rangle. \tag{3.14}$$

Since the average model is derived for a three-phase system, it can be analyzed by applying the space-vector theory. The analysis can be performed in synchronous reference frame, where the steady-state operating point required for linearization can be solved. Linearization is required for the sake of Laplace-transformation, which is applicaple only for linear systems. According to the space-vector theory, a three-phase variable can be expressed as a complex valued variable $\boldsymbol{x}(t)$ and real valued zero sequence component $x_{\text{z}}(t)$. However, since symmetrical and ideal grid condition is assumed, the zero sequence component is negligible.

Fig. 3.2 depicts a space vector $\overrightarrow{u}_{\text{ref}}$ in synchronous and stationary reference frames.
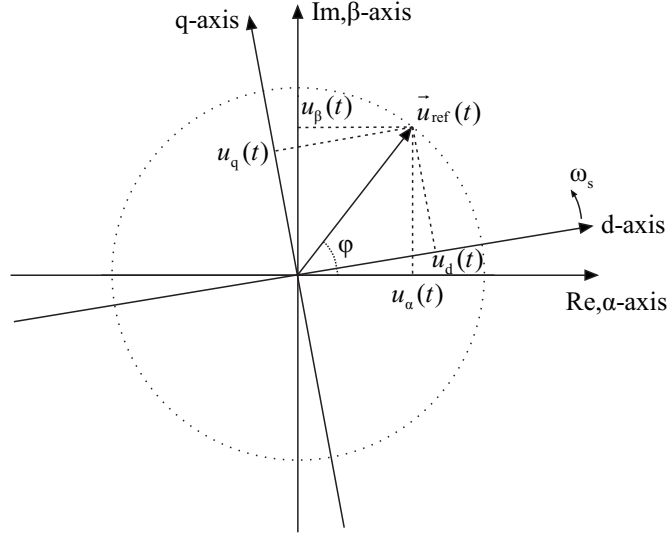
Figure 3.2: Space-vector in both stationary and synchronous reference frames.

In Fig. 3.2, the real and imaginary parts of the space vector $\vec{u}_{\text{ref}}$, i.e., the alpha and beta components can be expressed by

$$\boldsymbol{x}(t) = \frac{2}{3}(x_{\text{a}}(t)e^{j0} + x_{\text{b}}(t)e^{j2\pi/3} + x_{\text{c}}(t)e^{j4\pi/3}) = x_{\alpha}(t) + jx_{\beta}(t), \tag{3.15}$$

$$x_{\text{z}}(t) = \frac{1}{3}(x_{\text{a}}(t) + x_{\text{b}}(t) + x_{\text{c}}(t)). \tag{3.16}$$

The coefficent $2/3$ in (3.15) is a scalar, which scales the magnitude of the space vector equal to the peak value of the phase variables in a symmetrical and ideal grid conditions. In general, the coefficent can be either $2/3$ or $\sqrt{2/3}$ depending on if the amplitude or power-invariant transformation is used, respectively.

According to (3.15), the boost-inductor voltages, i.e., (3.1) - (3.6) can be expressed by

$$\langle \boldsymbol{u}_{\text{L1}} \rangle = -(r_{\text{eq}} + r_{\text{Ca}})\langle \boldsymbol{i}_{\text{L1}} \rangle + \boldsymbol{d}\langle u_{\text{in}} \rangle - \langle \boldsymbol{u}_{\text{Ca}} \rangle + r_{\text{Ca}}\langle \boldsymbol{i}_{\text{L2}} \rangle$$
$$- \frac{2}{3}(e^{j0} + e^{j2\pi/3} + e^{j4\pi/3})\langle \boldsymbol{u}_{\text{SN}} \rangle. \tag{3.17}$$

As the coefficent of the common-mode voltage $\boldsymbol{u}_{\text{SN}}$ becomes zero, (3.17) can be presented by

$$\langle \boldsymbol{u}_{\text{L1}} \rangle = -(r_{\text{eq}} + r_{\text{C}})\langle \boldsymbol{i}_{\text{L1}} \rangle + \boldsymbol{d}\langle u_{\text{in}} \rangle - \langle \boldsymbol{u}_{\text{C}} \rangle + r_{\text{C}}\langle \boldsymbol{i}_{\text{L2}} \rangle. \tag{3.18}$$

Equation for the grid-side inductor voltage can be expressed by

$$\langle \boldsymbol{u}_{\mathrm{L2}} \rangle = -(r_{\mathrm{L2}} + r_{\mathrm{C}})\langle \boldsymbol{i}_{\mathrm{L2}} \rangle + r_{\mathrm{C}}\langle \boldsymbol{i}_{\mathrm{L1}} \rangle + \langle \boldsymbol{u}_{\mathrm{C}} \rangle - \langle \boldsymbol{u}_{\mathrm{o}} \rangle, \qquad (3.19)$$

where $\boldsymbol{i}_{\mathrm{L1}}$, $\boldsymbol{i}_{\mathrm{L2}}$, $\boldsymbol{u}_{\mathrm{C}}$ and $\boldsymbol{u}_{\mathrm{o}}$ are the vectors of space-vector transformed inverter-side inductor currents, output-currents, output filter capacitor voltages and output-voltages, respectively. Moreover, the grid capacitor current can be presented as space-vectors by

$$\langle \boldsymbol{i}_{\mathrm{C}} \rangle = \langle \boldsymbol{i}_{\mathrm{L1}} \rangle - \langle \boldsymbol{i}_{\mathrm{L2}} \rangle. \qquad (3.20)$$

Many publications analyze the inverter in a stationary reference frame in order to decrease the complexity of the analysis and the computational burden as discussed, for example, in [7, 15–19]. However, there are also some inconsistencies since in a stationary reference frame the steady-state operating point cannot be solved nor the linearization performed in a consistent manner. Furthermore, the synchronous reference frame may simplify the analysis and controller design as discussed in [9].

In the rotating or synchronous reference frame, the AC-quantities become constant in the steady state, which makes the use of conventional PI-type controller possible. Analysis in the synchronous reference frame also enables the study of cross-coupling effects, which are not present if stationary reference frame is used. Cross-couplings should be included in the analysis as they may have an effect on the dynamic behavior of the system if, for example, large filtering components in high power applications are used.

Control method is also dependent on the frame selection. It is known that classical PI-type controllers do not provide sufficient performance with sinusoidial references present in a stationary reference frame. Therefore, a proportional-resonant controllers (PR-controllers) are often used to track the sinusoidial references as presented in [16]. Although the performance of a PR-controller in a stationary reference frame matches the PI-controller in a synchronous reference frame, possible effects of high resonant peaks caused by the controller as found, for example, in [20, 21] have to be considered carefully.

In this thesis, the small-signal modeling is performed in the synchronous reference frame as done in [6, 13, 16, 22]. With the space-vector theory a variable can be presented in a synchronous reference frame by $\boldsymbol{x}^{s}(t) = \boldsymbol{x}(t)e^{-j\omega_{\mathrm{s}}t}$, where the superscript 's' denotes the synchronous reference frame and ω_{s} is the angular frequency of the reference frame. The synchronous form for (3.18) - (3.20) can be derived by

$$\langle \boldsymbol{i}_{\mathrm{L1}} \rangle = \langle \boldsymbol{i}_{\mathrm{L1}}^{\mathrm{s}} \rangle e^{j\omega_{\mathrm{s}}t} \rightarrow \frac{d\langle \boldsymbol{i}_{\mathrm{L1}} \rangle}{dt} = \frac{d\langle \boldsymbol{i}_{\mathrm{L1}}^{\mathrm{s}} \rangle}{dt} e^{j\omega_{\mathrm{s}}t} + j\omega_{\mathrm{s}}\langle \boldsymbol{i}_{\mathrm{L1}}^{\mathrm{s}} \rangle e^{j\omega_{\mathrm{s}}t}. \tag{3.21}$$

By substituting (3.21) into (3.18) and rearranging yields

$$\frac{d\langle \boldsymbol{i}_{\mathrm{L1}}^{\mathrm{s}} \rangle}{dt} = \frac{1}{L_1} \Big[\boldsymbol{d}^{\mathrm{s}} \langle u_{\mathrm{in}} \rangle - (r_{\mathrm{eq}} + r_{\mathrm{C}} + j\omega_{\mathrm{s}}L_1)\langle \boldsymbol{i}_{\mathrm{L1}}^{\mathrm{s}} \rangle + r_{\mathrm{C}}\langle \boldsymbol{i}_{\mathrm{L2}}^{\mathrm{s}} \rangle - \langle \boldsymbol{u}_{\mathrm{C}}^{\mathrm{s}} \rangle \Big]. \tag{3.22}$$

Now by performing the same procedures, the time derivative for the grid-side inductor current can be expressed by

$$\frac{d\langle \boldsymbol{i}_{\mathrm{L2}}^{\mathrm{s}} \rangle}{dt} = \frac{1}{L_2} \Big[-(r_{\mathrm{L2}} + r_{\mathrm{C}} + j\omega_{\mathrm{s}}L_2)\langle \boldsymbol{i}_{\mathrm{L2}}^{\mathrm{s}} \rangle + r_{\mathrm{C}}\langle \boldsymbol{i}_{\mathrm{L1}}^{\mathrm{s}} \rangle + \langle \boldsymbol{u}_{\mathrm{C}}^{\mathrm{s}} \rangle - \langle \boldsymbol{u}_{\mathrm{o}}^{\mathrm{s}} \rangle \Big]. \tag{3.23}$$

Moreover, the time derivative of the output capacitor voltage in synchronous reference frame can be given by

$$\frac{d\langle \boldsymbol{u}_{\mathrm{C}}^{\mathrm{s}} \rangle}{dt} = \frac{1}{C} \Big[\langle \boldsymbol{i}_{\mathrm{L1}}^{\mathrm{s}} \rangle - \langle \boldsymbol{i}_{\mathrm{L2}}^{\mathrm{s}} \rangle - j\omega_{\mathrm{s}}C\boldsymbol{u}_{\mathrm{C}}^{\mathrm{s}} \Big]. \tag{3.24}$$

The input capacitor current i_{Cin} can be expressed in dq-domain with inverse Park's transformation as $d_{\mathrm{A}}\langle i_{\mathrm{L1a}} \rangle + d_{\mathrm{B}}\langle i_{\mathrm{L1b}} \rangle + d_{\mathrm{C}}\langle i_{\mathrm{L1c}} \rangle = \frac{3}{2}\mathrm{Re}\{\boldsymbol{d}^{\mathrm{s}}\langle \boldsymbol{i}_{\mathrm{L1}}^{\mathrm{s}} \rangle^*\}$ by

$$\langle i_{\mathrm{Cin}} \rangle = -\frac{3}{2} \Big[d_{\mathrm{d}}\langle i_{\mathrm{L1d}} \rangle + d_{\mathrm{q}}\langle i_{\mathrm{L1q}} \rangle \Big] + \langle i_{\mathrm{in}} \rangle. \tag{3.25}$$

Now the time derivative for the input capacitor voltage can be expressed by

$$\frac{d\langle u_{\mathrm{Cin}} \rangle}{dt} = \frac{1}{C_{\mathrm{in}}} \Big[-\frac{3}{2}(d_{\mathrm{d}}\langle i_{\mathrm{L1d}} \rangle + d_{\mathrm{q}}\langle i_{\mathrm{L1q}} \rangle) + \langle i_{\mathrm{in}} \rangle \Big]. \tag{3.26}$$

Furthermore, the input voltage and the ouput current can be expressed by

$$\langle u_{\mathrm{in}} \rangle = -\frac{3}{2}r_{\mathrm{Cin}}d_{\mathrm{d}}\langle i_{\mathrm{L1d}} \rangle - \frac{3}{2}r_{\mathrm{Cin}}d_{\mathrm{q}}\langle i_{\mathrm{L1q}} \rangle + \langle u_{\mathrm{Cin}} \rangle + r_{\mathrm{Cin}}\langle i_{\mathrm{in}} \rangle, \tag{3.27}$$

$$\langle \boldsymbol{i}_{\mathrm{o}}^{\mathrm{s}} \rangle = \langle \boldsymbol{i}_{\mathrm{L2}}^{\mathrm{s}} \rangle. \tag{3.28}$$

Finally, (3.22) - (3.28) in the synchronous reference are divided into direct and quadrature components as $\boldsymbol{x}^{\mathrm{s}}(t) = x_{\mathrm{d}}(t) + jx_{\mathrm{q}}(t)$. By substituting (3.27) into (3.22)

and dividing equations into d- and q-components yields

$$
\frac{d\langle i_{\mathrm{L1d}}\rangle}{dt} = \frac{1}{L_1}\Bigg[-\Big(r_{\mathrm{eq}} + r_{\mathrm{C}} + \frac{3}{2}r_{\mathrm{Cin}}d_{\mathrm{d}}^2\Big)\langle i_{\mathrm{L1d}}\rangle + \Big(\omega_{\mathrm{s}}L_1 + \frac{3}{2}r_{\mathrm{Cin}}d_{\mathrm{d}}d_{\mathrm{q}}\Big)\langle i_{\mathrm{L1q}}\rangle
$$
$$
+ r_{\mathrm{C}}\langle i_{\mathrm{L2d}}\rangle - \langle u_{\mathrm{Cd}}\rangle + d_{\mathrm{d}}\langle u_{\mathrm{Cin}}\rangle + r_{\mathrm{Cin}}d_{\mathrm{d}}\langle i_{\mathrm{in}}\rangle \Bigg], \quad (3.29)
$$

$$
\frac{d\langle i_{\mathrm{L1q}}\rangle}{dt} = \frac{1}{L_1}\Bigg[-\Big(r_{\mathrm{eq}} + r_{\mathrm{C}} + \frac{3}{2}r_{\mathrm{Cin}}d_{\mathrm{q}}^2\Big)\langle i_{\mathrm{L1q}}\rangle - \Big(\omega_{\mathrm{s}}L_1 + \frac{3}{2}r_{\mathrm{Cin}}d_{\mathrm{d}}d_{\mathrm{q}}\Big)\langle i_{\mathrm{L1d}}\rangle
$$
$$
+ r_{\mathrm{C}}\langle i_{\mathrm{L2q}}\rangle - \langle u_{\mathrm{Cq}}\rangle + d_{\mathrm{q}}\langle u_{\mathrm{Cin}}\rangle + r_{\mathrm{Cin}}d_{\mathrm{q}}\langle i_{\mathrm{in}}\rangle \Bigg], \quad (3.30)
$$

$$
\frac{d\langle i_{\mathrm{L2d}}\rangle}{dt} = \frac{1}{L_2}\Big[-(r_{\mathrm{L2}} + r_{\mathrm{C}})\langle i_{\mathrm{L2d}}\rangle + \omega_{\mathrm{s}}L_2\langle i_{\mathrm{L2q}}\rangle + r_{\mathrm{C}}\langle i_{\mathrm{L1d}}\rangle + \langle u_{\mathrm{Cd}}\rangle - \langle u_{\mathrm{od}}\rangle \Big], \quad (3.31)
$$

$$
\frac{d\langle i_{\mathrm{L2q}}\rangle}{dt} = \frac{1}{L_2}\Big[-(r_{\mathrm{L2}} + r_{\mathrm{C}})\langle i_{\mathrm{L2q}}\rangle - \omega_{\mathrm{s}}L_2\langle i_{\mathrm{L2d}}\rangle + r_{\mathrm{C}}\langle i_{\mathrm{L1q}}\rangle + \langle u_{\mathrm{Cq}}\rangle - \langle u_{\mathrm{oq}}\rangle \Big], \quad (3.32)
$$

$$
\frac{d\langle u_{\mathrm{Cin}}\rangle}{dt} = \frac{1}{C_{\mathrm{in}}}\Big[-\frac{3}{2}\Big(d_{\mathrm{d}}\langle i_{\mathrm{L1d}}\rangle + d_{\mathrm{q}}\langle i_{\mathrm{L1q}}\rangle\Big) + \langle i_{\mathrm{in}}\rangle \Big], \quad (3.33)
$$

$$
\frac{d\langle u_{\mathrm{Cd}}\rangle}{dt} = \frac{1}{C}\Big[\langle i_{\mathrm{L1d}}\rangle - \langle i_{\mathrm{L2d}}\rangle \Big) + \omega_{\mathrm{s}}C\langle u_{\mathrm{Cq}}\rangle \Big], \quad (3.34)
$$

$$
\frac{d\langle u_{\mathrm{Cq}}\rangle}{dt} = \frac{1}{C}\Big[\langle i_{\mathrm{L1q}}\rangle - \langle i_{\mathrm{L2q}}\rangle \Big) - \omega_{\mathrm{s}}C\langle u_{\mathrm{Cd}}\rangle \Big], \quad (3.35)
$$

$$
\langle u_{\mathrm{in}}\rangle = -\frac{3}{2}r_{\mathrm{Cin}}d_{\mathrm{d}}\langle i_{\mathrm{L1d}}\rangle - \frac{3}{2}r_{\mathrm{Cin}}d_{\mathrm{q}}\langle i_{\mathrm{L1q}}\rangle + \langle u_{\mathrm{Cin}}\rangle + r_{\mathrm{Cin}}\langle i_{\mathrm{in}}\rangle, \quad (3.36)
$$

$$
\langle i_{\mathrm{od}}\rangle = \langle i_{\mathrm{L2d}}\rangle, \quad (3.37)
$$

$$
\langle i_{\mathrm{oq}}\rangle = \langle i_{\mathrm{L2q}}\rangle. \quad (3.38)
$$

Eqs. (3.29) - (3.38) represent the synchronous-reference-frame average-valued model for a current-fed VSI.

3.2   Steady-state operating point

The steady-state operating point of the system can be solved from the average-valued model by setting the derivatives to zero and replacing the average-valued terms by their corresponding upper case steady-state values. It should be noted that the equations are simplified and rearranged as the derivation of the steady-

state operating point is otherwise relatively complex. In this thesis, the inverter-side inductor currents are controlled, thus, the dynamical model is derived with current feedback from the inverter-side inductors (i.e., the boost inductors). These currents are synchronized with the phase-voltages, which are measured from the grid-side. This feedback arrangement is often selected for safety reasons as otherwise there is no control in the inverter-side currents.

Here it is assumed that $I_{L1q} = 0$ and $U_{oq} = 0$, thus, the boost inductor currents are synchronized to the grid voltages and a small amount of reactive power is transferred to the grid (i.e., $I_{L2q} \neq 0$). It should be noted that if the inverter is desired to produce reactive power to the grid, aforementioned q-channel inverter-side inductor current I_{L1q} is not zero. This leads to more complicated steady-state calculation which, however, is not presented in this thesis.

The steady-state can now be derived as

$$0 = -(R_{eq} + \frac{3}{2}D_d^2 r_{Cin})I_{L1d} + r_C I_{L2d} - U_{Cd} + D_d U_{in} + r_{Cin} D_d I_{in}, \tag{3.39}$$

$$0 = -(k_3 + \frac{3}{2}D_d D_q r_{Cin})I_{L1d} + r_C I_{L2q} - U_{Cq} + D_q U_{in} + r_{Cin} D_q I_{in}, \tag{3.40}$$

$$U_{in} = U_{Cin}, \tag{3.41}$$

$$0 = -\frac{3}{2}D_d I_{L1d} + I_{in}, \tag{3.42}$$

$$0 = -k_1 I_{L2q} - U_{Cd}, \tag{3.43}$$

$$0 = k_1 I_{L2d} - k_1 I_{L1d} - U_{Cq}, \tag{3.44}$$

$$0 = k_2 U_{Cq} - k_2 R I_{L2q} - I_{L2d}, \tag{3.45}$$

$$0 = R k_2 I_{L2d} - k_2 r_C I_{L1d} - k_2 U_{Cd} + k_2 U_{od} - I_{L2q}, \tag{3.46}$$

where $k_1 = \frac{1}{\omega_s C}$, $k_2 = \frac{1}{\omega_s L_2}$, $k_3 = \omega_s L_1$, $R_{eq} = r_{eq} + r_C$ and $R = r_{L2} + r_C$. Now by substituting (3.43) and (3.44) into (3.45) and (3.46) and solving for I_{L1d}, I_{L2d}, I_{L2q},

U_{Cd} and U_{Cd} yields

$$I_{\mathrm{L1d}} = \frac{2I_{\mathrm{in}}}{3D_{\mathrm{d}}},$$ (3.47)

$$I_{\mathrm{L2d}} = \frac{2I_{\mathrm{in}}K_{\mathrm{ILd}} - 3D_{\mathrm{d}}RU_{\mathrm{od}}}{3D_{\mathrm{d}}K},$$ (3.48)

$$I_{\mathrm{L2q}} = -\frac{2I_{\mathrm{in}}K_{\mathrm{ILq}} + 3D_{\mathrm{d}}RU_{\mathrm{od}}K_{\mathrm{Uo}}}{3D_{\mathrm{d}}K},$$ (3.49)

$$U_{\mathrm{Cd}} = \frac{2I_{\mathrm{in}}k_1 K_{\mathrm{Ucd}} + 3D_{\mathrm{d}}U_{\mathrm{od}}k_1 K_{\mathrm{Uo}}}{3D_{\mathrm{d}}K},$$ (3.50)

$$U_{\mathrm{Cq}} = -\frac{k_1\left(2I_{\mathrm{in}}K_{\mathrm{Ucq}} + 3D_{\mathrm{d}}RU_{\mathrm{od}}\right)}{3D_{\mathrm{d}}K},$$ (3.51)

where $K_{\mathrm{ILd}} = k_1^2 - k_1 k_2 + R r_{\mathrm{C}}$, $K_{\mathrm{ILq}} = k_2 r_{\mathrm{C}} + k_1 R - k_1 r_{\mathrm{C}}$, $K_{\mathrm{Ucd}} = R k_1 - k_1 r_{\mathrm{C}} + k_2 r_{\mathrm{C}}$, $K_{\mathrm{Ucq}} = R^2 + k_2^2 - R r_{\mathrm{C}} - k_1 k_2$, $K_{\mathrm{Uo}} = k_1 - k_2$ and $K = R^2 + (k_1 - k_2)^2$. Now the steady-state values for D_{d} and D_{q} can be calculated by substituting (3.47) - (3.51) into (3.39) and (3.40). However, the final symbolic values for D_{d} and D_{q} are too complex to be presented with all the parasitic elements. Appendix A provides a complete MATLAB-code for calculating the steady state values. Simplified values for D_{d} and D_{q} without any parasitic elements can be presented by

$$D_{\mathrm{d}} = \frac{U_{\mathrm{od}}\frac{1}{\omega_{\mathrm{s}}^2 C L_2}}{U_{\mathrm{in}}\left(\frac{1}{\omega_{\mathrm{s}}^2 C L_2} - 1\right)},$$ (3.52)

$$D_{\mathrm{q}} = \frac{2I_{\mathrm{in}}\left(\frac{1}{\omega_{\mathrm{s}}C} - \omega_{\mathrm{s}}L_1 + \frac{L_1}{\omega_{\mathrm{s}}C L_2}\right)}{3U_{\mathrm{od}}\frac{1}{\omega_{\mathrm{s}}^2 C L_2}}.$$ (3.53)

The linearization process is described in detail in the next section.

3.3 Linearized model

The average-valued model is non-linear due to multiplication of duty ratios with other variables. Therefore, it has to be linearized at the operating point derived in the previous section. Linearization is performed by developing partial derivatives for all state, input and output variables, i.e., first-order approximation of the Taylor-series. Obtained linearized equations can be given by

$$
\frac{d\hat{i}_{L1d}}{dt} = \frac{1}{L_1}\Big[-(r_{eq} + r_C + \frac{3}{2}r_{Cin}D_d^2)\hat{i}_{L1d} + (\omega_s L_1 + \frac{3}{2}r_{Cin}D_d D_q)\hat{i}_{L1q}
$$
$$
+ r_C\hat{i}_{L2d} - \hat{u}_{Cd} + D_d\hat{u}_{Cin} + r_{Cin}D_d\hat{i}_{in} - (r_{Cin}I_{in} + U_{in})\hat{d}_d \Big], \quad (3.54)
$$

$$
\frac{d\hat{i}_{L1q}}{dt} = \frac{1}{L_1}\Big[-(r_{eq} + r_C + \frac{3}{2}r_{Cin}D_q^2)\hat{i}_{L1q} - (\omega_s L_1 + \frac{3}{2}r_{Cin}D_d D_q)\hat{i}_{L1d}
$$
$$
+ r_C\hat{i}_{L2q} - \hat{u}_{Cq} + D_q\hat{u}_{Cin} + r_{Cin}D_q\hat{i}_{in} + (-\frac{2D_q r_{Cin}I_{in}}{D_d})\hat{d}_d + U_{in}\hat{d}_q \Big], \quad (3.55)
$$

$$
\frac{d\hat{i}_{L2d}}{dt} = \frac{1}{L_2}\Big[-(r_{L2} + r_C)\hat{i}_{L2d} + \omega_s L_2\hat{i}_{L2q} + r_C\hat{i}_{L1d} + \hat{u}_{Cd} - \hat{u}_{od} \Big], \quad (3.56)
$$

$$
\frac{d\hat{i}_{L2q}}{dt} = \frac{1}{L_2}\Big[-(r_{L2} + r_C)\hat{i}_{L2q} - \omega_s L_2\hat{i}_{L2d} + r_C\hat{i}_{L1q} + \hat{u}_{Cq} - \hat{u}_{oq} \Big], \quad (3.57)
$$

$$
\frac{d\hat{u}_{Cin}}{dt} = \frac{1}{C_{in}}\Big[-\frac{3}{2}D_d\hat{i}_{L1d} - \frac{3}{2}D_q\hat{i}_{L1q} + \hat{i}_{in} - \frac{I_{in}}{D_d}\hat{d}_d \Big], \quad (3.58)
$$

$$
\frac{d\hat{u}_{Cd}}{dt} = \frac{1}{C}\Big[\hat{i}_{L1d} - \hat{i}_{L2d} + \omega_s C\hat{u}_{Cq} \Big], \quad (3.59)
$$

$$
\frac{d\hat{u}_{Cq}}{dt} = \frac{1}{C}\Big[\hat{i}_{L1q} - \hat{i}_{L2q} - \omega_s C\hat{u}_{Cd} \Big], \quad (3.60)
$$

$$
\hat{u}_{in} = -\frac{3}{2}D_d r_{cin}\hat{i}_{L1d} - \frac{3}{2}D_q r_{Cin}\hat{i}_{L1q} + \hat{u}_{Cin} + r_{Cin}\hat{i}_{in} - \frac{I_{in}r_{Cin}}{D_d}\hat{d}_d, \quad (3.61)
$$

$$
\hat{i}_{od} = \hat{i}_{L2d}, \quad (3.62)
$$

$$
\hat{i}_{oq} = \hat{i}_{L2q}. \quad (3.63)
$$

Now (3.54) - (3.63) can be expressed as a linearized state-space by

$$
\frac{\mathrm{d}\hat{\boldsymbol{x}}(t)}{\mathrm{d}t} = \mathbf{A}\hat{\boldsymbol{x}}(t) + \mathbf{B}\hat{\boldsymbol{u}}(t)
$$
$$
\hat{\boldsymbol{y}}(t) = \mathbf{C}\hat{\boldsymbol{x}}(t) + \mathbf{D}\hat{\boldsymbol{u}}(t)
$$

(3.64)

where $\hat{\boldsymbol{x}} = [\hat{i}_{\mathrm{L1d}}, \hat{i}_{\mathrm{L1q}}, \hat{i}_{\mathrm{L2d}}, \hat{i}_{\mathrm{L2q}}, \hat{u}_{\mathrm{Cd}}, \hat{u}_{\mathrm{Cq}}, \hat{u}_{\mathrm{Cin}}]$, $\hat{\boldsymbol{u}} = [\hat{i}_{\mathrm{in}}, \hat{u}_{\mathrm{od}}, \hat{u}_{\mathrm{oq}}, \hat{d}_{\mathrm{d}}, \hat{d}_{\mathrm{q}}]$ and $\hat{\boldsymbol{y}} = [\hat{i}_{\mathrm{L1d}}, \hat{i}_{\mathrm{L1q}}, \hat{u}_{\mathrm{in}}, \hat{i}_{\mathrm{od}}, \hat{i}_{\mathrm{oq}}]$ are the state, input and output variables, respectively. It is worth noting that the state variables $\hat{i}_{\mathrm{L1d}}$ and $\hat{i}_{\mathrm{L1q}}$ are also considered as output variables since they are the controlled variables at the inverter output. The state matrices in (3.64) can be given according to (3.54) - (3.63) by

$$
\mathbf{A} = \begin{bmatrix}
\frac{-(r_{\mathrm{eq}}+r_{\mathrm{C}}+\frac{3}{2}r_{\mathrm{Cin}}D_{\mathrm{d}}^2)}{L_1} & \frac{-(-\omega_{\mathrm{s}}L_1+\frac{3}{2}r_{\mathrm{Cin}}D_{\mathrm{d}}D_{\mathrm{q}})}{L_1} & \frac{r_{\mathrm{C}}}{L_1} & 0 & -\frac{1}{L_1} & 0 & \frac{D_{\mathrm{d}}}{L_1} \\
\frac{-(r_{\mathrm{eq}}+r_{\mathrm{C}}+\frac{3}{2}r_{\mathrm{Cin}}D_{\mathrm{d}}D_{\mathrm{q}})}{L_1} & \frac{-(\omega_{\mathrm{s}}L_1+\frac{3}{2}r_{\mathrm{Cin}}D_{\mathrm{q}}^2)}{L_1} & 0 & \frac{r_{\mathrm{C}}}{L_1} & 0 & -\frac{1}{L_1} & \frac{D_{\mathrm{q}}}{L_1} \\
\frac{r_{\mathrm{C}}}{L_2} & 0 & \frac{-(r_{\mathrm{L2}}+r_{\mathrm{C}})}{L_2} & \omega_{\mathrm{s}} & \frac{1}{L_2} & 0 & 0 \\
0 & \frac{r_{\mathrm{C}}}{L_2} & -\omega_{\mathrm{s}} & \frac{-(r_{\mathrm{L2}}+r_{\mathrm{C}})}{L_2} & 0 & \frac{1}{L_2} & 0 \\
\frac{1}{C} & 0 & -\frac{1}{C} & 0 & 0 & \omega_{\mathrm{s}} & 0 \\
0 & \frac{1}{C} & 0 & -\frac{1}{C} & -\omega_{\mathrm{s}} & 0 & 0 \\
-\frac{3}{2}\frac{D_{\mathrm{d}}}{C_{\mathrm{in}}} & -\frac{3}{2}\frac{D_{\mathrm{q}}}{C_{\mathrm{in}}} & 0 & 0 & 0 & 0 & 0
\end{bmatrix},
$$

(3.65)

$$
\mathbf{B} = \begin{bmatrix}
\frac{r_{\mathrm{Cin}}D_{\mathrm{d}}}{L_1} & 0 & 0 & -\frac{r_{\mathrm{Cin}}I_{\mathrm{in}}+U_{\mathrm{in}}}{L_1} & 0 \\
\frac{r_{\mathrm{Cin}}D_{\mathrm{q}}}{L_1} & 0 & 0 & -\frac{r_{\mathrm{Cin}}D_{\mathrm{q}}I_{\mathrm{in}}}{D_{\mathrm{d}}L_1} & \frac{U_{\mathrm{in}}}{L_1} \\
0 & -\frac{1}{L_2} & 0 & 0 & 0 \\
0 & 0 & -\frac{1}{L_2} & 0 & 0 \\
0 & 0 & 0 & 0 & 0 \\
0 & 0 & 0 & 0 & 0 \\
\frac{1}{C_{\mathrm{in}}} & 0 & 0 & -\frac{I_{\mathrm{in}}}{D_{\mathrm{d}}C_{\mathrm{in}}} & 0
\end{bmatrix},
$$

(3.66)

$$
\mathbf{C} = \begin{bmatrix}
1 & 0 & 0 & 0 & 0 & 0 & 0 \\
0 & 1 & 0 & 0 & 0 & 0 & 0 \\
-\frac{3}{2}D_{\mathrm{d}}r_{\mathrm{Cin}} & -\frac{3}{2}D_{\mathrm{q}}r_{\mathrm{Cin}} & 0 & 0 & 0 & 0 & 1 \\
0 & 0 & 1 & 0 & 0 & 0 & 0 \\
0 & 0 & 0 & 1 & 0 & 0 & 0
\end{bmatrix},
$$

(3.67)

$$\mathbf{D} = \begin{bmatrix} 0 & 0 & 0 & 0 & 0 \\ 0 & 0 & 0 & 0 & 0 \\ r_{\text{Cin}} & 0 & 0 & -\frac{r_{\text{Cin}}I_{\text{in}}}{D_{\text{d}}} & 0 \\ 0 & 0 & 0 & 0 & 0 \\ 0 & 0 & 0 & 0 & 0 \end{bmatrix}. \tag{3.68}$$

Furthermore, (3.64) can be Laplace-transformed since it is linearized and presented by

$$\begin{aligned} s\boldsymbol{X}(s) &= \mathbf{A}\boldsymbol{X}(s) + \mathbf{B}\boldsymbol{U}(s) \\ \boldsymbol{Y}(s) &= \mathbf{C}\boldsymbol{X}(s) + \mathbf{D}\boldsymbol{U}(s) \end{aligned}. \tag{3.69}$$

Now the transfer functions between input and output variables can be solved as given by the matrix $\mathbf{G}_{\text{H}}$ in (3.70)

$$\boldsymbol{Y}(s) = \left[\mathbf{C}(s\mathbf{I} - \mathbf{A})^{-1}\mathbf{B} + \mathbf{D}\right]\boldsymbol{U}(s) = \mathbf{G}_{\text{H}}\boldsymbol{U}(s). \tag{3.70}$$

Here the transfer function matrix $\mathbf{G}_{\text{H}}$ is commonly known as the H-parameter representation, i.e., the inverter is analyzed as current-input-current-output system. Transfer functions of the system can be presented in matrix form by

$$\begin{bmatrix} \hat{i}_{\text{L1d}} \\ \hat{i}_{\text{L1q}} \\ \hat{u}_{\text{in}} \\ \hat{i}_{\text{od}} \\ \hat{i}_{\text{oq}} \end{bmatrix} = \begin{bmatrix} G_{\text{ioL-d}}^{\text{H}} & -Y_{\text{L-d}}^{\text{H}} & G_{\text{crL-qd}}^{\text{H}} & G_{\text{cL-d}}^{\text{H}} & G_{\text{cL-qd}}^{\text{H}} \\ G_{\text{ioL-q}}^{\text{H}} & G_{\text{crL-dq}}^{\text{H}} & -Y_{\text{L-q}}^{\text{H}} & G_{\text{cL-dq}}^{\text{H}} & G_{\text{cL-q}}^{\text{H}} \\ Z_{\text{in}}^{\text{H}} & T_{\text{oi-d}}^{\text{H}} & T_{\text{oi-q}}^{\text{H}} & G_{\text{ci-d}}^{\text{H}} & G_{\text{ci-q}}^{\text{H}} \\ G_{\text{io-d}}^{\text{H}} & -Y_{\text{o-d}}^{\text{H}} & G_{\text{cr-qd}}^{\text{H}} & G_{\text{co-d}}^{\text{H}} & G_{\text{co-qd}}^{\text{H}} \\ G_{\text{io-q}}^{\text{H}} & G_{\text{cr-dq}}^{\text{H}} & -Y_{\text{o-q}}^{\text{H}} & G_{\text{co-dq}}^{\text{H}} & G_{\text{co-q}}^{\text{H}} \end{bmatrix} \begin{bmatrix} \hat{i}_{\text{in}} \\ \hat{u}_{\text{od}} \\ \hat{u}_{\text{oq}} \\ \hat{d}_{\text{d}} \\ \hat{d}_{\text{q}} \end{bmatrix}, \tag{3.71}$$

where the subscript 'L' denotes the inverter side inductor-related transfer functions. Presented transfer function matrix is modified as the actual current flows out of the inverter, thus, the admittances $Y_{\text{o-d}}^{\text{H}}$, $Y_{\text{o-q}}^{\text{H}}$, $Y_{\text{L-d}}^{\text{H}}$ and $Y_{\text{L-q}}^{\text{H}}$ have to be multiplied by -1. A linear network model can be presented according to the transfer function matrix as depicted in Fig. 3.3.

As can be seen from Fig. 3.3, the output voltage $\hat{u}_{\text{o(d,q)}}$ is present also in the inverter-side inductor current network model. This implies that perturbations of the output voltage $\hat{u}_{\text{o(d,q)}}$ affect the inverter-side inductor currents $\hat{i}_{\text{L1(d,q)}}$ via the corresponding transfer functions presented in the top two rows of the matrix in
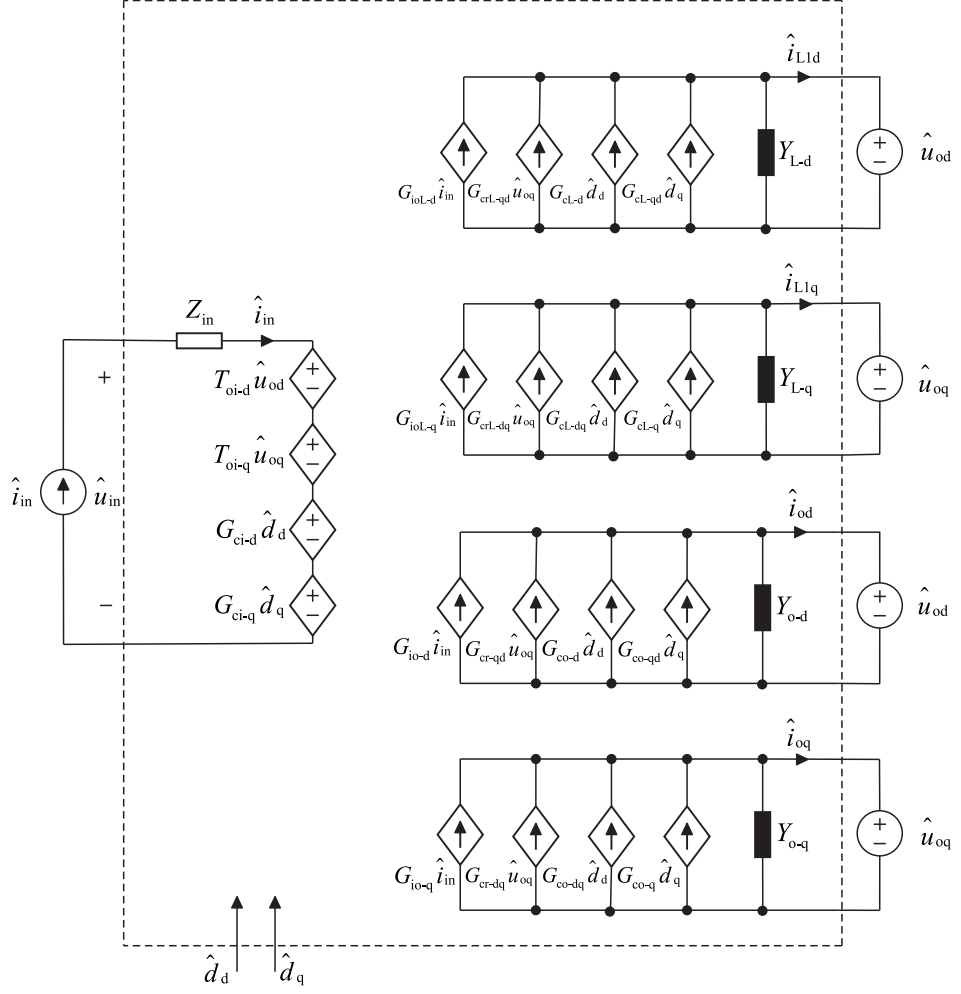
Figure 3.3: Linear network model of a CF-VSI.

(3.71). However, if the network model is modified, e.g., by adding a load, the load must be included to the real output seen from the grid side, i.e., to the $\hat{i}_{o(d,q)}$ related transfer functions. This procedure is presented in detail in Section 3.5.

The input dynamics of the system can be presented according to the transfer function matrix by

$$\hat{u}_{\text{in}} = Z_{\text{in}}^{\text{H}}\hat{i}_{\text{in}} + T_{\text{oi-d}}^{\text{H}}\hat{u}_{\text{od}} + T_{\text{oi-q}}^{\text{H}}\hat{u}_{\text{oq}} + G_{\text{ci-d}}^{\text{H}}\hat{d}_{\text{d}} + G_{\text{ci-q}}^{\text{H}}\hat{d}_{\text{q}}, \tag{3.72}$$

where Z_{in} is the input impedance of the system, $T_{\text{oi-(d,q)}}$ is known as the reverse transfer function, and $G_{\text{ci-(d,q)}}$ is the control-to-input-voltage transfer function. Dynamics related to inductor currents can be represented as in (3.73) and (3.74) regarding the boost-inductor currents and as in (3.75) and (3.76) regarding the grid-side output currents. Equations for the inductor currents can be given according to matrix in

(3.71) by

$$\hat{i}_{\text{L1d}} = G^{\text{H}}_{\text{ioL-d}}\hat{i}_{\text{in}} - Y^{\text{H}}_{\text{L-d}}\hat{u}_{\text{od}} + G^{\text{H}}_{\text{crL-qd}}\hat{u}_{\text{oq}} + G^{\text{H}}_{\text{cL-d}}\hat{d}_{\text{d}} + G^{\text{H}}_{\text{cL-qd}}\hat{d}_{\text{q}}, \tag{3.73}$$

$$\hat{i}_{\text{L1q}} = G^{\text{H}}_{\text{ioL-q}}\hat{i}_{\text{in}} + G^{\text{H}}_{\text{crL-dq}}\hat{u}_{\text{od}} - Y^{\text{H}}_{\text{L-q}}\hat{u}_{\text{oq}} + G^{\text{H}}_{\text{cL-dq}}\hat{d}_{\text{d}} + G^{\text{H}}_{\text{cL-q}}\hat{d}_{\text{q}}, \tag{3.74}$$

$$\hat{i}_{\text{od}} = G^{\text{H}}_{\text{io-d}}\hat{i}_{\text{in}} - Y^{\text{H}}_{\text{o-d}}\hat{u}_{\text{od}} + G^{\text{H}}_{\text{cr-qd}}\hat{u}_{\text{oq}} + G^{\text{H}}_{\text{co-d}}\hat{d}_{\text{d}} + G^{\text{H}}_{\text{co-qd}}\hat{d}_{\text{q}}, \tag{3.75}$$

$$\hat{i}_{\text{oq}} = G^{\text{H}}_{\text{io-q}}\hat{i}_{\text{in}} + G^{\text{H}}_{\text{cr-dq}}\hat{u}_{\text{od}} - Y^{\text{H}}_{\text{o-q}}\hat{u}_{\text{oq}} + G^{\text{H}}_{\text{co-dq}}\hat{d}_{\text{d}} + G^{\text{H}}_{\text{co-q}}\hat{d}_{\text{q}}, \tag{3.76}$$

where $G_{\text{io(L)(d,q)}}$ is the input-to-output transfer function or the forward current gain, $Y_{\text{(o,L)(d,q)}}$ is the output admittance, $G_{\text{cr(L)(dq,qd)}}$ is the cross-coupling term between the d-and q-channels, $G_{\text{c(o,L)(d,q)}}$ is known as the control-to-output-current transfer function, which is also cross-coupled to different channels as indicated by $G_{\text{c(o,L)(dq)}}$ and $G_{\text{c(o,L)(qd)}}$ in (3.73) - (3.76).

3.4   Source-affected model of a PV inverter

The dynamical model derived in the previous section does not include the effect of non-ideal source, which is often encountered in real systems. The effect of the non-ideal source may alter the dynamics of the system profoundly, thus, it is necessary to include it into the model. As discussed in Chapter 2, a PV generator has multiple operating points, which alter the behavior of the system due to the changes in dynamic resistance denoted earlier by r_{pv}. [2] The effect of the source can be modelled according to Fig. 3.4.

As can be seen from Fig. 3.4, the input current of the inverter can be presented by

$$\hat{i}_{\text{in}} = \hat{i}_{\text{inS}} - Y_{\text{s}}\hat{u}_{\text{in}}, \tag{3.77}$$

where $Y_{\text{s}} = \frac{1}{r_{\text{pv}}}$ i.e. the dynamic resistance of a PV generator. Now by substituting
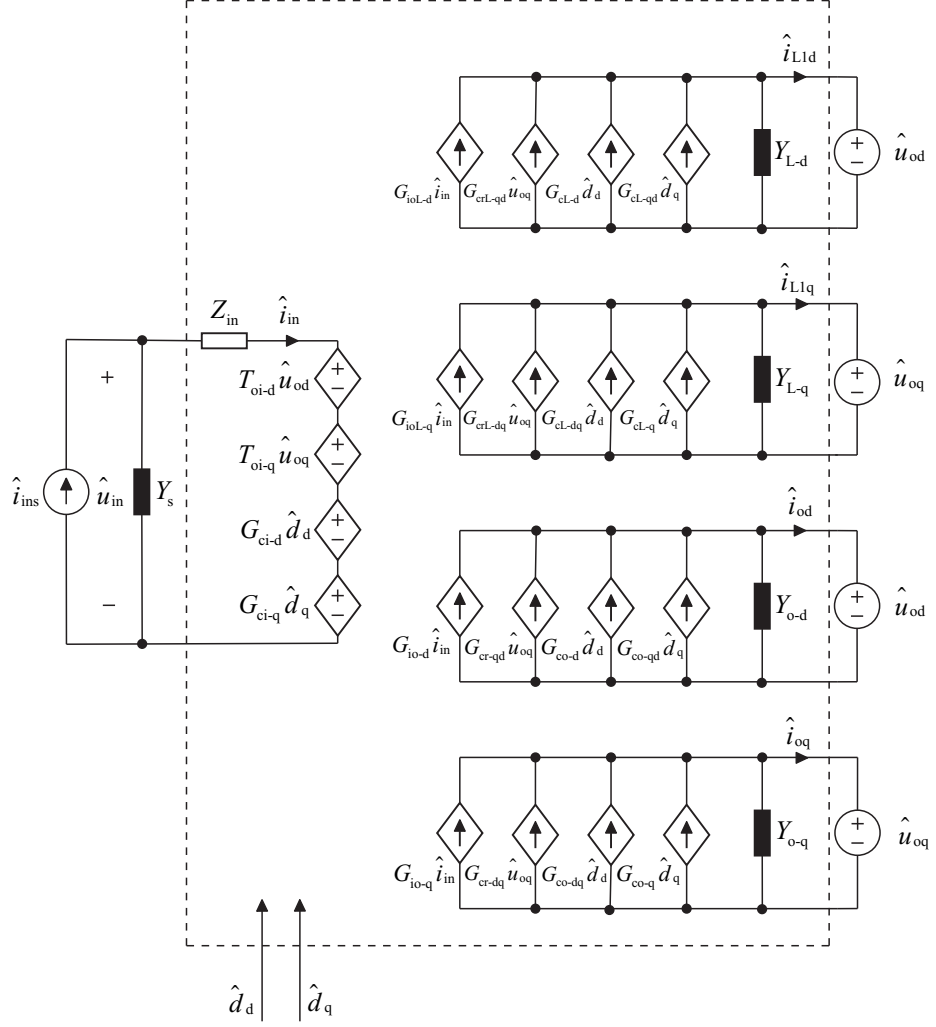
Figure 3.4: Linear model of a three-phase PV inverter with a non-ideal source.

$\hat{u}_{\text{in}}$ in (3.77) by the input-voltage dynamics given in (3.72) and solving for $\hat{i}_{\text{in}}$ yields

$$\hat{i}_{\text{in}} = \frac{1}{1 + Y_{\text{s}}Z_{\text{in}}^{\text{H}}}\hat{i}_{\text{inS}} - \frac{Y_{\text{s}}T_{\text{oi-d}}^{\text{H}}}{1 + Y_{\text{s}}Z_{\text{in}}^{\text{H}}}\hat{u}_{\text{od}} - \frac{Y_{\text{s}}T_{\text{oi-q}}^{\text{H}}}{1 + Y_{\text{s}}Z_{\text{in}}^{\text{H}}}\hat{u}_{\text{oq}} - \frac{Y_{\text{s}}G_{\text{ci-d}}^{\text{H}}}{1 + Y_{\text{s}}Z_{\text{in}}^{\text{H}}}\hat{d}_{\text{d}} - \frac{Y_{\text{s}}G_{\text{ci-q}}^{\text{H}}}{1 + Y_{\text{s}}Z_{\text{in}}^{\text{H}}}\hat{d}_{\text{q}}. \quad (3.78)$$

The stability of the interconnected subsystems at open loop can be analyzed by applying Nyquist stability criterion to the inverse minor loop-gain-term $Y_{\text{s}}Z_{\text{in}}^{\text{H}}$.

Now by substituting derived input-current $\hat{i}_{\text{in}}$ into the nominal open-loop dynamics presented by (3.73) - (3.76), the source-affected transfer functions can be solved. The input-voltage-related transfer functions can be given by

$$\hat{u}_{\text{in}} = Z_{\text{in}}^{\text{HS}}\hat{i}_{\text{inS}} + T_{\text{oi-d}}^{\text{HS}}\hat{u}_{\text{od}} + T_{\text{oi-q}}^{\text{HS}}\hat{u}_{\text{oq}} + G_{\text{ci-d}}^{\text{HS}}\hat{d}_{\text{d}} + G_{\text{ci-q}}^{\text{HS}}\hat{d}_{\text{q}}, \quad (3.79)$$

where

$$Z_{\text{in}}^{\text{HS}} = \frac{Z_{\text{in}}^{\text{H}}}{1 + Y_{\text{s}} Z_{\text{in}}^{\text{H}}}, \tag{3.80}$$

$$T_{\text{oi-d}}^{\text{HS}} = \frac{T_{\text{oi-d}}^{\text{H}}}{1 + Y_{\text{s}} Z_{\text{in}}^{\text{H}}}, \tag{3.81}$$

$$T_{\text{oi-q}}^{\text{HS}} = \frac{T_{\text{oi-q}}^{\text{H}}}{1 + Y_{\text{s}} Z_{\text{in}}^{\text{H}}}, \tag{3.82}$$

$$G_{\text{ci-d}}^{\text{HS}} = \frac{G_{\text{ci-d}}^{\text{H}}}{1 + Y_{\text{s}} Z_{\text{in}}^{\text{H}}}, \tag{3.83}$$

$$G_{\text{ci-q}}^{\text{HS}} = \frac{G_{\text{ci-q}}^{\text{H}}}{1 + Y_{\text{s}} Z_{\text{in}}^{\text{H}}}. \tag{3.84}$$

Now the source-affected inverter-side inductor current transfer functions can be solved by substituting (3.78) in (3.73) and (3.74). These transfer functions can be used, for example, to analyze the effect of the source (e.g., a PV generator) to the control loops, which are significantly affected. The d-channel boost-inductor current can be presented by

$$\hat{i}_{\text{L1d}} = G_{\text{ioL-d}}^{\text{HS}} \hat{i}_{\text{inS}} - Y_{\text{L-d}}^{\text{HS}} \hat{u}_{\text{od}} + G_{\text{crL-qd}}^{\text{HS}} \hat{u}_{\text{oq}} + G_{\text{cL-d}}^{\text{HS}} \hat{d}_{\text{d}} + G_{\text{cL-qd}}^{\text{HS}} \hat{d}_{\text{q}}, \tag{3.85}$$

where

$$G_{\text{ioL-d}}^{\text{HS}} = \frac{G_{\text{ioL-d}}^{\text{H}}}{1 + Y_{\text{s}} Z_{\text{in}}^{\text{H}}}, \tag{3.86}$$

$$Y_{\text{L-d}}^{\text{HS}} = -\frac{1 + Y_{\text{s}} Z_{\text{inL-d-oc}}^{\text{H}}}{1 + Y_{\text{s}} Z_{\text{in}}^{\text{H}}} Y_{\text{L-d}}^{\text{H}}, \tag{3.87}$$

$$G_{\text{crL-qd}}^{\text{HS}} = \frac{1 + Y_{\text{s}} Z_{\text{inL-qd-oc}}^{\text{H}}}{1 + Y_{\text{s}} Z_{\text{in}}^{\text{H}}} G_{\text{crL-qd}}^{\text{H}}, \tag{3.88}$$

$$G_{\text{cL-d}}^{\text{HS}} = \frac{1 + Y_{\text{s}} Z_{\text{inL-d-inf}}^{\text{H}}}{1 + Y_{\text{s}} Z_{\text{in}}^{\text{H}}} G_{\text{cL-d}}^{\text{H}}, \tag{3.89}$$

$$G_{\text{cL-qd}}^{\text{HS}} = \frac{1 + Y_{\text{s}} Z_{\text{inL-qd-inf}}^{\text{H}}}{1 + Y_{\text{s}} Z_{\text{in}}^{\text{H}}} G_{\text{cL-qd}}^{\text{H}}, \tag{3.90}$$

and the q-channel boost-inductor current by

$$\hat{i}_{\text{L1q}} = G_{\text{ioL-q}}^{\text{HS}} \hat{i}_{\text{inS}} + G_{\text{crL-dq}}^{\text{HS}} \hat{u}_{\text{od}} - Y_{\text{L-q}}^{\text{HS}} \hat{u}_{\text{oq}} + G_{\text{cL-dq}}^{\text{HS}} \hat{d}_{\text{d}} + G_{\text{cL-q}}^{\text{HS}} \hat{d}_{\text{q}}, \tag{3.91}$$

where

$$G_{\text{ioL-q}}^{\text{HS}} = \frac{G_{\text{ioL-q}}^{\text{H}}}{1 + Y_{\text{s}} Z_{\text{in}}^{\text{H}}}, \tag{3.92}$$

$$G_{\text{crL-dq}}^{\text{HS}} = \frac{1 + Y_{\text{s}} Z_{\text{inL-dq-oc}}^{\text{H}}}{1 + Y_{\text{s}} Z_{\text{in}}^{\text{H}}} G_{\text{crL-dq}}^{\text{H}}, \tag{3.93}$$

$$Y_{\text{L-q}}^{\text{HS}} = -\frac{1 + Y_{\text{s}} Z_{\text{inL-q-oc}}^{\text{H}}}{1 + Y_{\text{s}} Z_{\text{in}}^{\text{H}}} Y_{\text{L-q}}^{\text{H}}, \tag{3.94}$$

$$G_{\text{cL-dq}}^{\text{HS}} = \frac{1 + Y_{\text{s}} Z_{\text{inL-dq-inf}}^{\text{H}}}{1 + Y_{\text{s}} Z_{\text{in}}^{\text{H}}} G_{\text{cL-dq}}^{\text{H}}, \tag{3.95}$$

$$G_{\text{cL-q}}^{\text{HS}} = \frac{1 + Y_{\text{s}} Z_{\text{inL-q-inf}}^{\text{H}}}{1 + Y_{\text{s}} Z_{\text{in}}^{\text{H}}} G_{\text{cL-q}}^{\text{H}}. \tag{3.96}$$

The open-circuit and ideal input impedances in (3.86) - (3.96) are given explicitly

by (3.97) and (3.98), respectively.

$$Z_{\text{inL-d-oc}}^{\text{H}} = Z_{\text{in}}^{\text{H}} + \frac{T_{\text{oi-d}}^{\text{H}} G_{\text{ioL-d}}^{\text{H}}}{Y_{\text{L-d}}^{\text{H}}}, \quad Z_{\text{inL-qd-oc}}^{\text{H}} = Z_{\text{in}}^{\text{H}} - \frac{T_{\text{oi-q}}^{\text{H}} G_{\text{ioL-d}}^{\text{H}}}{G_{\text{crL-qd}}^{\text{H}}},$$
$$Z_{\text{inL-dq-oc}}^{\text{H}} = Z_{\text{in}}^{\text{H}} - \frac{T_{\text{oi-d}}^{\text{H}} G_{\text{ioL-q}}^{\text{H}}}{G_{\text{crL-dq}}^{\text{H}}}, \quad Z_{\text{inL-q-oc}}^{\text{H}} = Z_{\text{in}}^{\text{H}} + \frac{T_{\text{oi-q}}^{\text{H}} G_{\text{ioL-q}}^{\text{H}}}{Y_{\text{L-q}}^{\text{H}}}, \tag{3.97}$$

$$Z_{\text{inL-d-inf}}^{\text{H}} = Z_{\text{in}}^{\text{H}} - \frac{G_{\text{ci-d}}^{\text{H}} G_{\text{ioL-d}}^{\text{H}}}{G_{\text{cL-d}}^{\text{H}}}, \quad Z_{\text{inL-qd-inf}}^{\text{H}} = Z_{\text{in}}^{\text{H}} - \frac{G_{\text{ci-q}}^{\text{H}} G_{\text{ioL-d}}^{\text{H}}}{G_{\text{cL-qd}}^{\text{H}}},$$
$$Z_{\text{inL-dq-inf}}^{\text{H}} = Z_{\text{in}}^{\text{H}} - \frac{G_{\text{ci-d}}^{\text{H}} G_{\text{ioL-q}}^{\text{H}}}{G_{\text{cL-dq}}^{\text{H}}}, \quad Z_{\text{inL-q-inf}}^{\text{H}} = Z_{\text{in}}^{\text{H}} + \frac{G_{\text{ci-q}}^{\text{H}} G_{\text{ioL-q}}^{\text{H}}}{G_{\text{cL-q}}^{\text{H}}}. \tag{3.98}$$

Finally, by performing the same procedures as above, the source-affected transfer functions for the grid-side inductor current can be presented by

$$\hat{i}_{\text{od}} = G_{\text{io-d}}^{\text{HS}} \hat{i}_{\text{inS}} - Y_{\text{o-d}}^{\text{HS}} \hat{u}_{\text{od}} + G_{\text{cr-qd}}^{\text{HS}} \hat{u}_{\text{oq}} + G_{\text{co-d}}^{\text{HS}} \hat{d}_{\text{d}} + G_{\text{co-qd}}^{\text{HS}} \hat{d}_{\text{q}}, \tag{3.99}$$

$$\hat{i}_{\text{oq}} = G_{\text{io-q}}^{\text{HS}} \hat{i}_{\text{inS}} + G_{\text{cr-dq}}^{\text{HS}} \hat{u}_{\text{od}} - Y_{\text{o-q}}^{\text{HS}} \hat{u}_{\text{oq}} + G_{\text{co-dq}}^{\text{HS}} \hat{d}_{\text{d}} + G_{\text{co-q}}^{\text{HS}} \hat{d}_{\text{q}}, \tag{3.100}$$

where the d-channel-related transfer functions can be given by

$$G_{\text{io-d}}^{\text{HS}} = \frac{G_{\text{io-d}}^{\text{H}}}{1 + Y_{\text{s}} Z_{\text{in}}^{\text{H}}}, \tag{3.101}$$

$$Y_{\text{o-d}}^{\text{HS}} = -\frac{1 + Y_{\text{s}} Z_{\text{in-d-oc}}^{\text{H}}}{1 + Y_{\text{s}} Z_{\text{in}}^{\text{H}}} Y_{\text{o-d}}^{\text{H}}, \tag{3.102}$$

$$G_{\text{cr-qd}}^{\text{HS}} = \frac{1 + Y_{\text{s}} Z_{\text{in-qd-oc}}^{\text{H}}}{1 + Y_{\text{s}} Z_{\text{in}}^{\text{H}}} G_{\text{cr-qd}}^{\text{H}}, \tag{3.103}$$

$$G_{\text{co-d}}^{\text{HS}} = \frac{1 + Y_{\text{s}} Z_{\text{in-d-inf}}^{\text{H}}}{1 + Y_{\text{s}} Z_{\text{in}}^{\text{H}}} G_{\text{co-d}}^{\text{H}}, \tag{3.104}$$

$$G_{\text{co-qd}}^{\text{HS}} = \frac{1 + Y_{\text{s}} Z_{\text{in-qd-inf}}^{\text{H}}}{1 + Y_{\text{s}} Z_{\text{in}}^{\text{H}}} G_{\text{co-qd}}^{\text{H}}, \tag{3.105}$$

and the q-channel-related transfer functions by

$$G_{\text{io-q}}^{\text{HS}} = \frac{G_{\text{io-q}}^{\text{H}}}{1 + Y_{\text{s}} Z_{\text{in}}^{\text{H}}}, \tag{3.106}$$

$$G_{\text{cr-dq}}^{\text{HS}} = \frac{1 + Y_{\text{s}} Z_{\text{in-dq-oc}}^{\text{H}}}{1 + Y_{\text{s}} Z_{\text{in}}^{\text{H}}} G_{\text{cr-dq}}^{\text{H}}, \tag{3.107}$$

$$Y_{\text{o-q}}^{\text{HS}} = -\frac{1 + Y_{\text{s}} Z_{\text{in-q-oc}}^{\text{H}}}{1 + Y_{\text{s}} Z_{\text{in}}^{\text{H}}} Y_{\text{o-q}}^{\text{H}}, \tag{3.108}$$

$$G_{\text{co-dq}}^{\text{HS}} = \frac{1 + Y_{\text{s}} Z_{\text{in-dq-inf}}^{\text{H}}}{1 + Y_{\text{s}} Z_{\text{in}}^{\text{H}}} G_{\text{co-dq}}^{\text{H}}, \tag{3.109}$$

$$G_{\text{co-q}}^{\text{HS}} = \frac{1 + Y_{\text{s}} Z_{\text{in-q-inf}}^{\text{H}}}{1 + Y_{\text{s}} Z_{\text{in}}^{\text{H}}} G_{\text{co-q}}^{\text{H}}. \tag{3.110}$$

The open-circuit and the ideal input impedances in (3.101) - (3.110) are in explicit forms by (3.111) and (3.112).

$$\begin{aligned}
Z_{\text{in-d-oc}}^{\text{H}} &= Z_{\text{in}}^{\text{H}} + \frac{T_{\text{oi-d}}^{\text{H}} G_{\text{io-d}}^{\text{H}}}{Y_{\text{o-d}}^{\text{H}}}, \quad & Z_{\text{in-qd-oc}}^{\text{H}} &= Z_{\text{in}}^{\text{H}} - \frac{T_{\text{oi-q}}^{\text{H}} G_{\text{io-d}}^{\text{H}}}{G_{\text{cr-qd}}^{\text{H}}}, \\
Z_{\text{in-dq-oc}}^{\text{H}} &= Z_{\text{in}}^{\text{H}} - \frac{T_{\text{oi-d}}^{\text{H}} G_{\text{io-q}}^{\text{H}}}{G_{\text{cr-dq}}^{\text{H}}}, \quad & Z_{\text{in-q-oc}}^{\text{H}} &= Z_{\text{in}}^{\text{H}} + \frac{T_{\text{oi-q}}^{\text{H}} G_{\text{io-q}}^{\text{H}}}{Y_{\text{o-q}}^{\text{H}}},
\end{aligned} \tag{3.111}$$

$$\begin{aligned}
Z_{\text{in-d-inf}}^{\text{H}} &= Z_{\text{in}}^{\text{H}} - \frac{G_{\text{ci-d}}^{\text{H}} G_{\text{io-d}}^{\text{H}}}{G_{\text{co-d}}^{\text{H}}}, \quad & Z_{\text{in-qd-inf}}^{\text{H}} &= Z_{\text{in}}^{\text{H}} - \frac{G_{\text{ci-q}}^{\text{H}} G_{\text{io-d}}^{\text{H}}}{G_{\text{co-qd}}^{\text{H}}}, \\
Z_{\text{in-dq-inf}}^{\text{H}} &= Z_{\text{in}}^{\text{H}} - \frac{G_{\text{ci-d}}^{\text{H}} G_{\text{io-q}}^{\text{H}}}{G_{\text{co-dq}}^{\text{H}}}, \quad & Z_{\text{in-q-inf}}^{\text{H}} &= Z_{\text{in}}^{\text{H}} + \frac{G_{\text{ci-q}}^{\text{H}} G_{\text{io-q}}^{\text{H}}}{G_{\text{co-q}}^{\text{H}}}.
\end{aligned} \tag{3.112}$$

3.5 Load-affected model of a PV inverter

It is well known that the load impedance can significantly affect the dynamic behavior of the inverter. Therefore, the load-effect must be included into the model. It is worth noting that mathematically the load can be included either to the open-loop model or to the closed-loop model. However, the load is included to the open-loop model as its effect, e.g., to the control loop design can be analyzed.

The load effect can be calculated according to Fig. 3.5. It should be noted that for simplicity, it is assumed that no parallel components in the load impedance is present. However, this may be done as the connected load in this thesis is the three-phase grid and the impedance is the most interesting issue. The load is included with parallel components in [23] if further review of the topic is needed.
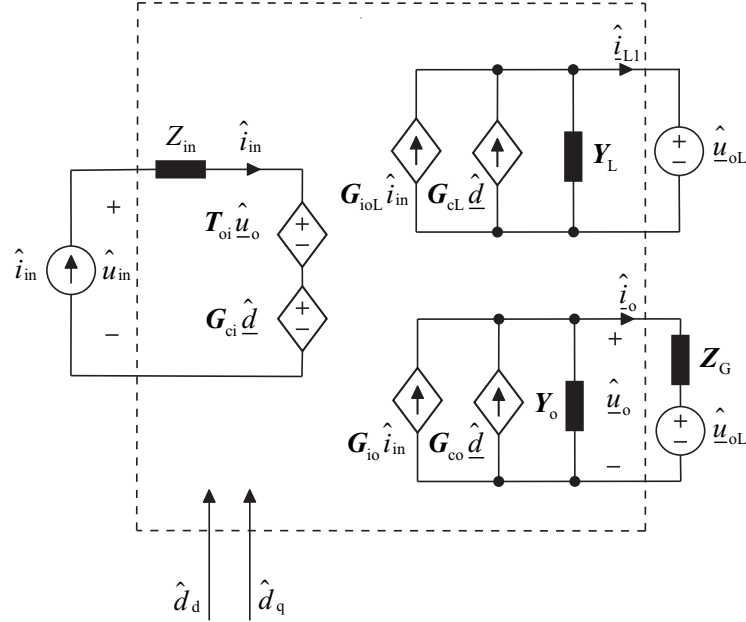

Figure 3.5: Load-affected model of a PV inverter at open loop.

Fig. 3.5 presents the impedance $\boldsymbol{Z}_{\mathrm{G}}$ and the grid voltage $\hat{\underline{u}}_{\mathrm{oL}}$. This grid impedance matrix can be estimated mathematically or it can be measured offline or online from the real grid using different techniques presented for example in [24–26].

As can be deduced from Fig. 3.5, the input voltage and the output grid-current can be presented with matrices by

$$\hat{u}_{\mathrm{in}} = Z_{\mathrm{in}}\hat{i}_{\mathrm{in}} + \boldsymbol{T}_{\mathrm{oi}}\hat{\underline{u}}_{\mathrm{o}} + \boldsymbol{G}_{\mathrm{ci}}\hat{\underline{d}}, \tag{3.113}$$

$$\hat{\underline{i}}_{\mathrm{o}} = \boldsymbol{G}_{\mathrm{io}}\hat{\underline{i}}_{\mathrm{in}} - \boldsymbol{Y}_{\mathrm{o}}\hat{\underline{u}}_{\mathrm{o}} + \boldsymbol{G}_{\mathrm{co}}\hat{\underline{d}}, \tag{3.114}$$

where the terms $\boldsymbol{T}_{\mathrm{oi}}, \boldsymbol{G}_{\mathrm{ci}}, \boldsymbol{G}_{\mathrm{io}}, \boldsymbol{Y}_{\mathrm{o}}$ and $\boldsymbol{G}_{\mathrm{co}}$ can be presented with the cross-coupling

effects by

$$\boldsymbol{T}_{\mathrm{oi}} = \begin{bmatrix} T_{\mathrm{oi\text{-}d}} \\ T_{\mathrm{oi\text{-}q}} \end{bmatrix}, \tag{3.115}$$

$$\boldsymbol{G}_{\mathrm{ci}} = \begin{bmatrix} G_{\mathrm{ci\text{-}d}} \\ G_{\mathrm{ci\text{-}q}} \end{bmatrix}, \tag{3.116}$$

$$\boldsymbol{G}_{\mathrm{io}} = \begin{bmatrix} G_{\mathrm{io\text{-}d}} \\ G_{\mathrm{io\text{-}q}} \end{bmatrix}, \tag{3.117}$$

$$\boldsymbol{Y}_{\mathrm{o}} = \begin{bmatrix} -Y_{\mathrm{o\text{-}d}} & G_{\mathrm{cr\text{-}qd}} \\ G_{\mathrm{cr\text{-}dq}} & -Y_{\mathrm{o\text{-}q}} \end{bmatrix}, \tag{3.118}$$

$$\boldsymbol{G}_{\mathrm{co}} = \begin{bmatrix} G_{\mathrm{co\text{-}d}} & G_{\mathrm{co\text{-}qd}} \\ G_{\mathrm{co\text{-}dq}} & G_{\mathrm{co\text{-}q}} \end{bmatrix}. \tag{3.119}$$

The output-voltage u_{o} can be given by

$$\underline{\hat{u}}_{\mathrm{o}} = \boldsymbol{Z}_{\mathrm{G}}\underline{\hat{i}}_{\mathrm{o}} + \underline{\hat{u}}_{\mathrm{oL}}, \tag{3.120}$$

where the grid impedance matrix can be presented by

$$\boldsymbol{Z}_{\mathrm{G}} = \begin{bmatrix} Z_{\mathrm{G\text{-}d}} & Z_{\mathrm{G\text{-}qd}} \\ Z_{\mathrm{G\text{-}dq}} & Z_{\mathrm{G\text{-}q}} \end{bmatrix}. \tag{3.121}$$

Now by substituting $\underline{\hat{u}}_{\mathrm{o}}$ in (3.114) by (3.120) yields

$$\underline{\hat{i}}_{\mathrm{o}} = \boldsymbol{G}_{\mathrm{io}}\underline{\hat{i}}_{\mathrm{in}} - \boldsymbol{Y}_{\mathrm{o}}\left(\boldsymbol{Z}_{\mathrm{G}}\underline{\hat{i}}_{\mathrm{o}} + \underline{\hat{u}}_{\mathrm{oL}}\right) + \boldsymbol{G}_{\mathrm{co}}\underline{\hat{d}}, \tag{3.122}$$

which can be rearranged as follows

$$\underline{\hat{i}}_{\mathrm{o}} = (\boldsymbol{I}+\boldsymbol{Y}_{\mathrm{o}}\boldsymbol{Z}_{\mathrm{G}})^{-1}\boldsymbol{G}_{\mathrm{io}}\underline{\hat{i}}_{\mathrm{in}} - (\boldsymbol{I}+\boldsymbol{Y}_{\mathrm{o}}\boldsymbol{Z}_{\mathrm{G}})^{-1}\boldsymbol{Y}_{\mathrm{o}}\underline{\hat{u}}_{\mathrm{oL}} + (\boldsymbol{I}+\boldsymbol{Y}_{\mathrm{o}}\boldsymbol{Z}_{\mathrm{G}})^{-1}\boldsymbol{G}_{\mathrm{co}}\underline{\hat{d}}, \tag{3.123}$$

where $\boldsymbol{I}$ is the unit matrix with suitable dimensions. It is worth noting that $\hat{\underline{i}}_\text{o}$ represents also the grid-side inductor current previously denoted as $\hat{\underline{i}}_\text{L2}$. From (3.123) the load-affected transfer functions for the output current can be presented by

$$\boldsymbol{G}_\text{io}^\text{L} = (\boldsymbol{I} + \boldsymbol{Y}_\text{o}\boldsymbol{Z}_\text{G})^{-1}\boldsymbol{G}_\text{io}, \tag{3.124}$$

$$\boldsymbol{Y}_\text{o}^\text{L} = -(\boldsymbol{I} + \boldsymbol{Y}_\text{o}\boldsymbol{Z}_\text{G})^{-1}\boldsymbol{Y}_\text{o}, \tag{3.125}$$

$$\boldsymbol{G}_\text{co}^\text{L} = (\boldsymbol{I} + \boldsymbol{Y}_\text{o}\boldsymbol{Z}_\text{G})^{-1}\boldsymbol{G}_\text{co}, \tag{3.126}$$

where the superscript 'L' denotes the load-affected transfer functions.

The effect of the grid impedance to the inverter-side inductor current $\hat{\underline{i}}_\text{L1}$ can be derived as follows. By substituting (3.123) into (3.120) and solving for $\hat{\underline{u}}_\text{o}$ yields

$$\hat{\underline{u}}_\text{o} = \Big[(\boldsymbol{I} + \boldsymbol{Y}_\text{o}\boldsymbol{Z}_\text{G})^{-1}\boldsymbol{G}_\text{io}\hat{\underline{i}}_\text{in} - (\boldsymbol{I} + \boldsymbol{Y}_\text{o}\boldsymbol{Z}_\text{G})^{-1}\boldsymbol{Y}_\text{o}\hat{\underline{u}}_\text{oL}$$
$$+ (\boldsymbol{I} + \boldsymbol{Y}_\text{o}\boldsymbol{Z}_\text{G})^{-1}\boldsymbol{G}_\text{co}\hat{\underline{d}}\Big]\boldsymbol{Z}_\text{G} + \hat{\underline{u}}_\text{oL}. \tag{3.127}$$

The equation for inverter-side inductor current can be presented by

$$\hat{\underline{i}}_\text{L1} = \boldsymbol{G}_\text{ioL}\hat{\underline{i}}_\text{in} - \boldsymbol{Y}_\text{oL}\hat{\underline{u}}_\text{o} + \boldsymbol{G}_\text{cL}\hat{\underline{d}}. \tag{3.128}$$

Now by substituting $\hat{\underline{u}}_\text{o}$ in (3.128) by (3.127) and solving for $\hat{\underline{i}}_\text{L1}$ gives the load-affected inverter-side inductor current, which can be now presented by

$$\hat{\underline{i}}_\text{L1} = \hat{\underline{i}}_\text{in}\big[\boldsymbol{G}_\text{ioL} - \boldsymbol{Y}_\text{oL}\boldsymbol{Z}_\text{G}\boldsymbol{G}_\text{io}(\boldsymbol{I} + \boldsymbol{Y}_\text{o}\boldsymbol{Z}_\text{G})^{-1}\big] + \hat{\underline{u}}_\text{oL}\big[-\boldsymbol{Y}_\text{oL}$$
$$+ \boldsymbol{Y}_\text{oL}\boldsymbol{Y}_\text{o}\boldsymbol{Z}_\text{G}(\boldsymbol{I} + \boldsymbol{Y}_\text{o}\boldsymbol{Z}_\text{G})^{-1}\big] + \hat{\underline{d}}\big[\boldsymbol{G}_\text{cL} - \boldsymbol{Y}_\text{oL}\boldsymbol{Z}_\text{G}\boldsymbol{G}_\text{co}(\boldsymbol{I} + \boldsymbol{Y}_\text{o}\boldsymbol{Z}_\text{G})^{-1}\big], \tag{3.129}$$

where

$$\boldsymbol{G}_\text{ioL} = \begin{bmatrix} G_\text{ioL-d} \\ G_\text{ioL-q} \end{bmatrix}, \tag{3.130}$$

$$\boldsymbol{Y}_{\text{L}} = \begin{bmatrix} -Y_{\text{L-d}} & G_{\text{crL-qd}} \\ G_{\text{crL-dq}} & -Y_{\text{L-q}} \end{bmatrix}, \tag{3.131}$$

$$\boldsymbol{G}_{\text{cL}} = \begin{bmatrix} G_{\text{cL-d}} & G_{\text{cL-qd}} \\ G_{\text{cL-dq}} & G_{\text{cL-q}} \end{bmatrix}. \tag{3.132}$$

The load-affected transfer functions for the inverter-side inductor can be given according to (3.129) by

$$\boldsymbol{G}_{\text{ioL}}^{\text{L}} = \boldsymbol{G}_{\text{ioL}} - \boldsymbol{Y}_{\text{oL}}\boldsymbol{Z}_{\text{G}}\boldsymbol{G}_{\text{io}}(\boldsymbol{I} + \boldsymbol{Y}_{\text{o}}\boldsymbol{Z}_{\text{G}})^{-1}, \tag{3.133}$$

$$\boldsymbol{Y}_{\text{L}}^{\text{L}} = \boldsymbol{Y}_{\text{oL}} - \boldsymbol{Y}_{\text{oL}}\boldsymbol{Y}_{\text{o}}\boldsymbol{Z}_{\text{G}}(\boldsymbol{I} + \boldsymbol{Y}_{\text{o}}\boldsymbol{Z}_{\text{G}})^{-1}, \tag{3.134}$$

$$\boldsymbol{G}_{\text{cL}}^{\text{L}} = \boldsymbol{G}_{\text{cL}} - \boldsymbol{Y}_{\text{oL}}\boldsymbol{Z}_{\text{G}}\boldsymbol{G}_{\text{co}}(\boldsymbol{I} + \boldsymbol{Y}_{\text{o}}\boldsymbol{Z}_{\text{G}})^{-1}. \tag{3.135}$$

As the purpose of this thesis is to present a complete dynamic model for the PV inverter, which can be subsequently used to analyze the effects of different grid impedances to the inverter dynamics, the most valuable information is found in the output impedances, i.e., $\boldsymbol{Z}_{\text{o}} = \boldsymbol{Y}_{\text{o}}^{-1}$ of the inverter. The inverter is interfaced with the grid according to Fig. 3.6 where the grid is assumed to be inductive.

Figure 3.6: Grid interfacing of a CF-VSI.

The stability of the system is determined by the term $\boldsymbol{Y}_\mathrm{o}\boldsymbol{Z}_\mathrm{G}$. The stability can be analyzed by applying the well-known Nyquist stability-criterion presented in [27] to the impedances $\boldsymbol{Y}_\mathrm{o}$ and $\boldsymbol{Z}_\mathrm{G}$ according to (3.136) [28]

$$\boldsymbol{L}_\mathrm{dq} = \begin{bmatrix} Y_\mathrm{o\text{-}d} & G_\mathrm{cr\text{-}qd} \\ G_\mathrm{cr\text{-}dq} & Y_\mathrm{o\text{-}q} \end{bmatrix} \begin{bmatrix} Z_\mathrm{G\text{-}d} & Z_\mathrm{G\text{-}qd} \\ Z_\mathrm{G\text{-}dq} & Z_\mathrm{G\text{-}q} \end{bmatrix}, \tag{3.136}$$

which may be simplified by neglecting the cross-coupling terms. Now the d-channel and q-channel impedance ratios can be given by

$$\boldsymbol{L}_\mathrm{d} = Y_\mathrm{o\text{-}d}Z_\mathrm{G\text{-}d} = \frac{Z_\mathrm{G\text{-}d}}{Z_\mathrm{o\text{-}d}}, \tag{3.137}$$

$$\boldsymbol{L}_\mathrm{q} = Y_\mathrm{o\text{-}q}Z_\mathrm{G\text{-}q} = \frac{Z_\mathrm{G\text{-}q}}{Z_\mathrm{o\text{-}q}}. \tag{3.138}$$

It is worth noting that even though the grid is often modeled as an inductive load as presented, for example, in [10, 24, 25, 29], the real load may vary significantly. Inverter may be accompanied with many other inverters and, therefore, the grid impedance should not be analyzed as a pure inductor. Research on the effect of other inverters and PE devices on the grid impedance would be valuable, however, it is not included in this thesis.

3.6 Closed-loop model

Due to nature of the discussed inverter, a cascaded-control scheme is used as a control strategy as done also in [23,30] and many other grid-connected inverter applications. The outer loop, i.e., the input-voltage control-loop provides the d-channel current reference to the inner output-current-loop. It should be noted that the q-channel output-current reference is usually set to zero to obtain unity power factor.

The inner current-control-loop is designed with high bandwidth to ensure high output impedance and sufficient power quality [31]. Thus, the current injected to the utility grid is less distorted, even though there is distortion in the grid voltages. The input-voltage controller is designed with lower bandwidth than the current loop, and the crossover frequency has to be higher than the RHP pole frequency and lower than twice the grid frequency. Usually this means a few tens of Hertz of bandwidth for a three-phase inverter. [32] These limitations are discussed more in detail in Chapter 4.

A block diagram of the complete dynamical model is depicted in Fig. 3.9. It is

worth noting that the effect of the grid-synchronization by the phase-locked loop is also included in the model, which induces a feed-forward effect to the control system from the q-channel output voltage $\hat{u}_{oq}$. This phenomenon is discussed in the following subsection.

3.6.1 Effect of the grid-synchronization

Theoretical derivation of the PLL-effect begins by analyzing the small-signal angle difference between the grid reference frame and the control system reference frame. According to [33], the control system d and q-components can be given as a function of grid d and q-components by

$$
\begin{aligned}
\hat{x}_{\text{d-c}} &= \hat{x}_{\text{d}} + \Theta_\Delta \hat{x}_{\text{q}} + X_{\text{q}} \theta_\Delta, \\
\hat{x}_{\text{q-c}} &= \hat{x}_{\text{q}} + \Theta_\Delta \hat{x}_{\text{d}} + X_{\text{d}} \theta_\Delta,
\end{aligned}
\tag{3.139}
$$

where the subscript extension 'c' denotes a variable in the reference frame tied to the control system variables. Eq. (3.139) is linearized at a predefined operating point, where Θ represents the steady state value of the error angle. However, in steady-state it is assumed that the error is zero as well as the grid voltage U_{oq}, q-component of the controlled current I_{L1q} and the q-component of the duty ratio D_{q}. Hence the grid variables can be given by means of the control system variables by

$$
\begin{aligned}
\hat{u}_{\text{od}} &= \hat{u}_{\text{od-c}}, \hat{u}_{\text{oq}} = \hat{u}_{\text{oq-c}} + U_{\text{od}} \hat{\theta}_\Delta, \\
\hat{i}_{\text{L1d}} &= \hat{i}_{\text{L1d-c}}, \hat{i}_{\text{L1q}} = \hat{i}_{\text{L1q-c}} + I_{\text{L1d}} \hat{\theta}_\Delta, \\
\hat{d}_{\text{d}} &= \hat{d}_{\text{d-c}}, \hat{d}_{\text{q}} = \hat{d}_{\text{q-c}} + D_{\text{d}} \hat{\theta}_\Delta.
\end{aligned}
\tag{3.140}
$$

As can be deduced, the PLL does not affect the d-channel current control, because the q-channel steady state duty ratio D_{q} is usually close to zero. Therefore, it may be assumed that $\hat{i}_{\text{L1d}} = \hat{i}_{\text{L1d-c}}$ in the block diagram presented in Fig. 3.9.

The small-signal presentation of a conventional PLL block diagram is presented in Fig. 3.7 according to [33].
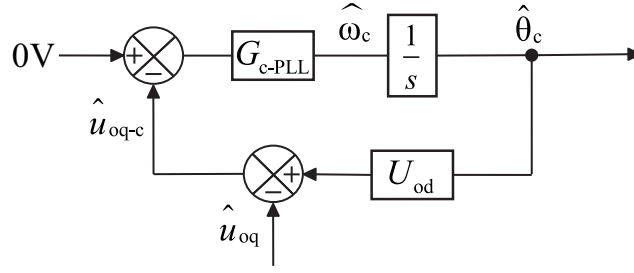
Figure 3.7: Small-signal block diagram of a PLL.

From Fig. 3.7, the small-signal angle can be solved (i.e., the PLL transfer function) and given by

$$\hat{\theta}_\Delta = \hat{\theta}_c = \frac{1}{U_{od}} \frac{L_{PLL}}{1 + L_{PLL}} \hat{u}_{oq},$$ (3.141)

where

$$L_{PLL} = -\frac{G_{c\text{-PLL}} U_{od}}{s}.$$ (3.142)

It is worth noting that the grid synchronization with the PLL alters the inverter output impedance as shown, for example, in [33, 34]. Because of the PLL, the phase of the q-channel output impedance is shifted to -180 degrees, which makes the inverter prone to instability or harmonic resonance if the inverter is connected to a weak grid. High bandwidth PLL increases the risk of instability since the phase stays close to -180 degrees over a wider frequency band. Fig. 3.8 shows predicted behavior of the output impedance under influence of a phase-locked loop.
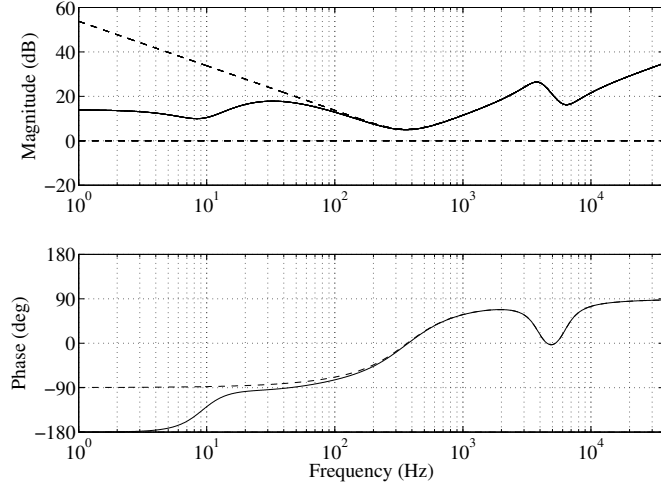
Figure 3.8: Predicted inverter q-channel output impedance $Z_{\text{o-q}}$ with PLL (solid line) and without PLL (dashed line)

3.6.2 Closed-loop model derivation

Closed-loop transfer functions for a cascaded control scheme can be derived by first computing the closed-loop transfer functions when only the output-current control is active and then treating the obtained model as an open-loop system for the input-voltage control-loop derivation. In the complete control block diagram, depicted in Fig. 3.9, G_{se} is the voltage-sensing transfer function, G_{vc} is the voltage controller, G_{a} is the modulator gain of the current controller (in digital control systems this can be neglected), R_{eq} is the current-sensing equivalent transfer function, G_{cc} is the current controller and G_{PLL} is the transfer function of the phase-locked loop, which was derived in previous subsection.

Control block diagram of an output-current-controlled inverter is presented in Fig. 3.10. According to Fig. 3.10, the d-channel duty ratio $\hat{d}_{\text{d}}$ can be given by

$$\hat{d}_{\text{d}} = -\frac{1}{G_{\text{cL-d}}}L_{\text{out-d}}\hat{i}_{\text{L1d}} + \frac{1}{G_{\text{cL-d}}R_{\text{eq-d}}}L_{\text{out-d}}\hat{u}_{\text{iL1d}}^{\text{ref}} + D_{\text{q}}G_{\text{PLL}}\hat{u}_{\text{oq}}, \qquad (3.143)$$

and the d-channel inverter-side inductor current can be presented by

$$\hat{i}_{\text{L1d}} = (-R_{\text{eq-d}}\hat{i}_{\text{L1d}} + \hat{u}_{\text{iL1d}}^{\text{ref}})G_{\text{cc-d}}G_{\text{a}}G_{\text{cL-d}} + G_{\text{ioL-d}}\hat{i}_{\text{in}} - Y_{\text{L-d}}\hat{u}_{\text{od}} + G_{\text{crL-qd}}\hat{u}_{\text{oq}}$$
$$+ G_{\text{cL-qd}}\hat{d}_{\text{q}} + D_{\text{q}}G_{\text{PLL}}G_{\text{cL-d}}\hat{u}_{\text{oq}}, \quad (3.144)$$

where

$$L_{\text{out-d}} = R_{\text{eq-d}}G_{\text{cc-d}}G_{\text{a}}G_{\text{cL-d}}. \tag{3.145}$$

From (3.143) and (3.144), the derivation of a general form for the d-channel duty ratio can be performed. However, the derivation of the duty ratios is relatively complex, and therefore, it is presented in detail only in Appendix B. Derived general form for the d-channel duty-ratio can be presented by

$$
\begin{aligned}
\hat{d}_{\text{d}} = {} & \frac{1}{1 - \frac{G_{\text{cL-dq}}G_{\text{cL-qd}}}{G_{\text{cL-q}}G_{\text{cL-d}}} \frac{L_{\text{out-q}}L_{\text{out-d}}}{(1+L_{\text{out-q}})(1+L_{\text{out-d}})}} \left\{ -\frac{1}{G_{\text{cL-d}}}L_{\text{out-d}} \left[\frac{G_{\text{ioL-d}}}{1 + L_{\text{out-d}}}\hat{i}_{\text{in}} - \frac{Y_{\text{L-d}}}{1 + L_{\text{out-d}}}\hat{u}_{\text{od}} \right. \right. \\
& + \frac{G_{\text{crL-qd}}}{1 + L_{\text{out-d}}}\hat{u}_{\text{oq}} + \frac{D_{\text{q}}G_{\text{cL-d}}G_{\text{PLL}}}{1 + L_{\text{out-d}}}\hat{u}_{\text{oq}} + \frac{1}{R_{\text{eq-d}}}\frac{L_{\text{out-d}}}{1 + L_{\text{out-d}}}\hat{u}_{\text{iL1d}}^{\text{ref}} + \frac{G_{\text{cL-qd}}}{1 + L_{\text{out-d}}} \\
& \times \left(-\frac{G_{\text{ioL-q}}}{G_{\text{cL-q}}}\frac{L_{\text{out-q}}}{1 + L_{\text{out-q}}}\hat{i}_{\text{in}} - \frac{G_{\text{crL-dq}}}{G_{\text{cL-q}}}\frac{L_{\text{out-q}}}{1 + L_{\text{out-q}}}\hat{u}_{\text{od}} + \frac{Y_{\text{L-q}}}{G_{\text{cL-q}}}\frac{L_{\text{out-q}}}{1 + L_{\text{out-q}}}\hat{u}_{\text{oq}} \right. \\
& \left. + \frac{1}{R_{\text{eq-q}}G_{\text{cL-q}}}\frac{L_{\text{out-q}}}{1 + L_{\text{out-q}}}\hat{u}_{\text{iL1q}}^{\text{ref}} + \frac{I_{\text{L1d}}G_{\text{PLL}}}{G_{\text{cL-q}}}\frac{L_{\text{out-q}}}{1 + L_{\text{out-q}}}\hat{u}_{\text{oq}} + D_{\text{d}}G_{\text{PLL}}\frac{1}{1 + L_{\text{out-q}}}\hat{u}_{\text{oq}} \right) \right] \\
& \left. + \frac{1}{G_{\text{cL-d}}R_{\text{eq-d}}}L_{\text{out-d}}\hat{u}_{\text{iL1d}}^{\text{ref}} + D_{\text{q}}G_{\text{PLL}}\hat{u}_{\text{oq}} \right\}. \tag{3.146}
\end{aligned}
$$

Respectively, the q-channel duty ratio derivation can be performed from equations obtained from Fig. 3.10, where $\hat{d}_{\text{q}}$ can be presented by

$$\hat{d}_{\text{q}} = -\frac{1}{G_{\text{cL-q}}}L_{\text{out-q}}\hat{i}_{\text{L1q}} + \frac{1}{G_{\text{cL-q}}R_{\text{eq-q}}}L_{\text{out-q}}\hat{u}_{\text{iL1q}}^{\text{ref}} + D_{\text{d}}G_{\text{PLL}}\hat{u}_{\text{oq}} + \frac{I_{\text{L1d}}G_{\text{PLL}}}{G_{\text{cL-q}}}L_{\text{out-q}}\hat{u}_{\text{oq}}. \tag{3.147}$$

From Fig. 3.10, the q-channel inverter-side inductor current can be given by

$$
\begin{aligned}
\hat{i}_{\text{L1q}} = {} & (-R_{\text{eq-q}}\hat{i}_{\text{L1q}} + \hat{u}_{\text{iL1q}}^{\text{ref}} + I_{\text{L1d}}G_{\text{PLL}}R_{\text{eq-q}}\hat{u}_{\text{oq}})G_{\text{cc-q}}G_{\text{a}}G_{\text{cL-q}} + G_{\text{ioL-q}}\hat{i}_{\text{in}} \\
& + G_{\text{crL-dq}}\hat{u}_{\text{od}} - Y_{\text{L-q}}\hat{u}_{\text{oq}} + G_{\text{cL-dq}}\hat{d}_{\text{d}} + D_{\text{d}}G_{\text{PLL}}G_{\text{cL-q}}\hat{u}_{\text{oq}}, \tag{3.148}
\end{aligned}
$$

where

$$L_{\text{out-q}} = R_{\text{eq-q}}G_{\text{cc-q}}G_{\text{a}}G_{\text{cL-q}}. \tag{3.149}$$

The detailed derivation of the equation can be found in Appendix B. The q-channel duty-ratio can be presented according to (3.150) by

$$
\begin{aligned}
\hat{d}_{\mathrm{q}} = \frac{1}{1 - \frac{G_{\mathrm{cL\text{-}dq}}G_{\mathrm{cL\text{-}qd}}}{G_{\mathrm{cL\text{-}q}}G_{\mathrm{cL\text{-}d}}}\frac{L_{\mathrm{out\text{-}q}}L_{\mathrm{out\text{-}d}}}{(1+L_{\mathrm{out\text{-}q}})(1+L_{\mathrm{out\text{-}d}})}} & \left\{ -\frac{1}{G_{\mathrm{cL\text{-}q}}}L_{\mathrm{out\text{-}q}}\left[\frac{G_{\mathrm{ioL\text{-}q}}}{1+L_{\mathrm{out\text{-}q}}}\hat{i}_{\mathrm{in}} + \frac{G_{\mathrm{crL\text{-}dq}}}{1+L_{\mathrm{out\text{-}q}}}\hat{u}_{\mathrm{od}} \right. \right. \\
& - \frac{Y_{\mathrm{L\text{-}q}}}{1+L_{\mathrm{out\text{-}q}}}\hat{u}_{\mathrm{oq}} + \frac{D_{\mathrm{d}}G_{\mathrm{cL\text{-}q}}G_{\mathrm{PLL}}}{1+L_{\mathrm{out\text{-}q}}}\hat{u}_{\mathrm{oq}} + I_{\mathrm{L1d}}G_{\mathrm{PLL}}\frac{L_{\mathrm{out\text{-}q}}}{1+L_{\mathrm{out\text{-}q}}}\hat{u}_{\mathrm{oq}} + \frac{1}{R_{\mathrm{eq\text{-}q}}}\frac{L_{\mathrm{out\text{-}q}}}{1+L_{\mathrm{out\text{-}q}}}\hat{u}_{\mathrm{iL1q}}^{\mathrm{ref}} \\
& + \frac{G_{\mathrm{cL\text{-}dq}}}{1+L_{\mathrm{out\text{-}q}}}\left(-\frac{G_{\mathrm{ioL\text{-}d}}}{G_{\mathrm{cL\text{-}d}}}\frac{L_{\mathrm{out\text{-}d}}}{1+L_{\mathrm{out\text{-}d}}}\hat{i}_{\mathrm{in}} + \frac{Y_{\mathrm{L\text{-}d}}}{G_{\mathrm{cL\text{-}d}}}\frac{L_{\mathrm{out\text{-}d}}}{1+L_{\mathrm{out\text{-}d}}}\hat{u}_{\mathrm{od}} - \frac{G_{\mathrm{crL\text{-}qd}}}{G_{\mathrm{cL\text{-}d}}}\frac{L_{\mathrm{out\text{-}d}}}{1+L_{\mathrm{out\text{-}d}}}\hat{u}_{\mathrm{oq}} \right. \\
& \left. + \frac{1}{R_{\mathrm{eq\text{-}d}}G_{\mathrm{cL\text{-}d}}}\frac{L_{\mathrm{out\text{-}d}}}{1+L_{\mathrm{out\text{-}d}}}\hat{u}_{\mathrm{iL1d}}^{\mathrm{ref}} + D_{\mathrm{q}}G_{\mathrm{PLL}}\frac{1}{1+L_{\mathrm{out\text{-}d}}}\hat{u}_{\mathrm{oq}} \right) \left. \right] + \frac{1}{G_{\mathrm{cL\text{-}q}}R_{\mathrm{eq\text{-}q}}}L_{\mathrm{out\text{-}q}}\hat{u}_{\mathrm{iL1q}}^{\mathrm{ref}} \\
& \left. + D_{\mathrm{d}}G_{\mathrm{PLL}}\hat{u}_{\mathrm{oq}} + \frac{I_{\mathrm{L1d}}G_{\mathrm{PLL}}}{G_{\mathrm{cL\text{-}q}}}L_{\mathrm{out\text{-}q}}\hat{u}_{\mathrm{oq}} \right\}. \quad (3.150)
\end{aligned}
$$

The d- and q-channel duty ratios can be substituted to the open-loop dynamics of the input voltage $\hat{u}_{\mathrm{in}}$ and the inductor currents $\hat{i}_{\mathrm{L1d}}$, $\hat{i}_{\mathrm{L1q}}$, $\hat{i}_{\mathrm{od}}$ and $\hat{i}_{\mathrm{oq}}$. Furthermore, the closed-loop transfer functions, when the output-current control-loops are closed, can be solved. Derived transfer functions are presented with all cross-coupling effects in Appendix C.

The closed-loop transfer functions, when all control loops are closed, can be solved according to Fig. 3.11, where the derived output-current-loop transfer functions are used as an open-loop system for the input voltage control-loop derivation. The d-channel output-current reference can be given according to Fig. 3.11 by

$$
\hat{u}_{\mathrm{iL1d}}^{\mathrm{ref}} = G_{\mathrm{se\text{-}v}}G_{\mathrm{vc}}\hat{u}_{\mathrm{in}} - G_{\mathrm{vc}}\hat{u}_{\mathrm{uin}}^{\mathrm{ref}}. \tag{3.151}
$$

Now by substituting (3.151) into the derived output-current-controlled input voltage dynamics yields

$$
\hat{u}_{\mathrm{in}} = Z_{\mathrm{in}}^{\mathrm{out}}\hat{i}_{\mathrm{in}} + T_{\mathrm{oi\text{-}d}}^{\mathrm{out}}\hat{u}_{\mathrm{od}} + T_{\mathrm{oi\text{-}q}}^{\mathrm{out}}\hat{u}_{\mathrm{oq}} + G_{\mathrm{ci\text{-}d}}^{\mathrm{out}}\left(G_{\mathrm{se\text{-}v}}G_{\mathrm{vc}}\hat{u}_{\mathrm{in}} - G_{\mathrm{vc}}\hat{u}_{\mathrm{uin}}^{\mathrm{ref}} \right) + G_{\mathrm{ci\text{-}q}}^{\mathrm{out}}\hat{u}_{\mathrm{iL1q}}^{\mathrm{ref}}, \tag{3.152}
$$

where the superscript 'out' denotes that only the output-current-control loop is connected. By solving (3.152) for $\hat{u}_{\mathrm{in}}$, the complete closed-loop transfer functions for input dynamics can be expressed by

$$
Z_{\mathrm{in}}^{\mathrm{tot}} = \frac{\hat{u}_{\mathrm{in}}}{\hat{i}_{\mathrm{in}}} = \frac{Z_{\mathrm{in}}^{\mathrm{out}}}{1 - L_{\mathrm{in}}}, \tag{3.153}
$$

$$T_{\text{oi-d}}^{\text{tot}} = \frac{\hat{u}_{\text{in}}}{\hat{u}_{\text{od}}} = \frac{T_{\text{oi-d}}^{\text{out}}}{1 - L_{\text{in}}}, \tag{3.154}$$

$$T_{\text{oi-q}}^{\text{tot}} = \frac{\hat{u}_{\text{in}}}{\hat{u}_{\text{oq}}} = \frac{T_{\text{oi-q}}^{\text{out}}}{1 - L_{\text{in}}}, \tag{3.155}$$

$$G_{\text{ci-d}}^{\text{tot}} = \frac{\hat{u}_{\text{in}}}{\hat{u}_{\text{uin}}^{\text{ref}}} = -\frac{1}{G_{\text{se-v}}} \frac{L_{\text{in}}}{1 - L_{\text{in}}}, \tag{3.156}$$

and

$$G_{\text{ci-q}}^{\text{tot}} = \frac{\hat{u}_{\text{in}}}{\hat{u}_{\text{iL1q}}^{\text{ref}}} = \frac{G_{\text{ci-q}}^{\text{out}}}{1 - L_{\text{in}}}, \tag{3.157}$$

where the input-voltage loop gain $L_{\text{in}} = G_{\text{ci-d}}^{\text{out}} G_{\text{se-v}} G_{\text{vc}}$ and the superscript 'tot' denotes the complete closed-loop transfer function. The inverter-side inductor current and output current dynamics can be solved by substituting derived expression for $\hat{u}_{\text{in}}$ into (3.151) and substituting (3.151) into (C.7), (C.13), (C.19) and (C.25). The inverter-side inductor current dynamics can be presented by

$$\hat{i}_{\text{L1d}} = G_{\text{ioL-d}}^{\text{tot}} \hat{i}_{\text{in}} - Y_{\text{L-d}}^{\text{tot}} \hat{u}_{\text{od}} + G_{\text{crL-qd}}^{\text{tot}} \hat{u}_{\text{oq}} + G_{\text{cL-d}}^{\text{tot}} \hat{u}_{\text{iL1d}}^{\text{ref}} + G_{\text{cL-qd}}^{\text{tot}} \hat{u}_{\text{iL1q}}^{\text{ref}}, \tag{3.158}$$

and

$$\hat{i}_{\text{L1q}} = G_{\text{ioL-q}}^{\text{tot}} \hat{i}_{\text{in}} + G_{\text{crL-dq}}^{\text{tot}} \hat{u}_{\text{od}} - Y_{\text{L-q}}^{\text{tot}} \hat{u}_{\text{oq}} + G_{\text{cL-dq}}^{\text{tot}} \hat{u}_{\text{iL1d}}^{\text{ref}} + G_{\text{cL-q}}^{\text{tot}} \hat{u}_{\text{iL1q}}^{\text{ref}}, \tag{3.159}$$

where the d-channel-related transfer function are given by

$$G_{\text{ioL-d}}^{\text{tot}} = \frac{\hat{i}_{\text{L1d}}}{\hat{i}_{\text{in}}} = G_{\text{ioL-d}}^{\text{out}} + \frac{L_{\text{in}}}{1 - L_{\text{in}}} \frac{Z_{\text{in}}^{\text{out}} G_{\text{cL-d}}^{\text{out}}}{G_{\text{ci-d}}^{\text{out}}}, \tag{3.160}$$

$$Y_{\text{L-d}}^{\text{tot}} = \frac{\hat{i}_{\text{L1d}}}{\hat{u}_{\text{od}}} = Y_{\text{L-d}}^{\text{out}} - \frac{L_{\text{in}}}{1 - L_{\text{in}}} \frac{T_{\text{oi-d}}^{\text{out}} G_{\text{cL-d}}^{\text{out}}}{G_{\text{ci-d}}^{\text{out}}}, \tag{3.161}$$

$$G_{\text{crL-qd}}^{\text{tot}} = \frac{\hat{i}_{\text{L1d}}}{\hat{u}_{\text{oq}}} = G_{\text{crL-qd}}^{\text{out}} + \frac{L_{\text{in}}}{1 - L_{\text{in}}} \frac{T_{\text{oi-q}}^{\text{out}} G_{\text{cL-d}}^{\text{out}}}{G_{\text{ci-d}}^{\text{out}}}, \tag{3.162}$$

$$G_{\text{cL-d}}^{\text{tot}} = \frac{\hat{i}_{\text{L1d}}}{\hat{u}_{\text{uin}}^{\text{ref}}} = -G_{\text{cL-d}}^{\text{out}} G_{\text{vc}} \left(\frac{L_{\text{in}}}{1 - L_{\text{in}}} + 1 \right), \tag{3.163}$$

and

$$G_{\text{crL-qd}}^{\text{tot}} = \frac{\hat{i}_{\text{L1d}}}{\hat{u}_{\text{IL1q}}^{\text{ref}}} = G_{\text{cL-qd}}^{\text{out}} + \frac{L_{\text{in}}}{1 - L_{\text{in}}} \frac{G_{\text{ci-q}}^{\text{out}} G_{\text{cL-d}}^{\text{out}}}{G_{\text{ci-d}}^{\text{out}}}. \tag{3.164}$$

Furthermore, the transfer functions for the q-channel inverter-side inductor current can be expressed by

$$G_{\text{ioL-q}}^{\text{tot}} = \frac{\hat{i}_{\text{L1q}}}{\hat{i}_{\text{in}}} = G_{\text{ioL-q}}^{\text{out}} + \frac{L_{\text{in}}}{1 - L_{\text{in}}} \frac{Z_{\text{in}}^{\text{out}} G_{\text{cL-dq}}^{\text{out}}}{G_{\text{ci-d}}^{\text{out}}}, \tag{3.165}$$

$$G_{\text{crL-dq}}^{\text{tot}} = \frac{\hat{i}_{\text{L1q}}}{\hat{u}_{\text{od}}} = G_{\text{crL-dq}}^{\text{out}} + \frac{L_{\text{in}}}{1 - L_{\text{in}}} \frac{T_{\text{oi-d}}^{\text{out}} G_{\text{cL-dq}}^{\text{out}}}{G_{\text{ci-d}}^{\text{out}}}, \tag{3.166}$$

$$Y_{\text{L-q}}^{\text{tot}} = \frac{\hat{i}_{\text{L1q}}}{\hat{u}_{\text{oq}}} = Y_{\text{L-q}}^{\text{out}} - \frac{L_{\text{in}}}{1 - L_{\text{in}}} \frac{T_{\text{oi-q}}^{\text{out}} G_{\text{cL-dq}}^{\text{out}}}{G_{\text{ci-d}}^{\text{out}}}, \tag{3.167}$$

$$G_{\text{cL-dq}}^{\text{tot}} = \frac{\hat{i}_{\text{L1q}}}{\hat{u}_{\text{uin}}^{\text{ref}}} = -G_{\text{cL-dq}}^{\text{out}} G_{\text{vc}} \left(\frac{L_{\text{in}}}{1 - L_{\text{in}}} + 1 \right), \tag{3.168}$$

and

$$G_{\text{cL-q}}^{\text{tot}} = \frac{\hat{i}_{\text{L1q}}}{\hat{u}_{\text{IL1q}}^{\text{ref}}} = G_{\text{cL-q}}^{\text{out}} + \frac{L_{\text{in}}}{1 - L_{\text{in}}} \frac{G_{\text{ci-q}}^{\text{out}} G_{\text{cL-dq}}^{\text{out}}}{G_{\text{ci-d}}^{\text{out}}}. \tag{3.169}$$

By performing the same procedures, the dynamics of the output currents i_{od} and i_{oq}

can be presented by

$$\hat{i}_{\text{od}} = G_{\text{io-d}}^{\text{tot}} \hat{i}_{\text{in}} - Y_{\text{o-d}}^{\text{tot}} \hat{u}_{\text{od}} + G_{\text{cr-qd}}^{\text{tot}} \hat{u}_{\text{oq}} + G_{\text{co-d}}^{\text{tot}} \hat{u}_{\text{iL1d}}^{\text{ref}} + G_{\text{co-qd}}^{\text{tot}} \hat{u}_{\text{iL1q}}^{\text{ref}}, \tag{3.170}$$

and

$$\hat{i}_{\text{oq}} = G_{\text{io-q}}^{\text{tot}} \hat{i}_{\text{in}} + G_{\text{cr-dq}}^{\text{tot}} \hat{u}_{\text{od}} - Y_{\text{o-q}}^{\text{tot}} \hat{u}_{\text{oq}} + G_{\text{co-dq}}^{\text{tot}} \hat{u}_{\text{iL1d}}^{\text{ref}} + G_{\text{co-q}}^{\text{tot}} \hat{u}_{\text{iL1q}}^{\text{ref}}, \tag{3.171}$$

where the d-channel closed-loop transfer functions are given by

$$G_{\text{io-d}}^{\text{tot}} = \frac{\hat{i}_{\text{od}}}{\hat{i}_{\text{in}}} = G_{\text{io-d}}^{\text{out}} + \frac{L_{\text{in}}}{1 - L_{\text{in}}} \frac{Z_{\text{in}}^{\text{out}} G_{\text{co-d}}^{\text{out}}}{G_{\text{ci-d}}^{\text{out}}}, \tag{3.172}$$

$$Y_{\text{o-d}}^{\text{tot}} = \frac{\hat{i}_{\text{od}}}{\hat{u}_{\text{od}}} = Y_{\text{o-d}}^{\text{out}} - \frac{L_{\text{in}}}{1 - L_{\text{in}}} \frac{T_{\text{oi-d}}^{\text{out}} G_{\text{co-d}}^{\text{out}}}{G_{\text{ci-d}}^{\text{out}}}, \tag{3.173}$$

$$G_{\text{cr-qd}}^{\text{tot}} = \frac{\hat{i}_{\text{od}}}{\hat{u}_{\text{oq}}} = G_{\text{cr-qd}}^{\text{out}} + \frac{L_{\text{in}}}{1 - L_{\text{in}}} \frac{T_{\text{oi-q}}^{\text{out}} G_{\text{co-d}}^{\text{out}}}{G_{\text{ci-d}}^{\text{out}}}, \tag{3.174}$$

$$G_{\text{co-d}}^{\text{tot}} = \frac{\hat{i}_{\text{od}}}{\hat{u}_{\text{uin}}^{\text{ref}}} = -G_{\text{co-d}}^{\text{out}} G_{\text{vc}} \left(\frac{L_{\text{in}}}{1 - L_{\text{in}}} + 1 \right), \tag{3.175}$$

and

$$G_{\text{co-qd}}^{\text{tot}} = \frac{\hat{i}_{\text{od}}}{\hat{u}_{\text{IL1q}}^{\text{ref}}} = G_{\text{co-qd}}^{\text{out}} + \frac{L_{\text{in}}}{1 - L_{\text{in}}} \frac{G_{\text{ci-q}}^{\text{out}} G_{\text{co-d}}^{\text{out}}}{G_{\text{ci-d}}^{\text{out}}}. \tag{3.176}$$

Moreover, the q-channel closed-loop transfer functions are as follows:

$$G_{\text{io-q}}^{\text{tot}} = \frac{\hat{i}_{\text{oq}}}{\hat{i}_{\text{in}}} = G_{\text{io-q}}^{\text{out}} + \frac{L_{\text{in}}}{1 - L_{\text{in}}} \frac{Z_{\text{in}}^{\text{out}} G_{\text{co-dq}}^{\text{out}}}{G_{\text{ci-d}}^{\text{out}}} \tag{3.177}$$

$$G_{\text{cr-dq}}^{\text{tot}} = \frac{\hat{i}_{\text{oq}}}{\hat{u}_{\text{od}}} = G_{\text{cr-dq}}^{\text{out}} + \frac{L_{\text{in}}}{1 - L_{\text{in}}} \frac{T_{\text{oi-d}}^{\text{out}} G_{\text{co-dq}}^{\text{out}}}{G_{\text{ci-d}}^{\text{out}}} \tag{3.178}$$

$$Y_{\text{o-q}}^{\text{tot}} = \frac{\hat{i}_{\text{oq}}}{\hat{u}_{\text{oq}}} = Y_{\text{o-q}}^{\text{out}} - \frac{L_{\text{in}}}{1 - L_{\text{in}}} \frac{T_{\text{oi-q}}^{\text{out}} G_{\text{co-dq}}^{\text{out}}}{G_{\text{ci-d}}^{\text{out}}} \tag{3.179}$$

$$G_{\text{co-dq}}^{\text{tot}} = \frac{\hat{i}_{\text{oq}}}{\hat{u}_{\text{uin}}^{\text{ref}}} = -G_{\text{co-dq}}^{\text{out}} G_{\text{vc}} \left(\frac{L_{\text{in}}}{1 - L_{\text{in}}} + 1 \right) \tag{3.180}$$

$$G_{\text{co-q}}^{\text{tot}} = \frac{\hat{i}_{\text{oq}}}{\hat{u}_{\text{IL1q}}^{\text{ref}}} = G_{\text{co-q}}^{\text{out}} + \frac{L_{\text{in}}}{1 - L_{\text{in}}} \frac{G_{\text{ci-q}}^{\text{out}} G_{\text{co-dq}}^{\text{out}}}{G_{\text{ci-d}}^{\text{out}}} \tag{3.181}$$

The controller design can be done according to $L_{\text{out-d}}$, $L_{\text{out-q}}$ and L_{in}, however, the design is discussed in detail in the next chapter.
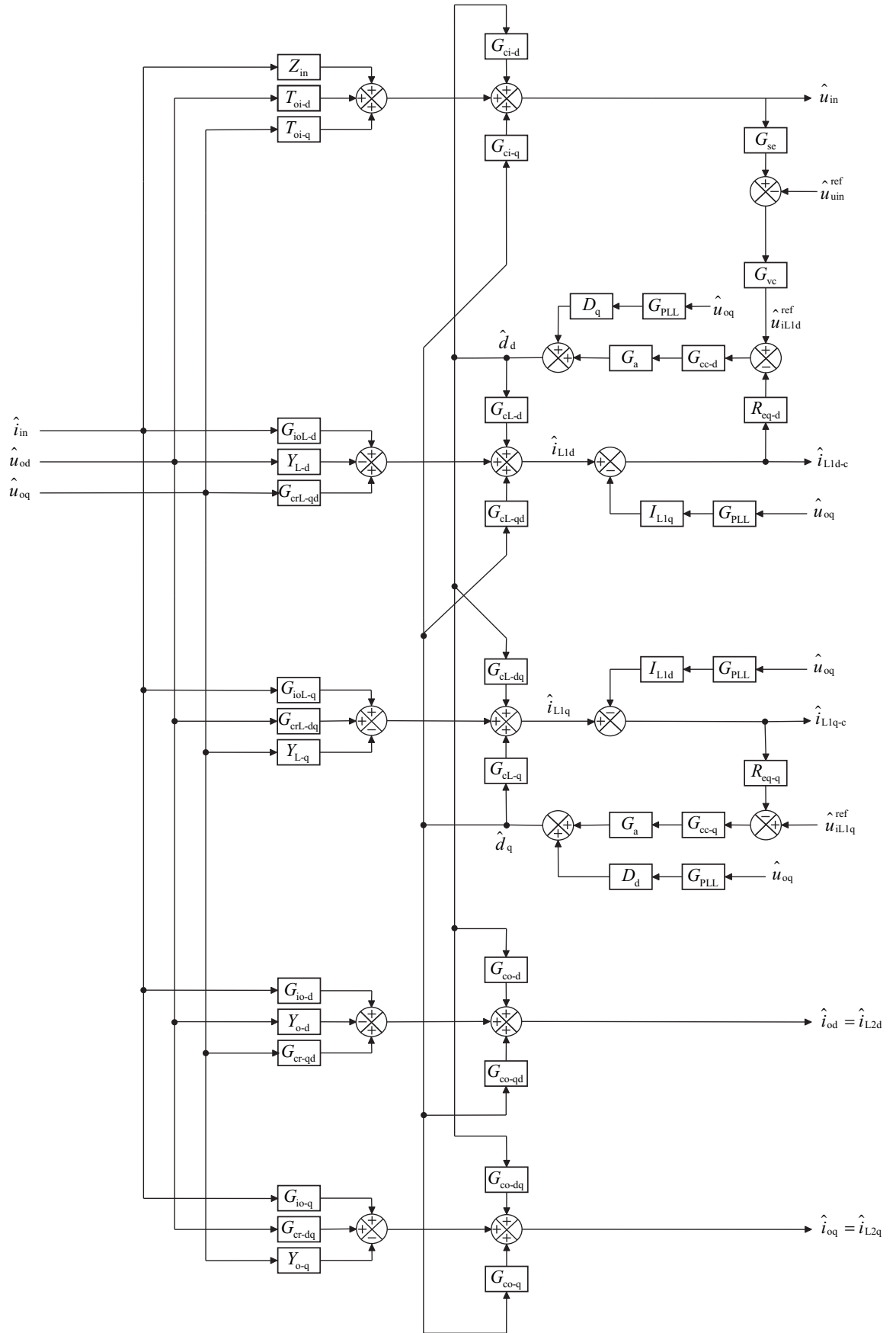
Figure 3.9: Control-block diagram of a grid-connected CF inverter with cascaded input-voltage-output-current control scheme.
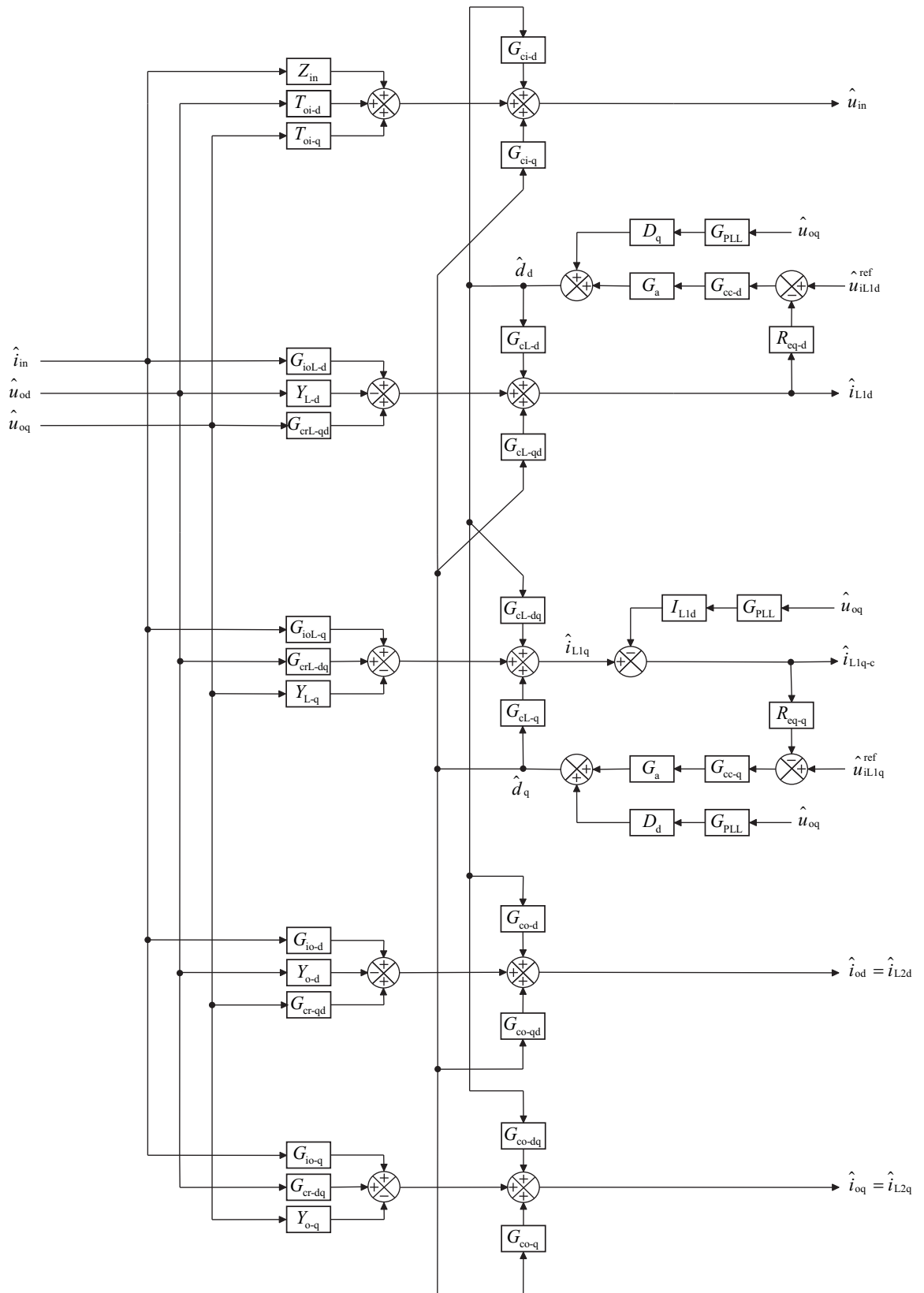
Figure 3.10: Control-block diagram of an output-current-controlled grid-connected CF inverter.
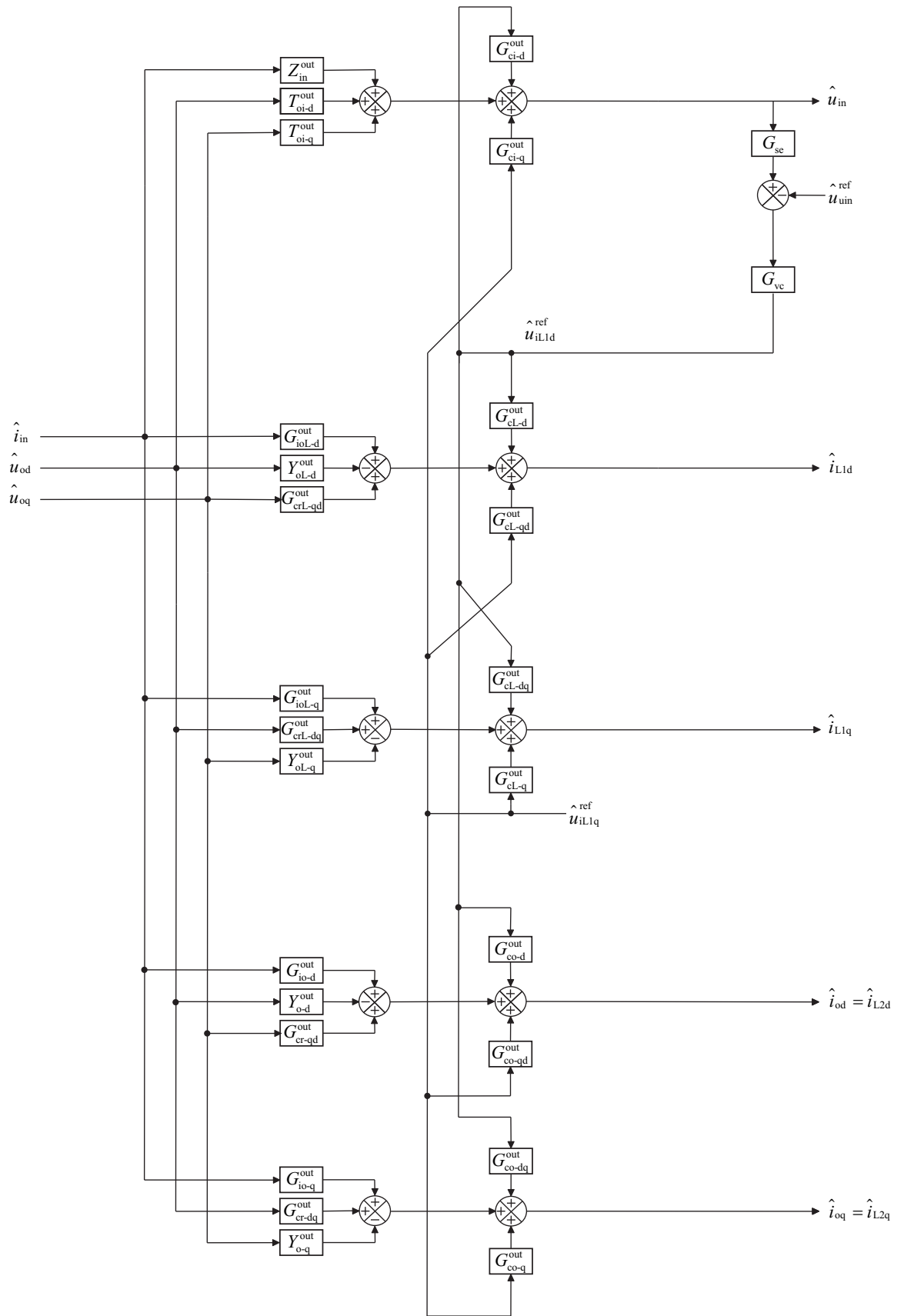
Figure 3.11: Control-block diagram of a input-voltage-controlled CF inverter.

4. MODEL VERIFICATION

This chapter presents the measurements from the scaled-down prototype inverter in order to verify the inverter model derived in Chapter 3. First the chapter presents the open-loop measurements and then the closed-loop measurements.

The prototype LCL-filter was designed for the verification process and the design procedures are presented in detail, for example, in [10,16]. The resonant frequency of the LCL-filter was designed to 6 kHz. In the measurement setup, the grid-simulator provides sinusoidal output-currents, which are generated with 10 kHz switching frequency.

The resonant frequency of the filter can be given according to [16] by

$$f_{\text{res}} = \frac{1}{2\pi} \sqrt{\frac{L_1 + L_2}{L_1 L_2 C_{\text{d}}}}, \tag{4.1}$$

where L_1 is the inverter-side inductance, L_2 is the grid-side inductance and C_{d} is the output filter capacitance. The inductance and the capacitance values were chosen according to the literature examples found in [10]. Table 4.1 presents the selected values for the LCL-filter. For passive damping, a power resistor was also included to avoid high resonant peaking as was discussed earlier. Parasitic resistances of the inductors were verified from the actual filter to ensure compliance to the simulations.

Table 4.1: LCL-filter passive component values.

Component	Value
L_1	365 μH
$r_{\text{L1-ESR}}$	40 mΩ
L_2	240 μH
$r_{\text{L1-ESR}}$	30 mΩ
C_{d}	4,7 μF
$r_{\text{C-ESR}}$	10 mΩ
R_{d}	2 Ω

The correct value for the damping resistor R_{d} can be derived from the impedance of the filter capacitor at the resonant frequency. Usually the damping value is one third of the corresponding impedance value [10].

Table 4.2 presents used operating point and power-stage component values.

Table 4.2: Operating point and power-stage component values.

Parameter	Value
$I_{\text{in-MPP}}$	1,9 A
$U_{\text{in-MPP}}$	31,7 V
$I_{\text{in-CCR}}$	2,1 A
$U_{\text{in-CCR}}$	25 V
$I_{\text{in-CVR}}$	1,5 A
$U_{\text{in-CVR}}$	35 V
$U_{\text{od-ref}}$	6,6 V
$U_{\text{oq-ref}}$	0 V
$r_{\text{pv-MPP}}$	$\frac{U_{\text{in-MPP}}}{I_{\text{in-MPP}}}$
$r_{\text{pv-CCR}}$	155,8 Ω
$r_{\text{pv-CVR}}$	3,4 Ω
C_{in}	1100 μF
r_{Cin}	10 mΩ
r_{sw}	100 mΩ
f_{s}	50 Hz
f_{sw}	75 kHz

The value of the input capacitor is dependent on the RHP zero frequency found in source-affected control-to-output-current transfer function and correct design is essential for stable operation of the inverter. As presented by Puukko in [23], the RHP zero frequency can be expressed by

$$\omega_{\text{RHP,max}} = \frac{I_{\text{in,max}}}{U_{\text{in,min}}C_{\text{in}}}. \tag{4.2}$$

Moreover, the minimum value for the input capacitor can be presented by

$$C_{\text{in,min}} = \frac{k_{\text{RHP}}k_{\text{i}}}{k_{\text{grid}}} \frac{I_{\text{sc}}}{U_{\text{in-min}}\omega_{\text{grid}}}, \tag{4.3}$$

where an inequality $k_{\text{grid}}\omega_{\text{grid}} = \omega_{\text{v-loop}} \geq k_{\text{RHP}}\omega_{\text{RHP}}$ must be satisfied [23]. The input-voltage control-loop bandwidth $\omega_{\text{v-loop}}$ should be within the range of 10 Hz - 50 Hz to avoid DC-link voltage ripple to affect the grid currents. Usually a safety factor $k_{\text{RHP}} = 2$ is chosen according to [35] and a safety factor for maximum input current can be chosen as $k_{\text{i}} = 1,5$, which presents the relation in $I_{\text{in,max}} = k_{\text{i}}I_{\text{sc}}$ [23]. The RHP zero has to be taken into account when designing a control system, which

is discussed in Section 4.2.

4.1 Open-loop verifications

This presents the measurement results to validate the derived inverter model at open loop. Important transfer function to be validated is the control-to-inductor-current transfer function $G_{\text{cL-d}}^{\text{HS}}$ as it change significantly when the operating point of the PV generator varies. Open-loop verifications were carried out using measurement setup depicted in Fig. 4.2. All measurements were processed and the control system was implemented by means of the digital signal processor eZdsp F28335.

The source (PV generator) was a modular solar-array simulator E4360 manufactured by Agilent. Real output impedances of the SAS were measured in both CVR and CCR to be used in the analytical predictions. Obtained impedances are presented in Fig. 4.1.
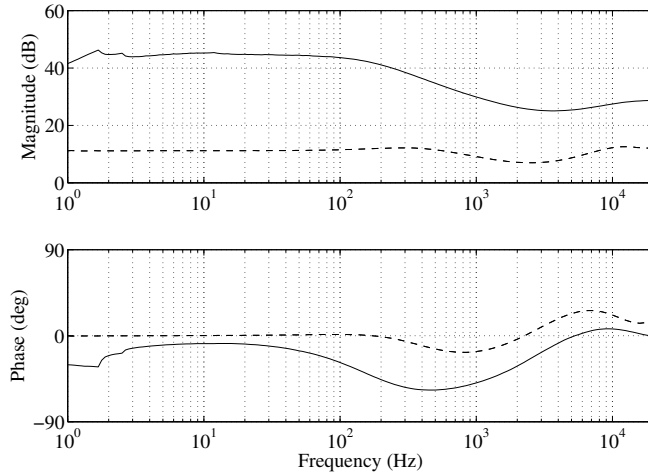
Figure 4.1: SAS output impedances in CCR (solid line) and in CVR (dashed line).

ELGAR SW 5250A voltage source was used as the three-phase grid voltage emulator. In practice, ELGAR cannot operate as a power sink, therefore, resistors (i.e., r_{load} in Fig. 4.2) were connected in parallel with ELGAR to consume the power produced by the inverter. At open loop, the grid emulator (i.e., the AC voltage source ELGAR) was synchronized with the DSP reference frame to provide as ideal synchronization with the grid as possible, because the effect of grid-synchronization was not included into the open-loop model.

At open loop, the inverter switches are controlled by constant steady-state duty ratios depending on the operating point, which were derived in Chapter 3. Measured and processed synchronous reference frame variables were transferred to the

frequency response analyzer by the DSP-board. It is also noteworthy that the injection from the frequency responce analyzer was processed in the DSP in order to add injection for the frequency response measurements. All the transfer functions were measured with frequency response analyzer Venable Model 3120 denoted in Fig 4.2 as FRA.
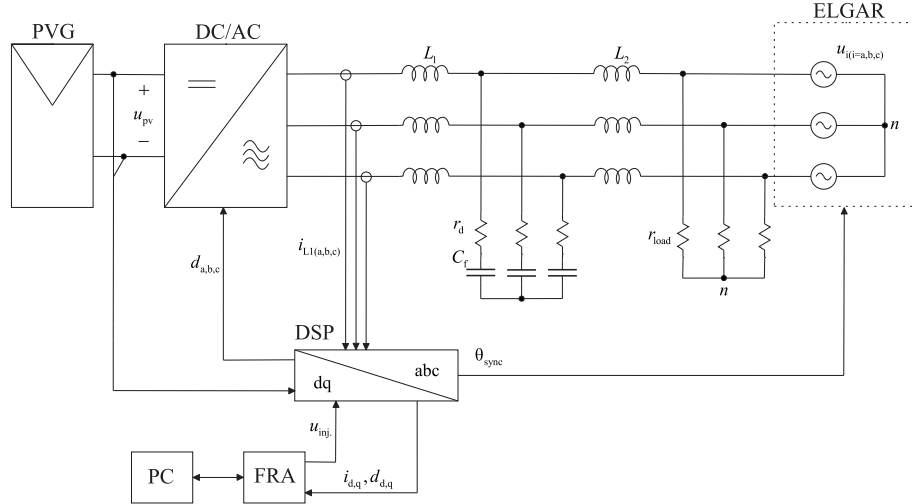
Figure 4.2: Open-loop measurement setup.

It should be noted that the delay effect caused by the digital control is included to the predictions as it decreases the phase in the measurements. First-order Padé approximation was used for the delay as given by

$$G_{\text{delay}} = \frac{1 - T_{\text{s}}s}{1 + T_{\text{s}}s}, \tag{4.4}$$

where T_{s} is the switching period.

As presented in [2] and [36], the selection of the input source alters the inverter behavior significantly. The inverter has to operate reliably at all operating points. However, a PV generator induces design constaints which have to be considered carefully. The effect of the changing operating point can be demonstrated by investigating the source-affected control-to-inductor-current transfer function $G_{\text{cL-d}}^{\text{HS}}$ presented in (4.5), which incorporates a RHP zero if the operating point is in the CCR.

$$G_{\text{cL-d}}^{\text{HS}} = \frac{1 + Y_{\text{s}}Z_{\text{inL-d-inf}}^{\text{H}}}{1 + Y_{\text{s}}Z_{\text{in}}^{\text{H}}}G_{\text{cL-d}}^{\text{H}}, \tag{4.5}$$

Transfer function in (4.5) is too complex to extract the frequency of the RHP zero

in a symbolic form even without parasitic elements. Therefore, the appearance of
the RHP zero is demonstrated by means of predicted transfer functions in Fig. 4.3.

As can be seen in Fig. 4.3, the operating point dependent zero is located in the
RHP when the inverter is operating in CCR. This affects significantly the control-
to-inductor-current transfer function by flipping the phase by 180 degrees, when a
transition from CVR to CCR (or *vice versa*) occurs.
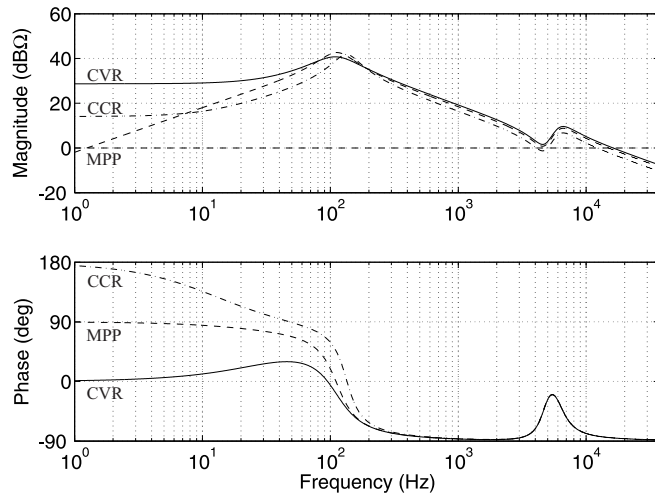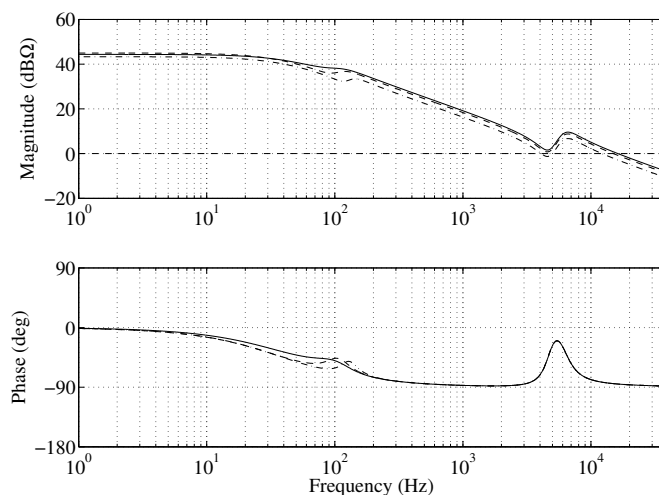

Figure 4.3: Predicted d-channel control-to-inductor-current transfer function $G_{\text{cL-d}}^{\text{HS}}$ at
MPP (dashed line), CCR (dash-dotted line) and CVR (solid line).

The RHP zero, induced by the control-to-inductor-current transfer function $G_{\text{cL-d}}^{\text{HS}}$,
has to be taken into account very carefully when designing the control system as it
may lead to system instability if the control system is designed poorly. However, the
inverter may be designed to be stable in both CCR and CVR due to the cascaded
control scheme, which is discussed in the next section. Measured control-to-inductor-
current $G_{\text{cL-d}}^{\text{HS}}$ transfer functions are presented in Fig. 4.4 in both CCR and CVR.
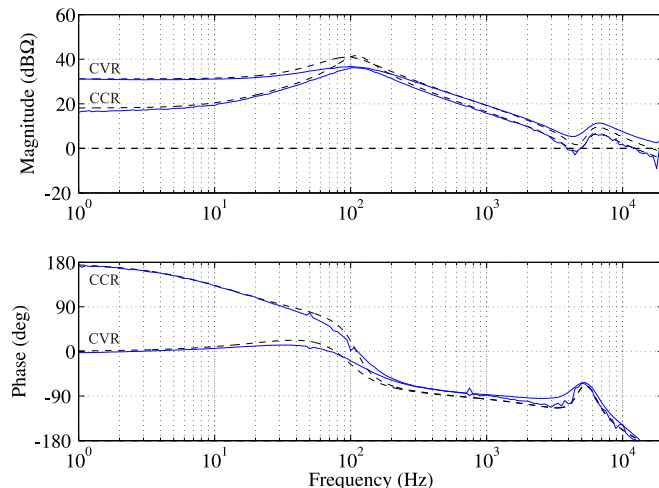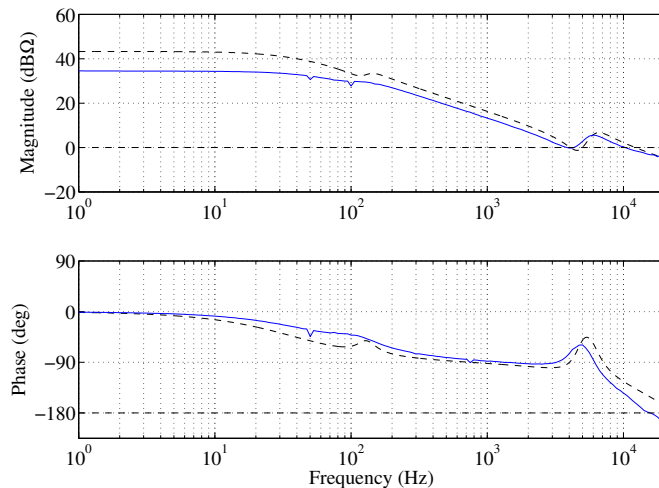
Figure 4.4: Measured (solid line) and predicted (dash-dotted line) d-channel control-to-inductor-current transfer functions $G_{\text{cL-d}}^{\text{HS}}$ in CCR and CVR.
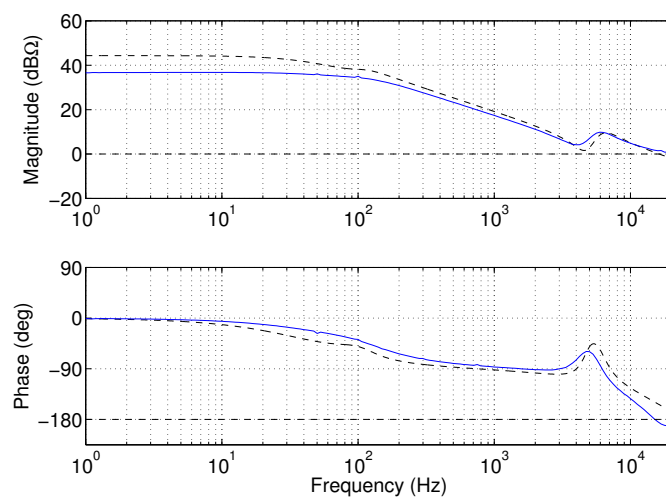
The q-channel control-to-inductor-current transfer function $G_{\text{cL-q}}^{\text{HS}}$ is not affected by the change of the operating point. This is due to the fact that the transfer function does not incorporate an RHP zero, when the operating point changes from CVR to CCR. Predicted bode-plot of the $G_{\text{cL-q}}^{\text{HS}}$ is presented in all operating points in Fig. 4.5.

Figure 4.5: Predicted q-channel control-to-inductor-current transfer function $G_{\text{cL-q}}^{\text{HS}}$ at MPP (dashed line), CCR (dash-dotted line) and CVR (solid line).

Measured q-channel control-to-inductor-current transfer functions are presented in both CCR and CVR in Figs. 4.6 and 4.7

Figure 4.6: Measured (solid line) and predicted (dash-dotted line) control-to-inductor-current transfer function $G_{\text{cL-q}}^{\text{HS}}$ in CCR.

Figure 4.7: Measured (solid line) and predicted (dash-dotted line) control-to-inductor-current transfer function $G_{\text{cL-q}}^{\text{HS}}$ in CVR.

According to Figs. 4.4 - 4.7, the predictions match well especially for the d-channel-related transfer functions. It can be seen that the prototype inverter has much higher damping values in the first resonant circuit formed by the input capacitor and the inverter-side inductor. Therefore, the resonant peaking at around 100 Hz is highly damped compared to the predictions.

As can be seen from Figs. 4.6 and 4.7, there is inaccuracy compared to the predictions. This may be caused by a little synchronization error between the DSP and the grid simulator ELGAR. Also the q-channel duty-ratio D_{q} is relatively small,

which makes the measurement setup more sensitive to distortions. Moreover, at open loop the system is affected greatly by all the unidealities, which could not be predicted accurately enough. This leads to mismatches between the predictions and measurements.

The control-to-input-voltage transfer function presents the relation between duty ratio and the input voltage and is not affected by the change of operating point, because the control-to-input transfer function does not incorporate any operating point-dependent zeros. This is visible in Figs. 4.8 and 4.9 where the $G_{\text{ci-d}}^{\text{HS}}$ is presented in both CCR and CVR, respectively.
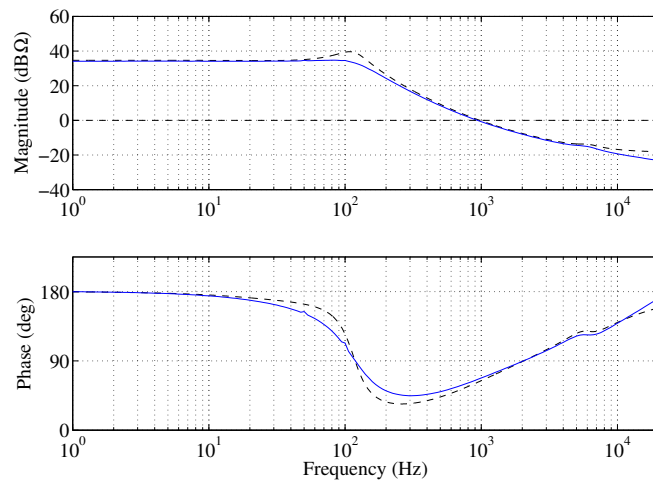
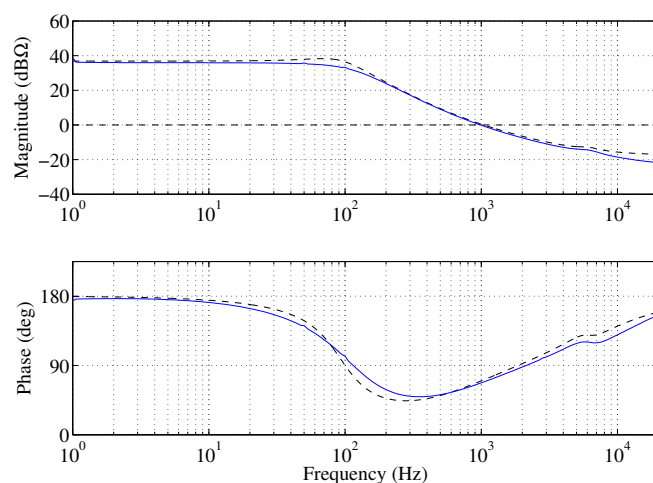**Figure 4.8:** Measured (solid line) and predicted (dash-dotted line) control-to-input-voltage transfer function $G_{\text{ci-d}}^{\text{HS}}$ in CCR.

Figure 4.9: Measured (solid line) and predicted (dash-dotted line) control-to-input-voltage transfer function $G_{\text{ci-d}}^{\text{HS}}$ in CVR.

As can be seen, the operating point does not affect the frequency responses of $G_{\text{ci-d}}^{\text{HS}}$ significantly at all as they are practically identical. However, it is noteworthy that the phase of frequency responses starts at 180 degrees.

Input impedance of the inverter is important when analyzing stability of the source and inverter input interface. Verification of the input impedances is presented in Figs. 4.10 and 4.11.
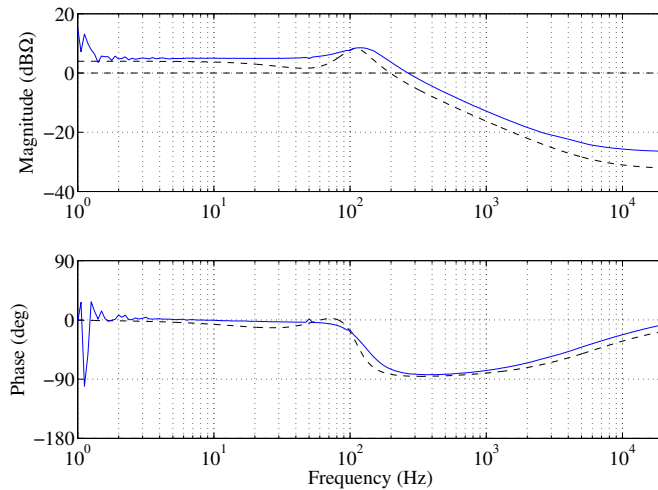
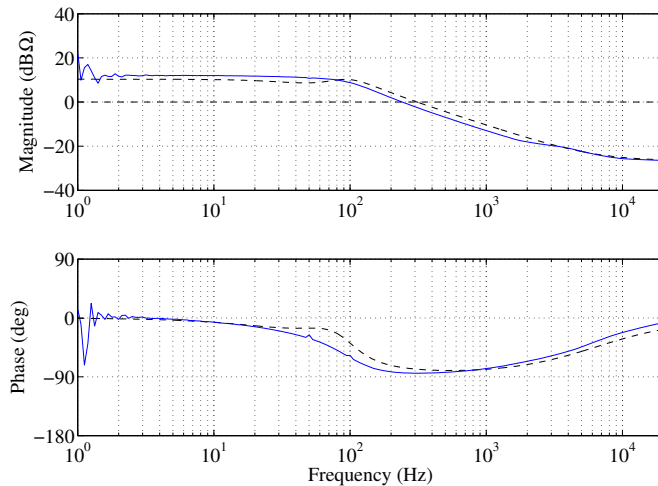**Figure 4.10:** Measured (solid line) and predicted (dash-dotted line) input impedance $Z_{\text{in}}^{\text{HS}}$ in CCR.

Figure 4.11: Measured (solid line) and predicted (dash-dotted line) input impedance $Z_{\text{in}}^{\text{HS}}$ in CVR.

As discussed earlier, the resonant peaking around the frequency of 100 Hz is greatly damped in the measured frequency responses. This implies that the system

has higher parasitic resistances, which are not estimated properly. However, the input impedance behaves correctly as it resembles a resistor-like behavior at low frequencies and a capacitive-like behavior at higher frequencies.

4.2 Closed-loop verifications

Closed-loop control system design begins by designing proper controllers. According to control engineering principles, the inner loop of the cascaded control scheme has to be designed first. As presented in Section 3.6, the inductor-current loop-gain is given by

$$L_{\text{out-d}} = R_{\text{eq-d}}G_{\text{cc-d}}G_{\text{a}}G_{\text{cL-d}}^{\text{HS}}, \tag{4.6}$$

where the current controller $G_{\text{cc-d}}$ is a conventional PI-type controller, which can be given by

$$G_{\text{cc-d}} = \frac{K_{\text{cc-d}}(s + \omega_{\text{z}})}{s(s + \omega_{\text{p}})}. \tag{4.7}$$

As discussed earlier, the source-affected control-to-inductor-current transfer function $G_{\text{cL-d}}^{\text{HS}}$ incorporates an RHP zero when the operating point of the PV generator is in CCR. According to the control engineering principles, the control bandwidth has to be limited below the RHP zero frequency for stable operation. However, as discussed earlier, highest frequency for a RHP zero can be given by (4.2), which results in too low bandwidth for grid-connected inverter, and therefore, poor power quality. This implies that the inverter would be stable only in the CVR, when only inductor-current control is active, because high current-control bandwidth is essential in grid-connected applications. Hence, the output-current controller is designed in the CVR to obtain high enough bandwidth and to ensure stable operation as the input-voltage-loop stabilizes the inductor-current-loop when inverter is operating in the CCR.

Closed-loop measurements were carried out with a setup depicted in Fig. 4.12. The setup was used to measure the output impedances as they are important for the future research. In Fig. 4.12, the grid emulator ELGAR was synchronized with the DSP 2, which also provided injection to the phase voltages in order to measure the frequency response. DSP 2 also performed necessary measurements from the grid-side phase voltages and currents. The purpose of DSP 1 was to perform grid-synchronization for the control system, because the PLL effect is visible only if the control system operates in different reference frame compared to the real grid
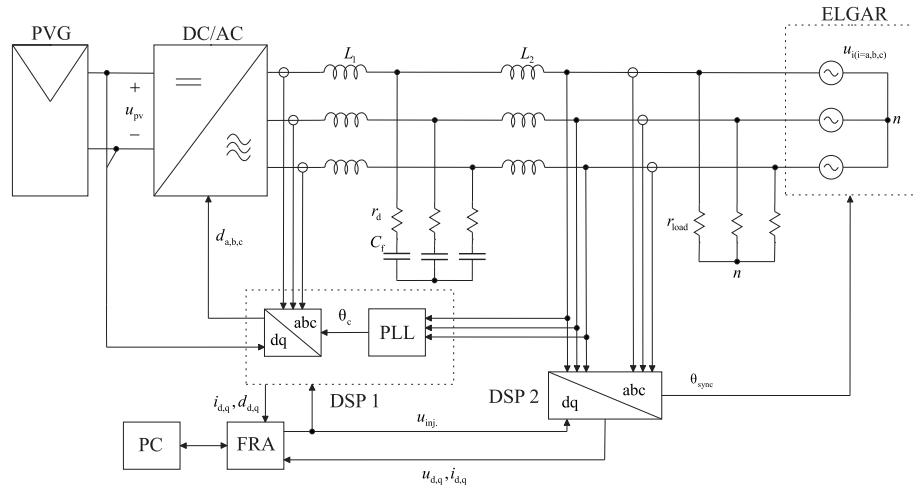
as discussed in Section 3.6.1.

Figure 4.12: Closed-loop measurement setup.

According to (4.6), the inductor-current loop-gain can be presented as in Fig. 4.13, where $K_{\text{cc-d}} = 141$, $\omega_z = 2\pi300$ Hz and $\omega_p = 2\pi37,5$ kHz. High pole frequency was desired to attenuate high frequency switching ripple.
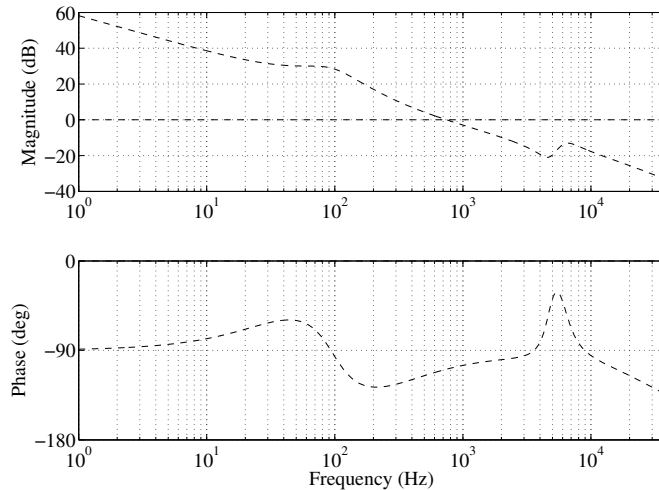

Figure 4.13: Output-current loop-gain $L_{\text{out-d}}$ in CCR.

As can be seen in Fig. 4.13, the crossover frequency of 800 Hz and phase margin of 72 degrees were obtained. The crossover frequency can be extended up to 2 kHz but was noticed to cause extra noise which disturbed the measurements. The q-channel loop-gain dynamics resemble the d-channel dynamics, and therefore, the same tuning parameters were used for the q-channel current control.

The input-voltage controller was designed in the CCR according to (C.5) found in App. C. It is worth noting that the source-affected control-to-inductor-current transfer function $G_{\text{cL-d}}^{\text{HS}}$ introduces an RHP pole to the control-to-input-voltage transfer function $G_{\text{ci-d}}^{\text{out}}$ as given in (C.5). This implies that the input-voltage loop given by

$$L_{\text{in}} = G_{\text{se}}G_{\text{vc}}G_{\text{ci-d}}^{\text{out}} \approx G_{\text{se}}G_{\text{vc}}G_{\text{ci-d}}^{\text{H}} \frac{1}{G_{\text{cL-d}}^{\text{H}}R_{\text{eq-d}}} \frac{L_{\text{out-d}}}{1 + L_{\text{out-d}}} \qquad (4.8)$$

incorporates an RHP pole if the operating point is in the CCR. According to the control engineering principles, the controller bandwidth has to be higher than the RHP pole frequency, which in this case is around 20 Hz. Input-voltage loop-gain in the CCR is depicted in Fig. 4.14, where $K_{\text{vc}} = 3,2$, $\omega_{\text{z}} = 2\pi 1$ Hz and $\omega_{\text{p}} = 2\pi 500$ Hz. The controller pole was placed at relatively low frequency to attenuate the 300 Hz ripple voltage present in the DC-link voltage of three-phase grid-connected inverters. For comparison, the input-voltage loop-gain is also presented in the CVR in Fig. 4.15, where the RHP pole is not present.
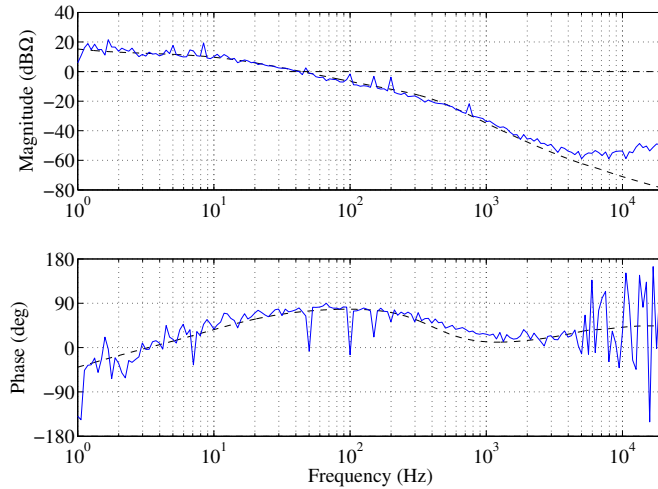

Figure 4.14: Measured (solid line) and predicted (dashed line) input-voltage loop-gain L_{in} in CCR.
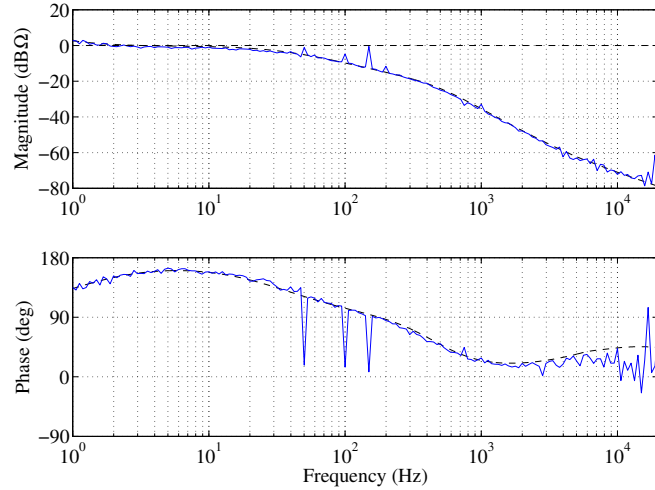
Figure 4.15: Measured (solid line) and predicted (dashed line) input-voltage loop-gain L_{in} in CVR.

As can be seen from Fig. 4.14, an attenuation of around 20 dB was achieved for the 100 Hz grid ripple. With the chosen gain value, crossover frequency of 40 Hz with 70 degrees phase margin was obtained.

As the stability analysis of the grid-interface is important, output impedances of the inverter were measured. Stability can be evaluated if the output impedance of the inverter is measured or predicted accurately. However, in practice, the impedance measurements from a time-varying system can be difficult. Therefore, accurate predictions are valuable in order to analyze the stability of the inverter. Measured and predicted output impedances presented in (C.21) and (C.28) are depicted in Figs. 4.16 - 4.19 in both CCR and CVR.
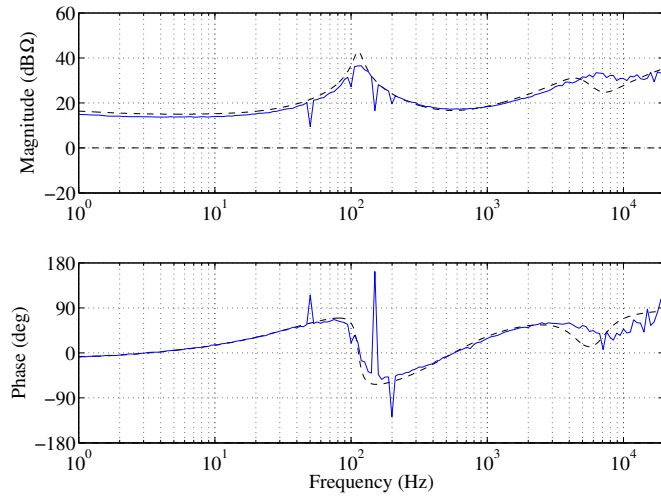
Figure 4.16: Measured (solid line) and predicted (dashed line) d-channel output impedance in CCR.
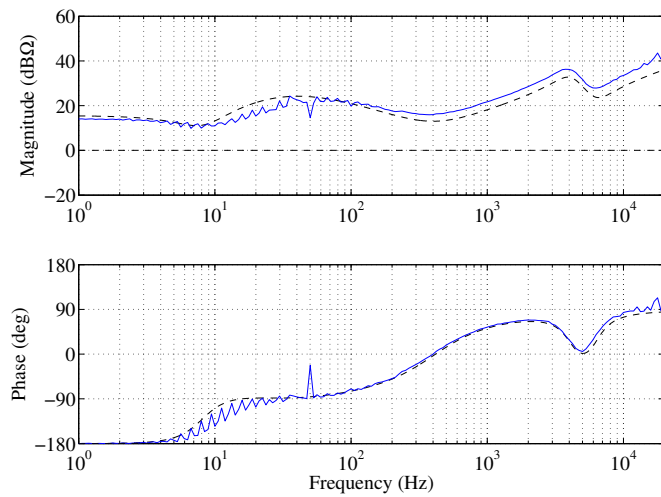
Figure 4.17: Measured (solid line) and predicted (dashed line) q-channel output impedance in CCR.
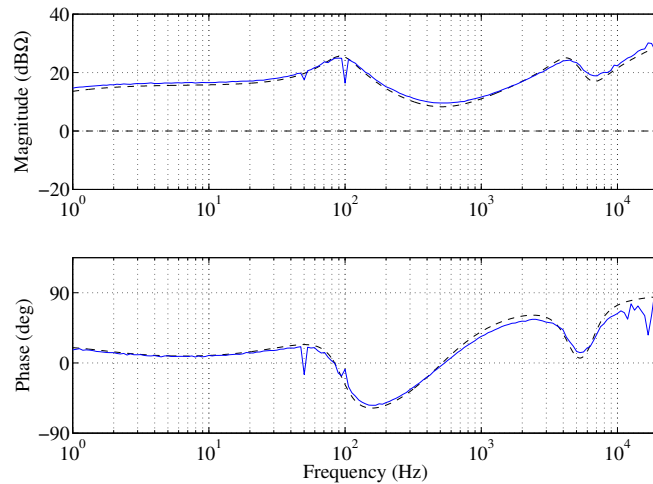
Figure 4.18: Measured (solid line) and predicted (dashed line) d-channel output impedance in CVR.
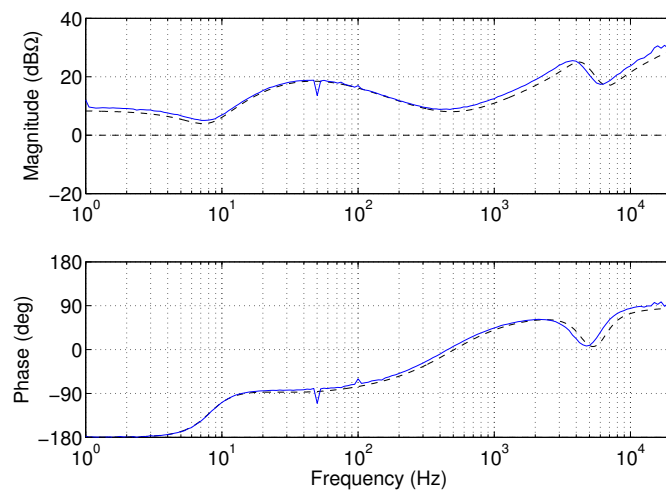
Figure 4.19: Measured (solid line) and predicted (dashed line) q-channel output impedance in CVR.

As can be seen from Fig. 4.16, the d-channel output impedance resembles the impedance of a passive circuit, because the phase is always in the range of -90 to 90 degrees. Actually, the d-channel impedance behaves like a pure resistor at lower frequencies, which induces beneficial damping to the network. As presented in Section 3.6.1, the q-channel output impedance has a negative-resistor-like behavior below the PLL bandwidth. This may cause harmonic resonance or instability when inverter is connected to a weak grid as presented for example in [28]. However, stability analysis of impedance interactions is not included in this thesis.

As can be deduced from the open-loop and closed-loop measurements, the closed-loop predictions match the measurements with good accuracy. Moreover, the resonant behavior of the LCL-filter is evident in the kilohertz range, and is correctly predicted by the model.

5. CONCLUSIONS

Photovoltaic generator is a unique power source with both constant-current and constant-voltage source characteristics, which are dependent on the operating point of the generator. As discussed in Chapter 2, in constant-current region (CCR) the source acts as a constant-current source with high output impedance. Moreover, in constant-voltage region the source acts as a voltage source with low output impedance. Due to this phenomenon, the PV generator introduces an operating point-dependent RHP zero to the control-to-inductor-current transfer function when operating point is in the CCR. This leads to a phase flip of 180 degrees, which causes major control system design constraints.

An LCL-type filter is gaining popularity in grid-current filtering because of its good filtering performance compared to a simple L-type filter. However, the use of LCL-filter causes also design issues as the LCL-filter has an inherent resonance at a spesific frequency, which is dependent on the values of the filtering components. This resonant behavior has to be taken into account by damping it with either passive or active methods. Passive damping is implemented by adding a series resistor to the grid-side filter-capacitor, whereas active damping is performed using different control methods.

In addition, the control topology is different compared to an ordinary L-filter since the current measurements are taken from the inverter-side inductors and voltage measurements from the grid side. This causes the inverter to produce a small amount of reactive power, because the currents of the boost-inductors are synchronized with the grid-voltages. However, if the current measurements are taken from the grid-side, it may introduce a safety issue, where there is no control in the boost-inductor-currents.

Due to the LCL-filter, small-signal modeling of the inverter becomes more complicated compared to an inverter with just an L-type filter since the LCL-type filter introduces new state variables to the model (i.e., the capacitor voltages $u_{c(d,q)}$ and boost-inductor currents $i_{L1(d,q)}$). However, modeling can be performed and the system steady-state values calculated.

As customary in three-phase grid-connected applications, a cascaded control-scheme was used. In cascaded control scheme, the control system consists of two control loops connected in cascade. In this thesis, the input-voltage and the inverter-

side inductor-currents are the controllable variables. Thus, in the cascaded control system, the outer loop controls the input voltage, which generates a reference for the inner loop controlling the inverter-side inductor current. According to control engineering principles, the inner loop must have faster dynamics compared to the outer loop, which also applies the control system presented in this thesis.

Some interesting observations may be drawn from the thesis. It is clear that even though the LCL-filter leads to a very complex small-signal model, the inverter can be modeled very accurately without neglecting any parasitic elements or cross-coupling effects. As discussed in Section 3.6.1, the grid-synchronization causes a negative-resistor-like behavior in the q-channel output impedance. This may lead to instability if the input impedance of interfaced load matches the output impedance of the inverter with 180 degree phase difference. Therefore, it would be valuable to study if the q-channel output impedance could be somehow passivated.

The effect of the LCL-filter on the control system of the inverter was minimal. The resonant frequency of the LCL-filter was designed to be around 6 kHz. Moreover, the resonant peaking may be taken into account in the design and it has negligible effect on the inverter dynamics if the control loops are designed properly. In this thesis, the current control loop has a bandwidth below the resonant frequency. Thus, the resonant peaking does not affect the current control loop. Bandwidth over the resonant frequency was not realisable due to inadequate measurement devices. However, this may be done with proper equipment if higher bandwidth is needed as the filter does not present any major constraints to it.

As can be deduced from the thesis and measurements, the inverter model derived was accurate. Thus, it can be used in further research such as in stability analysis. Stability of an interconnected photovoltaic power system should be guaranteed since the grid has always finite input impedance and may exhibit inductive or even resonant behavior at the point of common coupling (PCC). Stability can be evaluated if the shape of the inverter input and output impedances are measured or predicted accurately. In practice, measuring the impedances from a time-varying system, such as a PV inverter is not straight-forward but can be performed using proper measurement equipment. However, with accurate small-signal model, only the grid impedance has to be measured or estimated.

Moreover, at open loop the measurements included more gain and phase errors due to parasitic mismatches between the analytical model and the inverter prototype. However, they were accurate enough to present the behavior of the inverter at open loop. At closed loop, the good match between predictions and measured responses was evident.

BIBLIOGRAPHY

[1] B. K. Bose, "Energy, environmental pollution, and the impact of power electronics," *IEEE Ind. Electron. Mag.*, pp. 6–17, Mar. 2010.

[2] L. Nousiainen, J. Puukko, A. Mäki, T. Messo, J. Huusari, J. Jokipii, J. Viinamäki, D. T. Lobera, S. Valkealahti, and T. Suntio, "Photovoltaic generator as an input source for power electronic converters," *IEEE Trans. Power Electron.*, vol. 28, no. 6, pp. 3028–3038, Jun. 2013.

[3] X. Zhang, J. W. Spencer, and J. M. Guerrero, "Small-signal modeling of digitally controlled grid-connected inverters with LCL filters," *IEEE Trans. Ind. Electron.*, vol. 60, no. 9, pp. 3752–3765, Sep. 2013.

[4] B. Hoff, W. Sulkowski, and P. Sharma, "Cascaded model predictive control of voltage source inverter with active damped LCL filter," *2013 IEEE Energy Conversion Congress and Exposition*, pp. 4119–4125, Sep. 2013.

[5] K. H. Masoud and G. Ledwich, "Dynamics of grid connected PV inverters," *2010 IEEE International Energy Conference*, pp. 484–489, Dec. 2010.

[6] X. Bao, F. Zhuo, Y. Tian, and P. Tan, "Simplified feedback linearization control of three-phase photovoltaic inverter with an LCL filter," *IEEE Trans. Power Electron.*, vol. 28, no. 6, pp. 2739–2752, Jun. 2013.

[7] Y. Jia, J. Zhao, and X. Fu, "Direct grid current control of LCL-filtered grid-connected inverter mitigating grid voltage disturbance," *IEEE Trans. Power Electron.*, vol. 29, no. 3, pp. 1532–1541, Mar. 2014.

[8] Y. Li, S. Jiang, and J. G. Cintron-rivera, "Modeling and control of quasi-Z-source inverter for distributed generation applications," *IEEE Trans. Ind. Electron.*, vol. 60, no. 4, pp. 1532–1541, Apr. 2013.

[9] P. P. Dash and M. Kazerani, "Dynamic modeling and performance analysis of a grid-connected current-source inverter-based photovoltaic system," *IEEE Trans. Sustain. Energy*, vol. 2, no. 4, pp. 443–450, Oct. 2011.

[10] M. Liserre, F. Blaabjerg, and S. Hansen, "Design and control of an LCL-filter-based three-phase active rectifier," *IEEE Trans. Ind. Appl.*, vol. 41, no. 5, pp. 1281–1291, Sep. 2005.

[11] B. Ren, X. Sun, S. An, X. Cao, and Q. Zhang, "Analysis and design of an LCL filter for the three-level grid-connected inverter," *IEEE 7th International Power Electronics and Motion Control Conference*, pp. 2023–2027, Jun. 2012.

[12] C. Bao, X. Ruan, X. Wang, and W. Li, "Step-by-step controller design for LCL-type grid-connected inverter with capacitorcurrent-feedback active-damping," *IEEE Trans. Power Electron.*, vol. 29, no. 3, pp. 1239–1253, Mar. 2014.

[13] X. Wei, L. Xiao, Z. Yao, and C. Gong, "Design of LCL filter for wind power inverter," *2010 World Non-Grid-Connected Wind Power and Energy Conference*, pp. 1–6, Nov. 2010.

[14] J. M. Sosa and P. R. Mart, "Model based controller for an LCL coupling filter for transformerless grid connected inverters in PV applications," *39th Annual Conference of the IEEE Industrial Electronics Society, IECON 2013*, pp. 1723–1728, Nov. 2013.

[15] Y. Chen and F. Liu, "Design and control for three-phase grid-connected photovoltaic inverter with LCL filter," *IEEE Circuits and Systems International Conference on Testing and Diagnosis*, pp. 1–4, Apr. 2009.

[16] M. Liserre, R. Teodorescu, and F. Blaabjerg, "Stability of photovoltaic and wind turbine grid-connected inverters for a large set of grid impedance values," *IEEE Trans. Power Electron.*, vol. 21, no. 1, pp. 263–272, Jan. 2006.

[17] V. Yaramasu and B. Wu, "Predictive power control of grid-connected four-level inverters in stationary reference frame," *International Conference on Circuits, Power and Computing Technologies (ICCPCT)*, pp. 636–641, Mar. 2013.

[18] M. Shahparasti, M. Mohamadian, and A. Yazdian, "Derivation of a stationary-frame single-loop controller for three-phase standalone inverter supplying nonlinear loads," *IEEE Trans. Power Electron.*, vol. 29, no. 9, pp. 5063–5071, Sep. 2014.

[19] D. N. Zmood, S. Member, and D. G. Holmes, "Stationary frame current fegulation of PWM inverters with zero steady-state error," *IEEE Trans. Power Electron.*, vol. 18, no. 3, pp. 814–822, May 2003.

[20] J. C. Vasquez, J. M. Guerrero, M. Savaghebi, J. Eloy-Garcia, and R. Teodorescu, "Modeling, analysis and design of parallel three-phase voltage source inverters," *IEEE Trans. Power Electron.*, vol. 60, no. 4, pp. 1271–1280, Apr. 2013.

[21] M. Castilla, J. Miret, J. Matas, L. G. D. Vicuña, and J. M. Guerrero, "Linear current control scheme with series resonant harmonic compensator for single-phase grid-connected photovoltaic inverters," *IEEE Trans. Ind. Electron.*, vol. 55, no. 7, pp. 2724–2733, Jul. 2008.

[22] E. Figueres, A. Member, G. Garcerá, J. Sandia, F. González-espín, S. Member, J. C. Rubio, and A. A. Model, "Sensitivity study of the dynamics of three-phase photovoltaic inverters with an LCL grid filter," *IEEE Trans. Ind. Electron.*, vol. 56, no. 3, pp. 706–717, Mar. 2009.

[23] J. Puukko, "*Issues on Dynamic Modeling and Design of Grid- Connected Three-Phase VSIs in Photovoltaic Applications*," Dissertation, Publication 1087, Tampere University of Technology, Tampere, 2012.

[24] M. Liserre, S. Member, F. Blaabjerg, and R. Teodorescu, "Grid impedance estimation via excitation of LCL-filter resonance," *IEEE Trans. Ind. Appl.*, vol. 43, no. 5, pp. 1401–1407, Sep. 2007.

[25] M. Cespedes and J. Sun, "Adaptive control of grid-connected inverters based on online grid impedance measurements," *IEEE Trans. Sustain. Energy*, vol. 5, no. 2, pp. 516–523, Apr. 2014.

[26] M. J.-B. Ghorbal, W. Ghzaiel, I. Slama-Belkhodja, and J. M. Guerrero, "Online detection and estimation of grid impedance variation for distributed power generation," *16th IEEE Mediterranean Electrotechnical Conference*, pp. 555–560, Mar. 2012.

[27] J. Sun, "Impedance-based stability criterion for grid-connected inverters," *IEEE Trans. Power Electron.*, vol. 26, no. 11, pp. 3075–3078, Nov. 2011.

[28] T. Messo, J. Jokipii, A. Aapro, and T. Suntio, "Time and frequency-domain evidence on power quality issues caused by grid-connected three-phase photovoltaic inverters," *IEEE 2014 16th European Conference on Power Electronics and Applications (EPE'14-ECCE Europe)*, pp. 1–9, Aug. 2014.

[29] D. Pan, X. Ruan, and C. Bao, "Capacitor-current-feedback active damping with reduced computation delay for improving robustness of LCL-type grid-connected inverter," *IEEE Trans. Power Electron.*, vol. 29, no. 7, pp. 3414–3427, Jul. 2014.

[30] M. Liserre, A. Dell'Aquila, and F. Blaabjerg, "Genetic algorithm-based design of the active damping for an LCL-filter three-phase active rectifier," *IEEE Trans. Power Electron.*, vol. 19, no. 1, pp. 76–86, Jan. 2004.

[31] F. Blaabjerg, R. Teodorescu, M. Liserre, and A. V. Timbus, "Overview of control and grid synchronization for distributed power generation systems," *IEEE Trans. Ind. Electron.*, vol. 53, no. 5, pp. 1398–1409, Oct. 2006.

[32] T. Messo, J. Jokipii, J. Puukko, and T. Suntio, "Determining the value of DC-link capacitance to ensure stable operation of a three-phase photovoltaic inverter," *IEEE Trans. Power Electron.*, vol. 29, no. 2, pp. 665–673, Feb. 2014.

[33] T. Messo, J. Jokipii, A. Mäkinen, and T. Suntio, "Modeling the grid synchronization induced negative-resistor-like behavior in the output impedance of a three-phase photovoltaic inverter," *IEEE 4th International Symposium on Power Electronics for Distributed Generation Systems*, pp. 1–7, Jul. 2014.

[34] D. Yang, X. Ruan, and H. Wu, "Impedance shaping of the grid-connected inverter with LCL filter to improve its adaptability to the weak grid condition," *IEEE Trans. Power Electron.*, vol. 29, no. 11, pp. 5795–5805, Nov. 2014.

[35] J. W. Kolar, T. Friedli, F. Krismer, A. Looser, M. Schweizer, P. Steimer, and J. Bevirt, "Conceptualization and multi-objective optimization of the electric system of an airborne wind turbine," *IEEE International Symposium on Industrial Electronics*, pp. 32–55, Jun. 2011.

[36] J. Puukko, T. Messo, and T. Suntio, "Effect of photovoltaic generator on a typical VSI-based three-phase grid-connected photovoltaic inverter dynamics," in *IET Conference on Renewable Power Generation*, Sep. 2011, pp. 72–72.

A. MATLAB CODE FOR CF-VSI STEADY STATE CALCULATION

```
% ########### operating point ###########

eq1='-k1*IL2q=Ucd'
eq2='k1*IL2d-k1*IL1d=Ucq'
eq3='k2*IL2d+R*IL2q=Ucq'
eq4='R*IL2d-rC*IL1d-k2*IL2q+Uod=Ucd'
eq5='IL1d=2*Iin/(3*Dd)'

f=solve(eq1,eq2,eq3,eq4,eq5,'IL2d','IL2q','Ucd','Ucq','IL1d')

%
% % ### simplified IL2d IL2q ###
%

eq10='IL2d=(2*Iin*K_ild-3*Dd*R*Uod)/(3*Dd*K)'
eq11='IL2q=-(2*Iin*K_ilq+3*Dd*Uod*Kuo)/(3*Dd*K)'
eq12='Uin*Dd^2+rC*IL2d*Dd+IL2q*Dd*k1-2*Iin*Req/3=0'
eq13='Dq*Uin-k1*(IL2d-2*Iin/(3*Dd))+rC*IL2q-2*Iin*k3/(3*Dd)=0'

g=solve(eq10,eq11,eq12,eq13,'Dd','Dq','IL2d','IL2q')


% ### Without parasitic elements ###

eq1='-k1*IL2q=Ucd'
eq2='k1*IL2d-k1*IL1d=Ucq'
eq3='k2*IL2d+0*IL2q=Ucq'
eq4='0*IL2d-0*IL1d-k2*IL2q+Uod=Ucd'
eq5='IL1d=2*Iin/(3*Dd)'
```

```
h=solve(eq1,eq2,eq3,eq4,eq5,'IL2d','IL2q','Ucd','Ucq','IL1d')


%
% % ### simplified IL2d IL2q ###
%


eq10='IL2d=(2*Iin*K_ild-3*Dd*0*Uod)/(3*Dd*K)'
eq11='IL2q=-(2*Iin*0+3*Dd*Uod*Kuo)/(3*Dd*K)'
eq12='Uin*Dd^2+0*IL2d*Dd+IL2q*Dd*k1-2*Iin*0/3=0'
eq13='Dq*Uin-k1*(IL2d-2*Iin/(3*Dd))+0*IL2q-2*Iin*k3/(3*Dd)=0'


y=solve(eq10,eq11,eq12,eq13,'Dd','Dq','IL2d','IL2q')


% now the symbolic values for Dd and Dq


Dd = ((K*Req*(K_ilq*((8*Iin*Req*Uin*K^2)/3 + (8*Iin*K_ilq*Uin*K*k1)/3 -
 (8*Iin*K_ild*Uin*K*rC)/3 + Kuo^2*Uod^2*k1^2 + 2*Kuo*R*Uod^2*k1*rC
 + R^2*Uod^2*rC^2)^(1/2) + 2*K*Kuo*Req*Uod + K_ilq*Kuo*Uod*k1
 - 2*K_ild*Kuo*Uod*rC - K_ilq*R*Uod*rC))/(2*(K_ilq*k1 - K_ild*rC + K*Req))
 + (K_ilq*k1*(K_ilq*((8*Iin*Req*Uin*K^2)/3 + (8*Iin*K_ilq*Uin*K*k1)/3
 - (8*Iin*K_ild*Uin*K*rC)/3 + Kuo^2*Uod^2*k1^2 + 2*Kuo*R*Uod^2*k1*rC
 + R^2*Uod^2*rC^2)^(1/2) + 2*K*Kuo*Req*Uod + K_ilq*Kuo*Uod*k1
 - 2*K_ild*Kuo*Uod*rC - K_ilq*R*Uod*rC))/(2*(K_ilq*k1 - K_ild*rC + K*Req))
 - (K_ild*rC*(K_ilq*((8*Iin*Req*Uin*K^2)/3 + (8*Iin*K_ilq*Uin*K*k1)/3
 - (8*Iin*K_ild*Uin*K*rC)/3 + Kuo^2*Uod^2*k1^2 + 2*Kuo*R*Uod^2*k1*rC
 + R^2*Uod^2*rC^2)^(1/2) + 2*K*Kuo*Req*Uod + K_ilq*Kuo*Uod*k1
 - 2*K_ild*Kuo*Uod*rC - K_ilq*R*Uod*rC))/(2*(K_ilq*k1 - K_ild*rC + K*Req))
 - K*Kuo*Req*Uod + K_ild*Kuo*Uod*rC + K_ilq*R*Uod*rC)/(K*K_ilq*Uin)


Dq =  -((K*k1*(K_ilq*((8*Iin*Req*Uin*K^2)/3 + (8*Iin*K_ilq*Uin*K*k1)/3 -
 (8*Iin*K_ild*Uin*K*rC)/3 + Kuo^2*Uod^2*k1^2 + 2*Kuo*R*Uod^2*k1*rC +
 R^2*Uod^2*rC^2)^(1/2) + 2*K*Kuo*Req*Uod + K_ilq*Kuo*Uod*k1
 - 2*K_ild*Kuo*Uod*rC - K_ilq*R*Uod*rC))/(2*(K_ilq*k1 - K_ild*rC + K*Req)) -
 (K*k3*(K_ilq*((8*Iin*Req*Uin*K^2)/3 + (8*Iin*K_ilq*Uin*K*k1)/3 -
 (8*Iin*K_ild*Uin*K*rC)/3 + Kuo^2*Uod^2*k1^2 + 2*Kuo*R*Uod^2*k1*rC +
 R^2*Uod^2*rC^2)^(1/2) + 2*K*Kuo*Req*Uod + K_ilq*Kuo*Uod*k1
  - 2*K_ild*Kuo*Uod*rC - K_ilq*R*Uod*rC))/(2*(K_ilq*k1 - K_ild*rC + K*Req)) -
 (K_ild*k1*(K_ilq*((8*Iin*Req*Uin*K^2)/3 + (8*Iin*K_ilq*Uin*K*k1)/3 -
 (8*Iin*K_ild*Uin*K*rC)/3 + Kuo^2*Uod^2*k1^2 + 2*Kuo*R*Uod^2*k1*rC +
```

```
R^2*Uod^2*rC^2)^(1/2) + 2*K*Kuo*Req*Uod + K_ilq*Kuo*Uod*k1
 - 2*K_ild*Kuo*Uod*rC - K_ilq*R*Uod*rC))/(2*(K_ilq*k1 - K_ild*rC + K*Req)) -
(K_ilq*rC*(K_ilq*((8*Iin*Req*Uin*K^2)/3 + (8*Iin*K_ilq*Uin*K*k1)/3 -
(8*Iin*K_ild*Uin*K*rC)/3 + Kuo^2*Uod^2*k1^2 + 2*Kuo*R*Uod^2*k1*rC +
R^2*Uod^2*rC^2)^(1/2) + 2*K*Kuo*Req*Uod + K_ilq*Kuo*Uod*k1
 - 2*K_ild*Kuo*Uod*rC - K_ilq*R*Uod*rC))/(2*(K_ilq*k1 - K_ild*rC + K*Req))
 - K*Kuo*Uod*k1 + K*Kuo*Uod*k3 + K_ild*Kuo*Uod*k1
 + K_ilq*R*Uod*k1)/(K*K_ilq*Uin)

% where the steady state coefficents are as follows:

k1=1/(ws*C)
k2=ws*L2
k3=ws*L1
R=rL2+rC
Req=req+rC
K=R^2+(k1-k2)^2
K_ild=k1^2-k1*k2+R*rC
K_ilq=k2*rC+R*k1-k1*rC
Kuo=k1-k2
```

B. DUTY RATIO DERIVATION FOR OUTPUT-CURRENT LOOPS

This appendix provides the closed-loop duty ratio derivation, which is subsequently used to calculate the closed-loop transfer functions. According to the block diagram of the closed-loop model presented in Fig. 3.10, the duty ratio can be presented by

$$\hat{d}_{\mathrm{d}} = -\frac{1}{G_{\mathrm{cL\text{-}d}}} L_{\mathrm{out\text{-}d}} \hat{i}_{\mathrm{L1d}} + \frac{1}{G_{\mathrm{cL\text{-}d}} R_{\mathrm{eq\text{-}d}}} L_{\mathrm{out\text{-}d}} \hat{u}_{\mathrm{iL1d}}^{\mathrm{ref}} + D_{\mathrm{q}} G_{\mathrm{PLL}} \hat{u}_{\mathrm{oq}}, \tag{B.1}$$

and the inverter-side d-channel output-current can be presented by

$$\hat{i}_{\mathrm{L1d}} = (-R_{\mathrm{eq\text{-}d}} \hat{i}_{\mathrm{L1d}} + \hat{u}_{\mathrm{iL1d}}^{\mathrm{ref}}) G_{\mathrm{cc\text{-}d}} G_{\mathrm{a}} G_{\mathrm{cL\text{-}d}} + G_{\mathrm{ioL\text{-}d}} \hat{i}_{\mathrm{in}} - Y_{\mathrm{L\text{-}d}} \hat{u}_{\mathrm{od}} + G_{\mathrm{crL\text{-}qd}} \hat{u}_{\mathrm{oq}}$$
$$+ G_{\mathrm{cL\text{-}qd}} \hat{d}_{\mathrm{q}} + D_{\mathrm{q}} G_{\mathrm{PLL}} G_{\mathrm{cL\text{-}d}} \hat{u}_{\mathrm{oq}} \quad \text{(B.2)}$$

Furthermore, in Fig. 3.10 the q-channel duty ratio $\hat{d}_{\mathrm{q}}$ can be presented by

$$\hat{d}_{\mathrm{q}} = [-(G_{\mathrm{ioL\text{-}q}} \hat{i}_{\mathrm{in}} + G_{\mathrm{crL\text{-}dq}} \hat{u}_{\mathrm{od}} - Y_{\mathrm{L\text{-}q}} \hat{u}_{\mathrm{oq}} + G_{\mathrm{cL\text{-}dq}} \hat{d}_{\mathrm{d}} + G_{\mathrm{cL\text{-}q}} \hat{d}_{\mathrm{q}}$$
$$- I_{\mathrm{L1d}} G_{\mathrm{PLL}} \hat{u}_{\mathrm{oq}}) R_{\mathrm{eq\text{-}q}} + \hat{u}_{\mathrm{iL1q}}^{\mathrm{ref}}] G_{\mathrm{cc\text{-}q}} G_{\mathrm{a}} + D_{\mathrm{d}} G_{\mathrm{PLL}} \hat{u}_{\mathrm{oq}}, \quad \text{(B.3)}$$

where $\hat{i}_{\mathrm{L1q}}$ is presented with the input variables. Now by solving (B.3) for $\hat{d}_{\mathrm{q}}$ and rearranging yields

$$\hat{d}_{\mathrm{q}} = -\frac{G_{\mathrm{ioL\text{-}q}}}{G_{\mathrm{cL\text{-}q}}} \frac{L_{\mathrm{out\text{-}q}}}{1 + L_{\mathrm{out\text{-}q}}} \hat{i}_{\mathrm{in}} - \frac{G_{\mathrm{crL\text{-}dq}}}{G_{\mathrm{cL\text{-}q}}} \frac{L_{\mathrm{out\text{-}q}}}{1 + L_{\mathrm{out\text{-}q}}} \hat{u}_{\mathrm{od}} + \frac{Y_{\mathrm{L\text{-}q}}}{G_{\mathrm{cL\text{-}q}}} \frac{L_{\mathrm{out\text{-}q}}}{1 + L_{\mathrm{out\text{-}q}}} \hat{u}_{\mathrm{oq}}$$
$$- \frac{G_{\mathrm{cL\text{-}dq}}}{G_{\mathrm{cL\text{-}q}}} \frac{L_{\mathrm{out\text{-}q}}}{1 + L_{\mathrm{out\text{-}q}}} \hat{d}_{\mathrm{d}} + \frac{1}{R_{\mathrm{eq\text{-}q}} G_{\mathrm{cL\text{-}q}}} \frac{L_{\mathrm{out\text{-}q}}}{1 + L_{\mathrm{out\text{-}q}}} \hat{u}_{\mathrm{iL1q}}^{\mathrm{ref}} + \frac{I_{\mathrm{L1d}} G_{\mathrm{PLL}}}{G_{\mathrm{cL\text{-}q}}} \frac{L_{\mathrm{out\text{-}q}}}{1 + L_{\mathrm{out\text{-}q}}} \hat{u}_{\mathrm{oq}}$$
$$+ D_{\mathrm{d}} G_{\mathrm{PLL}} \frac{1}{1 + L_{\mathrm{out\text{-}q}}} \hat{u}_{\mathrm{oq}} \quad \text{(B.4)}$$

Now $\hat{i}_{\mathrm{L1d}}$ can be solved by substituting obtained value for $\hat{d}_{\mathrm{q}}$ into (B.2). Hence, $\hat{i}_{\mathrm{L1d}}$ can be given by

$$\hat{i}_{\text{L1d}} = \frac{G_{\text{ioL-q}}}{1 + L_{\text{out-d}}}\hat{i}_{\text{in}} - \frac{Y_{\text{L-d}}}{1 + L_{\text{out-d}}}\hat{u}_{\text{od}} + \frac{G_{\text{crL-qd}}}{1 + L_{\text{out-d}}}\hat{u}_{\text{oq}} + \frac{D_{\text{q}}G_{\text{cL-d}}G_{\text{PLL}}}{1 + L_{\text{out-d}}}\hat{u}_{\text{oq}}$$

$$+ \frac{1}{R_{\text{eq-d}}}\frac{L_{\text{out-d}}}{1 + L_{\text{out-d}}}\hat{u}_{\text{iL1d}}^{\text{ref}} + \frac{G_{\text{cL-qd}}}{1 + L_{\text{out-d}}}\left(-\frac{G_{\text{ioL-q}}}{G_{\text{cL-q}}}\frac{L_{\text{out-q}}}{1 + L_{\text{out-q}}}\hat{i}_{\text{in}} - \frac{G_{\text{crL-dq}}}{G_{\text{cL-q}}}\frac{L_{\text{out-q}}}{1 + L_{\text{out-q}}}\hat{u}_{\text{od}} \right.$$

$$+ \frac{Y_{\text{L-q}}}{G_{\text{cL-q}}}\frac{L_{\text{out-q}}}{1 + L_{\text{out-q}}}\hat{u}_{\text{oq}} - \frac{G_{\text{cL-dq}}}{G_{\text{cL-q}}}\frac{L_{\text{out-q}}}{1 + L_{\text{out-q}}}\hat{d}_{\text{d}} + \frac{1}{R_{\text{eq-q}}G_{\text{cL-q}}}\frac{L_{\text{out-q}}}{1 + L_{\text{out-q}}}\hat{u}_{\text{iL1q}}^{\text{ref}}$$

$$\left. + \frac{I_{\text{L1d}}G_{\text{PLL}}}{G_{\text{cL-q}}}\frac{L_{\text{out-q}}}{1 + L_{\text{out-q}}}\hat{u}_{\text{oq}} + D_{\text{d}}G_{\text{PLL}}\frac{1}{1 + L_{\text{out-q}}}\hat{u}_{\text{oq}} \right). \quad \text{(B.5)}$$

A general form for $\hat{d}_{\text{d}}$ can now be obtained by substituting (B.5) into (B.1) yielding

$$\hat{d}_{\text{d}} = -\frac{1}{G_{\text{cL-d}}}L_{\text{out-d}}\left[\frac{G_{\text{ioL-q}}}{1 + L_{\text{out-d}}}\hat{i}_{\text{in}} - \frac{Y_{\text{L-d}}}{1 + L_{\text{out-d}}}\hat{u}_{\text{od}} + \frac{G_{\text{crL-qd}}}{1 + L_{\text{out-d}}}\hat{u}_{\text{oq}} + \frac{D_{\text{q}}G_{\text{cL-d}}G_{\text{PLL}}}{1 + L_{\text{out-d}}}\hat{u}_{\text{oq}} \right.$$

$$+ \frac{1}{R_{\text{eq-d}}}\frac{L_{\text{out-d}}}{1 + L_{\text{out-d}}}\hat{u}_{\text{iL1d}}^{\text{ref}} + \frac{G_{\text{cL-qd}}}{1 + L_{\text{out-d}}}\left(-\frac{G_{\text{ioL-q}}}{G_{\text{cL-q}}}\frac{L_{\text{out-q}}}{1 + L_{\text{out-q}}}\hat{i}_{\text{in}} - \frac{G_{\text{crL-dq}}}{G_{\text{cL-q}}}\frac{L_{\text{out-q}}}{1 + L_{\text{out-q}}}\hat{u}_{\text{od}} \right.$$

$$+ \frac{Y_{\text{L-q}}}{G_{\text{cL-q}}}\frac{L_{\text{out-q}}}{1 + L_{\text{out-q}}}\hat{u}_{\text{oq}} - \frac{G_{\text{cL-dq}}}{G_{\text{cL-q}}}\frac{L_{\text{out-q}}}{1 + L_{\text{out-q}}}\hat{d}_{\text{d}} + \frac{1}{R_{\text{eq-q}}G_{\text{cL-q}}}\frac{L_{\text{out-q}}}{1 + L_{\text{out-q}}}\hat{u}_{\text{iL1q}}^{\text{ref}}$$

$$\left. + \frac{I_{\text{L1d}}G_{\text{PLL}}}{G_{\text{cL-q}}}\frac{L_{\text{out-q}}}{1 + L_{\text{out-q}}}\hat{u}_{\text{oq}} + D_{\text{d}}G_{\text{PLL}}\frac{1}{1 + L_{\text{out-q}}}\hat{u}_{\text{oq}} \right)\bigg] + \frac{1}{G_{\text{cL-d}}R_{\text{eq-d}}}L_{\text{out-d}}\hat{u}_{\text{iL1d}}^{\text{ref}}$$

$$+ D_{\text{q}}G_{\text{PLL}}\hat{u}_{\text{oq}}, \quad \text{(B.6)}$$

which now can be rearranged and presented by

$$\hat{d}_{\text{d}} = \frac{1}{1 - \frac{G_{\text{cL-dq}}G_{\text{cL-qd}}}{G_{\text{cL-q}}G_{\text{cL-d}}}\frac{L_{\text{out-q}}L_{\text{out-d}}}{(1+L_{\text{out-q}})(1+L_{\text{out-d}})}}\left\{ -\frac{1}{G_{\text{cL-d}}}L_{\text{out-d}}\left[\frac{G_{\text{ioL-d}}}{1 + L_{\text{out-d}}}\hat{i}_{\text{in}} - \frac{Y_{\text{L-d}}}{1 + L_{\text{out-d}}}\hat{u}_{\text{od}} \right.\right.$$

$$+ \frac{G_{\text{crL-qd}}}{1 + L_{\text{out-d}}}\hat{u}_{\text{oq}} + \frac{D_{\text{q}}G_{\text{cL-d}}G_{\text{PLL}}}{1 + L_{\text{out-d}}}\hat{u}_{\text{oq}} + \frac{1}{R_{\text{eq-d}}}\frac{L_{\text{out-d}}}{1 + L_{\text{out-d}}}\hat{u}_{\text{iL1d}}^{\text{ref}} + \frac{G_{\text{cL-qd}}}{1 + L_{\text{out-d}}}$$

$$\text{x}\left(-\frac{G_{\text{ioL-q}}}{G_{\text{cL-q}}}\frac{L_{\text{out-q}}}{1 + L_{\text{out-q}}}\hat{i}_{\text{in}} - \frac{G_{\text{crL-dq}}}{G_{\text{cL-q}}}\frac{L_{\text{out-q}}}{1 + L_{\text{out-q}}}\hat{u}_{\text{od}} + \frac{Y_{\text{L-q}}}{G_{\text{cL-q}}}\frac{L_{\text{out-q}}}{1 + L_{\text{out-q}}}\hat{u}_{\text{oq}} \right.$$

$$\left.\left. + \frac{1}{R_{\text{eq-q}}G_{\text{cL-q}}}\frac{L_{\text{out-q}}}{1 + L_{\text{out-q}}}\hat{u}_{\text{iL1q}}^{\text{ref}} + \frac{I_{\text{L1d}}G_{\text{PLL}}}{G_{\text{cL-q}}}\frac{L_{\text{out-q}}}{1 + L_{\text{out-q}}}\hat{u}_{\text{oq}} + D_{\text{d}}G_{\text{PLL}}\frac{1}{1 + L_{\text{out-q}}}\hat{u}_{\text{oq}} \right) \right]$$

$$\left. + \frac{1}{G_{\text{cL-d}}R_{\text{eq-d}}}L_{\text{out-d}}\hat{u}_{\text{iL1d}}^{\text{ref}} + D_{\text{q}}G_{\text{PLL}}\hat{u}_{\text{oq}} \right\}. \quad \text{(B.7)}$$

Respectively, the q-channel duty ratio $\hat{d}_{\text{q}}$ and boost-inductor current $\hat{i}_{\text{L1q}}$ can be

given by

$$\hat{d}_{q} = -\frac{1}{G_{\text{cL-q}}}L_{\text{out-q}}\hat{i}_{\text{L1q}} + \frac{1}{G_{\text{cL-q}}R_{\text{eq-q}}}L_{\text{out-q}}\hat{u}_{\text{iL1q}}^{\text{ref}} + D_{\text{d}}G_{\text{PLL}}\hat{u}_{\text{oq}} + \frac{I_{\text{L1d}}G_{\text{PLL}}}{G_{\text{cL-q}}}L_{\text{out-q}}\hat{u}_{\text{oq}},$$

(B.8)

$$\hat{i}_{\text{L1q}} = (-R_{\text{eq-q}}\hat{i}_{\text{L1q}} + \hat{u}_{\text{iL1q}}^{\text{ref}} + I_{\text{L1d}}G_{\text{PLL}}R_{\text{eq-q}}\hat{u}_{\text{oq}})G_{\text{cc-q}}G_{\text{a}}G_{\text{cL-q}} + G_{\text{ioL-q}}\hat{i}_{\text{in}}$$
$$+ G_{\text{crL-dq}}\hat{u}_{\text{od}} - Y_{\text{L-q}}\hat{u}_{\text{oq}} + G_{\text{cL-dq}}\hat{d}_{\text{d}} + D_{\text{d}}G_{\text{PLL}}G_{\text{cL-q}}\hat{u}_{\text{oq}}.$$

(B.9)

The d-channel duty ratio found in (B.9) can be given according to Fig. 3.10 by

$$\hat{d}_{\text{d}} = [-(G_{\text{ioL-d}}\hat{i}_{\text{in}} - Y_{\text{L-d}}\hat{u}_{\text{od}} + G_{\text{crL-qd}}\hat{u}_{\text{oq}} + G_{\text{cL-d}}\hat{d}_{\text{d}} + G_{\text{cL-qd}}\hat{d}_{\text{q}})R_{\text{eq-d}}$$
$$+ \hat{u}_{\text{iL1d}}^{\text{ref}}]G_{\text{cc-d}}G_{\text{a}} + D_{\text{q}}G_{\text{PLL}}\hat{u}_{\text{oq}} \quad (B.10)$$

Now by solving for $\hat{d}_{\text{d}}$ yields

$$\hat{d}_{\text{d}} = -\frac{G_{\text{ioL-d}}}{G_{\text{cL-d}}}\frac{L_{\text{out-d}}}{1 + L_{\text{out-d}}}\hat{i}_{\text{in}} + \frac{Y_{\text{L-d}}}{G_{\text{cL-d}}}\frac{L_{\text{out-d}}}{1 + L_{\text{out-d}}}\hat{u}_{\text{od}} - \frac{G_{\text{crL-qd}}}{G_{\text{cL-d}}}\frac{L_{\text{out-d}}}{1 + L_{\text{out-d}}}\hat{u}_{\text{oq}}$$
$$- \frac{G_{\text{cL-qd}}}{G_{\text{cL-d}}}\frac{L_{\text{out-d}}}{1 + L_{\text{out-d}}}\hat{d}_{\text{q}} + \frac{1}{R_{\text{eq-d}}G_{\text{cL-d}}}\frac{L_{\text{out-d}}}{1 + L_{\text{out-d}}}\hat{u}_{\text{iL1d}}^{\text{ref}} + D_{\text{q}}G_{\text{PLL}}\frac{1}{1 + L_{\text{out-d}}}\hat{u}_{\text{oq}}.$$

(B.11)

Now $\hat{i}_{\text{L1q}}$ can be solved by substituting obtained value for $\hat{d}_{\text{d}}$ into (B.9) yielding

$$\hat{i}_{\text{L1q}} = \frac{G_{\text{ioL-q}}}{1 + L_{\text{out-q}}}\hat{i}_{\text{in}} + \frac{G_{\text{crL-dq}}}{1 + L_{\text{out-q}}}\hat{u}_{\text{od}} - \frac{Y_{\text{L-q}}}{1 + L_{\text{out-q}}}\hat{u}_{\text{oq}} + \frac{D_{\text{d}}G_{\text{cL-q}}G_{\text{PLL}}}{1 + L_{\text{out-q}}}\hat{u}_{\text{oq}}$$
$$+ I_{\text{L1d}}G_{\text{PLL}}\frac{L_{\text{out-q}}}{1 + L_{\text{out-q}}}\hat{u}_{\text{oq}} + \frac{1}{R_{\text{eq-q}}}\frac{L_{\text{out-q}}}{1 + L_{\text{out-q}}}\hat{u}_{\text{iL1q}}^{\text{ref}} + \frac{G_{\text{cL-dq}}}{1 + L_{\text{out-q}}}\left(-\frac{G_{\text{ioL-d}}}{G_{\text{cL-d}}}\frac{L_{\text{out-d}}}{1 + L_{\text{out-d}}}\hat{i}_{\text{in}}\right.$$
$$+ \frac{Y_{\text{L-d}}}{G_{\text{cL-d}}}\frac{L_{\text{out-d}}}{1 + L_{\text{out-d}}}\hat{u}_{\text{od}} - \frac{G_{\text{crL-qd}}}{G_{\text{cL-d}}}\frac{L_{\text{out-d}}}{1 + L_{\text{out-d}}}\hat{u}_{\text{oq}} - \frac{G_{\text{cL-qd}}}{G_{\text{cL-d}}}\frac{L_{\text{out-d}}}{1 + L_{\text{out-d}}}\hat{d}_{\text{q}}$$
$$\left. + \frac{1}{R_{\text{eq-d}}G_{\text{cL-d}}}\frac{L_{\text{out-d}}}{1 + L_{\text{out-d}}}\hat{u}_{\text{iL1d}}^{\text{ref}} + D_{\text{q}}G_{\text{PLL}}\frac{1}{1 + L_{\text{out-d}}}\hat{u}_{\text{oq}}\right). \quad (B.12)$$

A general form for $\hat{d}_{\text{q}}$ can now be obtained by substituting (B.12) into (B.8) and presented by

$$\hat{d}_{\mathrm{q}} = -\frac{1}{G_{\mathrm{cL\text{-}q}}}L_{\mathrm{out\text{-}q}}\Bigg[\frac{G_{\mathrm{ioL\text{-}q}}}{1+L_{\mathrm{out\text{-}q}}}\hat{i}_{\mathrm{in}}+\frac{G_{\mathrm{crL\text{-}dq}}}{1+L_{\mathrm{out\text{-}q}}}\hat{u}_{\mathrm{od}}-\frac{Y_{\mathrm{L\text{-}q}}}{1+L_{\mathrm{out\text{-}q}}}\hat{u}_{\mathrm{oq}}+\frac{D_{\mathrm{d}}G_{\mathrm{cL\text{-}q}}G_{\mathrm{PLL}}}{1+L_{\mathrm{out\text{-}q}}}\hat{u}_{\mathrm{oq}}$$

$$+I_{\mathrm{L1d}}G_{\mathrm{PLL}}\frac{L_{\mathrm{out\text{-}q}}}{1+L_{\mathrm{out\text{-}q}}}\hat{u}_{\mathrm{oq}}+\frac{1}{R_{\mathrm{eq\text{-}q}}}\frac{L_{\mathrm{out\text{-}q}}}{1+L_{\mathrm{out\text{-}q}}}\hat{u}_{\mathrm{iL1q}}^{\mathrm{ref}}+\frac{G_{\mathrm{cL\text{-}dq}}}{1+L_{\mathrm{out\text{-}q}}}\left(-\frac{G_{\mathrm{ioL\text{-}d}}}{G_{\mathrm{cL\text{-}d}}}\frac{L_{\mathrm{out\text{-}d}}}{1+L_{\mathrm{out\text{-}d}}}\hat{i}_{\mathrm{in}}\right.$$

$$+\frac{Y_{\mathrm{L\text{-}d}}}{G_{\mathrm{cL\text{-}d}}}\frac{L_{\mathrm{out\text{-}d}}}{1+L_{\mathrm{out\text{-}d}}}\hat{u}_{\mathrm{od}}-\frac{G_{\mathrm{crL\text{-}qd}}}{G_{\mathrm{cL\text{-}d}}}\frac{L_{\mathrm{out\text{-}d}}}{1+L_{\mathrm{out\text{-}d}}}\hat{u}_{\mathrm{oq}}-\frac{G_{\mathrm{cL\text{-}qd}}}{G_{\mathrm{cL\text{-}d}}}\frac{L_{\mathrm{out\text{-}d}}}{1+L_{\mathrm{out\text{-}d}}}\hat{d}_{\mathrm{q}}$$

$$+\frac{1}{R_{\mathrm{eq\text{-}d}}G_{\mathrm{cL\text{-}d}}}\frac{L_{\mathrm{out\text{-}d}}}{1+L_{\mathrm{out\text{-}d}}}\hat{u}_{\mathrm{iL1d}}^{\mathrm{ref}}+D_{\mathrm{q}}G_{\mathrm{PLL}}\frac{1}{1+L_{\mathrm{out\text{-}d}}}\hat{u}_{\mathrm{oq}}\Bigg)\Bigg]+\frac{1}{G_{\mathrm{cL\text{-}q}}R_{\mathrm{eq\text{-}q}}}L_{\mathrm{out\text{-}q}}\hat{u}_{\mathrm{iL1q}}^{\mathrm{ref}}$$

$$+D_{\mathrm{d}}G_{\mathrm{PLL}}\hat{u}_{\mathrm{oq}}+\frac{I_{\mathrm{L1d}}G_{\mathrm{PLL}}}{G_{\mathrm{cL\text{-}q}}}L_{\mathrm{out\text{-}q}}\hat{u}_{\mathrm{oq}}. \quad \text{(B.13)}$$

By further arranging the equation, the general form for the q-channel duty ratio can be given by

$$\hat{d}_{\mathrm{q}} = \frac{1}{1-\frac{G_{\mathrm{cL\text{-}dq}}G_{\mathrm{cL\text{-}qd}}}{G_{\mathrm{cL\text{-}q}}G_{\mathrm{cL\text{-}d}}}\frac{L_{\mathrm{out\text{-}q}}L_{\mathrm{out\text{-}d}}}{(1+L_{\mathrm{out\text{-}q}})(1+L_{\mathrm{out\text{-}d}})}}\Bigg\{-\frac{1}{G_{\mathrm{cL\text{-}q}}}L_{\mathrm{out\text{-}q}}\Bigg[\frac{G_{\mathrm{ioL\text{-}q}}}{1+L_{\mathrm{out\text{-}q}}}\hat{i}_{\mathrm{in}}+\frac{G_{\mathrm{crL\text{-}dq}}}{1+L_{\mathrm{out\text{-}q}}}\hat{u}_{\mathrm{od}}$$

$$-\frac{Y_{\mathrm{L\text{-}q}}}{1+L_{\mathrm{out\text{-}q}}}\hat{u}_{\mathrm{oq}}+\frac{D_{\mathrm{d}}G_{\mathrm{cL\text{-}q}}G_{\mathrm{PLL}}}{1+L_{\mathrm{out\text{-}q}}}\hat{u}_{\mathrm{oq}}+I_{\mathrm{L1d}}G_{\mathrm{PLL}}\frac{L_{\mathrm{out\text{-}q}}}{1+L_{\mathrm{out\text{-}q}}}\hat{u}_{\mathrm{oq}}+\frac{1}{R_{\mathrm{eq\text{-}q}}}\frac{L_{\mathrm{out\text{-}q}}}{1+L_{\mathrm{out\text{-}q}}}\hat{u}_{\mathrm{iL1q}}^{\mathrm{ref}}$$

$$+\frac{G_{\mathrm{cL\text{-}dq}}}{1+L_{\mathrm{out\text{-}q}}}\left(-\frac{G_{\mathrm{ioL\text{-}d}}}{G_{\mathrm{cL\text{-}d}}}\frac{L_{\mathrm{out\text{-}d}}}{1+L_{\mathrm{out\text{-}d}}}\hat{i}_{\mathrm{in}}+\frac{Y_{\mathrm{L\text{-}d}}}{G_{\mathrm{cL\text{-}d}}}\frac{L_{\mathrm{out\text{-}d}}}{1+L_{\mathrm{out\text{-}d}}}\hat{u}_{\mathrm{od}}-\frac{G_{\mathrm{crL\text{-}qd}}}{G_{\mathrm{cL\text{-}d}}}\frac{L_{\mathrm{out\text{-}d}}}{1+L_{\mathrm{out\text{-}d}}}\hat{u}_{\mathrm{oq}}\right.$$

$$+\frac{1}{R_{\mathrm{eq\text{-}d}}G_{\mathrm{cL\text{-}d}}}\frac{L_{\mathrm{out\text{-}d}}}{1+L_{\mathrm{out\text{-}d}}}\hat{u}_{\mathrm{iL1d}}^{\mathrm{ref}}+D_{\mathrm{q}}G_{\mathrm{PLL}}\frac{1}{1+L_{\mathrm{out\text{-}d}}}\hat{u}_{\mathrm{oq}}\Bigg)\Bigg]+\frac{1}{G_{\mathrm{cL\text{-}q}}R_{\mathrm{eq\text{-}q}}}L_{\mathrm{out\text{-}q}}\hat{u}_{\mathrm{iL1q}}^{\mathrm{ref}}$$

$$+D_{\mathrm{d}}G_{\mathrm{PLL}}\hat{u}_{\mathrm{oq}}+\frac{I_{\mathrm{L1d}}G_{\mathrm{PLL}}}{G_{\mathrm{cL\text{-}q}}}L_{\mathrm{out\text{-}q}}\hat{u}_{\mathrm{oq}}\Bigg\}. \quad \text{(B.14)}$$

C. OUTPUT-CURRENT LOOP TRANSFER FUNCTIONS

This chapter presents the transfer functions when only the output-current control-loops are connected. The input-voltage can be presented by

$$\hat{u}_{\text{in}} = Z_{\text{in}}^{\text{out}}\hat{i}_{\text{in}} + T_{\text{oi-d}}^{\text{out}}\hat{u}_{\text{od}} + T_{\text{oi-q}}^{\text{out}}\hat{u}_{\text{oq}} + G_{\text{ci-d}}^{\text{out}}\hat{u}_{\text{iL1q}}^{\text{ref}} + G_{\text{ci-q}}^{\text{out}}\hat{u}_{\text{iL1q}}^{\text{ref}}, \tag{C.1}$$

where

$$Z_{\text{in}}^{\text{out}} = Z_{\text{in}}^{\text{H}} + G_{\text{ci-d}}^{\text{H}} \frac{-\frac{L_{\text{out-d}}}{G_{\text{cL-d}}^{\text{H}}}\left(\frac{G_{\text{ioL-d}}^{\text{H}}}{1+L_{\text{out-d}}} - \frac{G_{\text{cL-qd}}^{\text{H}}}{1+L_{\text{out-d}}}\frac{G_{\text{ioL-q}}^{\text{H}}}{G_{\text{cL-q}}^{\text{H}}}\frac{L_{\text{out-q}}}{1+L_{\text{out-q}}}\right)}{1 - \frac{G_{\text{cL-dq}}^{\text{H}}G_{\text{cL-qd}}^{\text{H}}}{G_{\text{cL-q}}^{\text{H}}G_{\text{cL-d}}^{\text{H}}}\frac{L_{\text{out-q}}L_{\text{out-d}}}{(1+L_{\text{out-q}})(1+L_{\text{out-d}})}}$$

$$+ G_{\text{ci-q}}^{\text{H}} \frac{-\frac{L_{\text{out-q}}}{G_{\text{cL-q}}^{\text{H}}}\left(\frac{G_{\text{ioL-q}}^{\text{H}}}{1+L_{\text{out-q}}} - \frac{G_{\text{cL-dq}}^{\text{H}}}{1+L_{\text{out-q}}}\frac{G_{\text{ioL-d}}^{\text{H}}}{G_{\text{cL-d}}^{\text{H}}}\frac{L_{\text{out-d}}}{1+L_{\text{out-d}}}\right)}{1 - \frac{G_{\text{cL-dq}}^{\text{H}}G_{\text{cL-qd}}^{\text{H}}}{G_{\text{cL-q}}^{\text{H}}G_{\text{cL-d}}^{\text{H}}}\frac{L_{\text{out-q}}L_{\text{out-d}}}{(1+L_{\text{out-q}})(1+L_{\text{out-d}})}}, \tag{C.2}$$

$$T_{\text{oi-d}}^{\text{out}} = T_{\text{oi-d}}^{\text{H}} + G_{\text{ci-d}}^{\text{H}} \frac{-\frac{L_{\text{out-d}}}{G_{\text{cL-d}}^{\text{H}}}\left(-\frac{Y_{\text{L-d}}^{\text{H}}}{1+L_{\text{out-d}}} - \frac{G_{\text{cL-qd}}^{\text{H}}}{1+L_{\text{out-d}}}\frac{G_{\text{crL-dq}}^{\text{H}}}{G_{\text{cL-q}}^{\text{H}}}\frac{L_{\text{out-q}}}{1+L_{\text{out-q}}}\right)}{1 - \frac{G_{\text{cL-dq}}^{\text{H}}G_{\text{cL-qd}}^{\text{H}}}{G_{\text{cL-q}}^{\text{H}}G_{\text{cL-d}}^{\text{H}}}\frac{L_{\text{out-q}}L_{\text{out-d}}}{(1+L_{\text{out-q}})(1+L_{\text{out-d}})}}$$

$$+ G_{\text{ci-q}}^{\text{H}} \frac{-\frac{L_{\text{out-q}}}{G_{\text{cL-q}}^{\text{H}}}\left(\frac{G_{\text{crL-dq}}^{\text{H}}}{1+L_{\text{out-q}}} - \frac{G_{\text{cL-dq}}^{\text{H}}}{1+L_{\text{out-q}}}\frac{Y_{\text{L-d}}^{\text{H}}}{G_{\text{cL-d}}^{\text{H}}}\frac{L_{\text{out-d}}}{1+L_{\text{out-d}}}\right)}{1 - \frac{G_{\text{cL-dq}}^{\text{H}}G_{\text{cL-qd}}^{\text{H}}}{G_{\text{cL-q}}^{\text{H}}G_{\text{cL-d}}^{\text{H}}}\frac{L_{\text{out-q}}L_{\text{out-d}}}{(1+L_{\text{out-q}})(1+L_{\text{out-d}})}}, \tag{C.3}$$

$$T_{\text{oi-q}}^{\text{out}} = T_{\text{oi-q}}^{\text{H}} + G_{\text{ci-d}}^{\text{H}} \frac{-\frac{L_{\text{out-d}}}{G_{\text{cL-d}}^{\text{H}}} \left(\frac{G_{\text{crL-qd}}^{\text{H}}}{1+L_{\text{out-d}}} + \frac{G_{\text{cL-qd}}^{\text{H}}}{1+L_{\text{out-d}}} \frac{Y_{\text{L-q}}^{\text{H}}}{G_{\text{cL-q}}^{\text{H}}} \frac{L_{\text{out-q}}}{1+L_{\text{out-q}}} \right)}{1 - \frac{G_{\text{cL-dq}}^{\text{H}} G_{\text{cL-qd}}^{\text{H}}}{G_{\text{cL-q}}^{\text{H}} G_{\text{cL-d}}^{\text{H}}} \frac{L_{\text{out-q}} L_{\text{out-d}}}{(1+L_{\text{out-q}})(1+L_{\text{out-d}})}}$$

$$+ G_{\text{ci-d}}^{\text{H}} \frac{D_{\text{q}} G_{\text{PLL}} - \frac{L_{\text{out-d}}}{G_{\text{cL-d}}^{\text{H}}} \left[\frac{D_{\text{q}} G_{\text{cL-d}}^{\text{H}} G_{\text{PLL}}}{1+L_{\text{out-d}}} + \frac{G_{\text{cL-qd}}^{\text{H}}}{1+L_{\text{out-d}}} \left(\frac{I_{\text{L1d}} G_{\text{PLL}}}{G_{\text{cL-q}}^{\text{H}}} \frac{L_{\text{out-q}}}{1+L_{\text{out-q}}} + \frac{D_{\text{d}} G_{\text{PLL}}}{1+L_{\text{out-q}}} \right) \right]}{1 - \frac{G_{\text{cL-dq}}^{\text{H}} G_{\text{cL-qd}}^{\text{H}}}{G_{\text{cL-q}}^{\text{H}} G_{\text{cL-d}}^{\text{H}}} \frac{L_{\text{out-q}} L_{\text{out-d}}}{(1+L_{\text{out-q}})(1+L_{\text{out-d}})}}$$

$$+ G_{\text{ci-q}}^{\text{H}} \frac{-\frac{L_{\text{out-q}}}{G_{\text{cL-q}}^{\text{H}}} \left(-\frac{Y_{\text{L-q}}^{\text{H}}}{1+L_{\text{out-q}}} - \frac{G_{\text{cL-dq}}^{\text{H}}}{1+L_{\text{out-q}}} \frac{G_{\text{crL-qd}}^{\text{H}}}{G_{\text{cL-d}}^{\text{H}}} \frac{L_{\text{out-d}}}{1+L_{\text{out-d}}} \right)}{1 - \frac{G_{\text{cL-dq}}^{\text{H}} G_{\text{cL-qd}}^{\text{H}}}{G_{\text{cL-q}}^{\text{H}} G_{\text{cL-d}}^{\text{H}}} \frac{L_{\text{out-q}} L_{\text{out-d}}}{(1+L_{\text{out-q}})(1+L_{\text{out-d}})}}$$

$$+ G_{\text{ci-q}}^{\text{H}} \left\{ \frac{D_{\text{d}} G_{\text{PLL}} + \frac{I_{\text{L1d}} G_{\text{PLL}}}{G_{\text{cL-q}}^{\text{H}}} L_{\text{out-q}}}{1 - \frac{G_{\text{cL-dq}}^{\text{H}} G_{\text{cL-qd}}^{\text{H}}}{G_{\text{cL-q}}^{\text{H}} G_{\text{cL-d}}^{\text{H}}} \frac{L_{\text{out-q}} L_{\text{out-d}}}{(1+L_{\text{out-q}})(1+L_{\text{out-d}})}} \right.$$

$$\left. - \frac{\frac{L_{\text{out-q}}}{G_{\text{cL-q}}^{\text{H}}} \left[\frac{D_{\text{d}} G_{\text{cL-q}}^{\text{H}} G_{\text{PLL}}}{1+L_{\text{out-q}}} + I_{\text{L1d}} G_{\text{PLL}} \frac{L_{\text{out-q}}}{1+L_{\text{out-q}}} + \frac{G_{\text{cL-dq}}^{\text{H}}}{1+L_{\text{out-q}}} \frac{D_{\text{q}} G_{\text{PLL}}}{1+L_{\text{out-d}}} \right]}{1 - \frac{G_{\text{cL-dq}}^{\text{H}} G_{\text{cL-qd}}^{\text{H}}}{G_{\text{cL-q}}^{\text{H}} G_{\text{cL-d}}^{\text{H}}} \frac{L_{\text{out-q}} L_{\text{out-d}}}{(1+L_{\text{out-q}})(1+L_{\text{out-d}})}} \right\}, \quad \text{(C.4)}$$

$$G_{\text{ci-d}}^{\text{out}} = G_{\text{ci-d}}^{\text{H}} \frac{-\frac{L_{\text{out-d}}}{G_{\text{cL-d}}^{\text{H}} R_{\text{eq-d}}} \left(\frac{L_{\text{out-d}}}{1+L_{\text{out-d}}} - 1 \right)}{1 - \frac{G_{\text{cL-dq}}^{\text{H}} G_{\text{cL-qd}}^{\text{H}}}{G_{\text{cL-q}}^{\text{H}} G_{\text{cL-d}}^{\text{H}}} \frac{L_{\text{out-q}} L_{\text{out-d}}}{(1+L_{\text{out-q}})(1+L_{\text{out-d}})}}$$

$$+ G_{\text{ci-q}}^{\text{H}} \frac{-\frac{G_{\text{cL-dq}}^{\text{H}}}{R_{\text{eq-d}} G_{\text{cL-q}}^{\text{H}}} \frac{L_{\text{out-q}}}{1+L_{\text{out-q}}} \frac{L_{\text{out-d}}}{1+L_{\text{out-d}}}}{1 - \frac{G_{\text{cL-dq}}^{\text{H}} G_{\text{cL-qd}}^{\text{H}}}{G_{\text{cL-q}}^{\text{H}} G_{\text{cL-d}}^{\text{H}}} \frac{L_{\text{out-q}} L_{\text{out-d}}}{(1+L_{\text{out-q}})(1+L_{\text{out-d}})}}, \quad \text{(C.5)}$$

$$G_{\text{ci-q}}^{\text{out}} = G_{\text{ci-d}}^{\text{H}} \frac{-\frac{G_{\text{cL-qd}}^{\text{H}}}{G_{\text{cL-d}}^{\text{H}} G_{\text{cL-q}}^{\text{H}} R_{\text{eq-d}}} \frac{L_{\text{out-d}}}{1+L_{\text{out-d}}} \frac{L_{\text{out-q}}}{1+L_{\text{out-q}}}}{1 - \frac{G_{\text{cL-dq}}^{\text{H}} G_{\text{cL-qd}}^{\text{H}}}{G_{\text{cL-q}}^{\text{H}} G_{\text{cL-d}}^{\text{H}}} \frac{L_{\text{out-q}} L_{\text{out-d}}}{(1+L_{\text{out-q}})(1+L_{\text{out-d}})}}$$

$$+ G_{\text{ci-q}}^{\text{H}} \frac{-\frac{L_{\text{out-q}}}{G_{\text{cL-q}}^{\text{H}} R_{\text{eq-q}}} \left(\frac{L_{\text{out-q}}}{1+L_{\text{out-q}}} - 1 \right)}{1 - \frac{G_{\text{cL-dq}}^{\text{H}} G_{\text{cL-qd}}^{\text{H}}}{G_{\text{cL-q}}^{\text{H}} G_{\text{cL-d}}^{\text{H}}} \frac{L_{\text{out-q}} L_{\text{out-d}}}{(1+L_{\text{out-q}}(1+L_{\text{out-d}})}}. \quad \text{(C.6)}$$

The d-channel inverter-side inductor current transfer functions, when only the output-current loops are closed, can be given by

$$\hat{i}_{\text{L1d}} = G_{\text{ioL-d}}^{\text{out}} \hat{i}_{\text{in}} - Y_{\text{L-d}}^{\text{out}} \hat{u}_{\text{od}} + G_{\text{crL-qd}}^{\text{out}} \hat{u}_{\text{oq}} + G_{\text{cL-d}}^{\text{out}} \hat{u}_{\text{iL1d}}^{\text{ref}} + G_{\text{cL-qd}}^{\text{out}} \hat{u}_{\text{iL1q}}^{\text{ref}}, \quad \text{(C.7)}$$

where

$$G_{\text{ioL-d}}^{\text{out}} = G_{\text{ioL-d}}^{\text{H}} + \frac{-L_{\text{out-d}} \left(\frac{G_{\text{ioL-d}}^{\text{H}}}{1+L_{\text{out-d}}} - \frac{G_{\text{ioL-q}}^{\text{H}}}{G_{\text{cL-q}}^{\text{H}}} \frac{G_{\text{cL-qd}}^{\text{H}}}{1+L_{\text{out-d}}} \frac{L_{\text{out-q}}}{1+L_{\text{out-q}}} \right)}{1 - \frac{G_{\text{cL-dq}}G_{\text{cL-qd}}}{G_{\text{cL-q}}G_{\text{cL-d}}} \frac{L_{\text{out-q}}L_{\text{out-d}}}{(1+L_{\text{out-q}})(1+L_{\text{out-d}})}}$$

$$+ \frac{-L_{\text{out-q}} \frac{G_{\text{cL-qd}}}{G_{\text{cL-q}}} \left(\frac{G_{\text{ioL-q}}^{\text{H}}}{1+L_{\text{out-q}}} - \frac{G_{\text{ioL-d}}^{\text{H}}}{G_{\text{cL-d}}^{\text{H}}} \frac{G_{\text{cL-dq}}^{\text{H}}}{1+L_{\text{out-q}}} \frac{L_{\text{out-d}}}{1+L_{\text{out-d}}} \right)}{1 - \frac{G_{\text{cL-dq}}^{\text{H}}G_{\text{cL-qd}}^{\text{H}}}{G_{\text{cL-q}}^{\text{H}}G_{\text{cL-d}}^{\text{H}}} \frac{L_{\text{out-q}}L_{\text{out-d}}}{(1+L_{\text{out-q}})(1+L_{\text{out-d}})}}, \quad (C.8)$$

$$Y_{\text{L-d}}^{\text{out}} = Y_{\text{L-d}}^{\text{H}} - \frac{-L_{\text{out-d}} \left(-\frac{Y_{\text{L-d}}^{\text{H}}}{1+L_{\text{out-d}}} - \frac{G_{\text{crL-dq}}^{\text{H}}}{G_{\text{cL-q}}^{\text{H}}} \frac{G_{\text{cL-qd}}^{\text{H}}}{1+L_{\text{out-d}}} \frac{L_{\text{out-q}}}{1+L_{\text{out-q}}} \right)}{1 - \frac{G_{\text{cL-dq}}^{\text{H}}G_{\text{cL-qd}}^{\text{H}}}{G_{\text{cL-q}}^{\text{H}}G_{\text{cL-d}}^{\text{H}}} \frac{L_{\text{out-q}}L_{\text{out-d}}}{(1+L_{\text{out-q}})(1+L_{\text{out-d}})}}$$

$$- \frac{-L_{\text{out-q}} \frac{G_{\text{cL-qd}}}{G_{\text{cL-q}}} \left(\frac{G_{\text{crL-dq}}^{\text{H}}}{1+L_{\text{out-q}}} + \frac{Y_{\text{L-d}}^{\text{H}}}{G_{\text{cL-d}}^{\text{H}}} \frac{G_{\text{cL-dq}}^{\text{H}}}{1+L_{\text{out-q}}} \frac{L_{\text{out-d}}}{1+L_{\text{out-d}}} \right)}{1 - \frac{G_{\text{cL-dq}}^{\text{H}}G_{\text{cL-qd}}^{\text{H}}}{G_{\text{cL-q}}^{\text{H}}G_{\text{cL-d}}^{\text{H}}} \frac{L_{\text{out-q}}L_{\text{out-d}}}{(1+L_{\text{out-q}})(1+L_{\text{out-d}})}}, \quad (C.9)$$

$$G_{\text{crL-qd}}^{\text{out}} = G_{\text{crL-qd}}^{\text{H}} + G_{\text{cL-d}}^{\text{H}} \frac{-\frac{L_{\text{out-d}}}{G_{\text{cL-d}}^{\text{H}}} \left(\frac{G_{\text{crL-qd}}^{\text{H}}}{1+L_{\text{out-d}}} + \frac{G_{\text{cL-qd}}^{\text{H}}}{1+L_{\text{out-d}}} \frac{Y_{\text{L-q}}^{\text{H}}}{G_{\text{cL-q}}^{\text{H}}} \frac{L_{\text{out-q}}}{1+L_{\text{out-q}}} \right)}{1 - \frac{G_{\text{cL-dq}}^{\text{H}}G_{\text{cL-qd}}^{\text{H}}}{G_{\text{cL-q}}^{\text{H}}G_{\text{cL-d}}^{\text{H}}} \frac{L_{\text{out-q}}L_{\text{out-d}}}{(1+L_{\text{out-q}})(1+L_{\text{out-d}})}}$$

$$+ G_{\text{cL-d}}^{\text{H}} \frac{D_{\text{q}}G_{\text{PLL}} - \frac{L_{\text{out-d}}}{G_{\text{cL-d}}^{\text{H}}} \left[\frac{D_{\text{q}}G_{\text{cL-d}}^{\text{H}}G_{\text{PLL}}}{1+L_{\text{out-d}}} + \frac{G_{\text{cL-qd}}^{\text{H}}}{1+L_{\text{out-d}}} \left(\frac{I_{\text{L1d}}G_{\text{PLL}}}{G_{\text{cL-q}}^{\text{H}}} \frac{L_{\text{out-q}}}{1+L_{\text{out-q}}} + \frac{D_{\text{d}}G_{\text{PLL}}}{1+L_{\text{out-q}}} \right) \right]}{1 - \frac{G_{\text{cL-dq}}^{\text{H}}G_{\text{cL-qd}}^{\text{H}}}{G_{\text{cL-q}}^{\text{H}}G_{\text{cL-d}}^{\text{H}}} \frac{L_{\text{out-q}}L_{\text{out-d}}}{(1+L_{\text{out-q}})(1+L_{\text{out-d}})}}$$

$$+ G_{\text{cL-qd}}^{\text{H}} \frac{-\frac{L_{\text{out-q}}}{G_{\text{cL-q}}^{\text{H}}} \left(-\frac{Y_{\text{L-q}}^{\text{H}}}{1+L_{\text{out-q}}} - \frac{G_{\text{cL-dq}}^{\text{H}}}{1+L_{\text{out-q}}} \frac{G_{\text{crL-qd}}^{\text{H}}}{G_{\text{cL-d}}^{\text{H}}} \frac{L_{\text{out-d}}}{1+L_{\text{out-d}}} \right)}{1 - \frac{G_{\text{cL-dq}}^{\text{H}}G_{\text{cL-qd}}^{\text{H}}}{G_{\text{cL-q}}^{\text{H}}G_{\text{cL-d}}^{\text{H}}} \frac{L_{\text{out-q}}L_{\text{out-d}}}{(1+L_{\text{out-q}})(1+L_{\text{out-d}})}}$$

$$+ G_{\text{cL-qd}}^{\text{H}} \left\{ \frac{D_{\text{d}}G_{\text{PLL}} + \frac{I_{\text{L1d}}G_{\text{PLL}}}{G_{\text{cL-q}}^{\text{H}}} L_{\text{out-q}}}{1 - \frac{G_{\text{cL-dq}}^{\text{H}}G_{\text{cL-qd}}^{\text{H}}}{G_{\text{cL-q}}^{\text{H}}G_{\text{cL-d}}^{\text{H}}} \frac{L_{\text{out-q}}L_{\text{out-d}}}{(1+L_{\text{out-q}})(1+L_{\text{out-d}})}} \right.$$

$$\left. - \frac{\frac{L_{\text{out-q}}}{G_{\text{cL-q}}^{\text{H}}} \left[\frac{D_{\text{d}}G_{\text{cL-q}}^{\text{H}}G_{\text{PLL}}}{1+L_{\text{out-q}}} + I_{\text{L1d}}G_{\text{PLL}} \frac{L_{\text{out-q}}}{1+L_{\text{out-q}}} + \frac{G_{\text{cL-dq}}^{\text{H}}}{1+L_{\text{out-q}}} \frac{D_{\text{q}}G_{\text{PLL}}}{1+L_{\text{out-d}}} \right]}{1 - \frac{G_{\text{cL-dq}}^{\text{H}}G_{\text{cL-qd}}^{\text{H}}}{G_{\text{cL-q}}^{\text{H}}G_{\text{cL-d}}^{\text{H}}} \frac{L_{\text{out-q}}L_{\text{out-d}}}{(1+L_{\text{out-q}})(1+L_{\text{out-d}})}} \right\}, \quad (C.10)$$

$$G_{\text{cL-d}}^{\text{out}} = G_{\text{cL-d}}^{\text{H}} \frac{-\frac{L_{\text{out-d}}}{G_{\text{cL-d}}^{\text{H}} R_{\text{eq-d}}} \left(\frac{L_{\text{out-d}}}{1+L_{\text{out-d}}} - 1 \right)}{1 - \frac{G_{\text{cL-dq}}^{\text{H}} G_{\text{cL-qd}}^{\text{H}}}{G_{\text{cL-q}}^{\text{H}} G_{\text{cL-d}}^{\text{H}}} \frac{L_{\text{out-q}} L_{\text{out-d}}}{(1+L_{\text{out-q}})(1+L_{\text{out-d}})}}$$

$$+ G_{\text{cL-qd}}^{\text{H}} \frac{-\frac{G_{\text{cL-dq}}^{\text{H}}}{R_{\text{eq-d}} G_{\text{cL-q}}^{\text{H}}} \frac{L_{\text{out-q}}}{1+L_{\text{out-q}}} \frac{L_{\text{out-d}}}{1+L_{\text{out-d}}}}{1 - \frac{G_{\text{cL-dq}}^{\text{H}} G_{\text{cL-qd}}^{\text{H}}}{G_{\text{cL-q}}^{\text{H}} G_{\text{cL-d}}^{\text{H}}} \frac{L_{\text{out-q}} L_{\text{out-d}}}{(1+L_{\text{out-q}})(1+L_{\text{out-d}})}}, \quad \text{(C.11)}$$

$$G_{\text{cL-qd}}^{\text{out}} = G_{\text{cL-d}}^{\text{H}} \frac{-\frac{G_{\text{cL-qd}}^{\text{H}}}{G_{\text{cL-d}}^{\text{H}} G_{\text{cL-q}}^{\text{H}} R_{\text{eq-d}}} \frac{L_{\text{out-d}}}{1+L_{\text{out-d}}} \frac{L_{\text{out-q}}}{1+L_{\text{out-q}}}}{1 - \frac{G_{\text{cL-dq}}^{\text{H}} G_{\text{cL-qd}}^{\text{H}}}{G_{\text{cL-q}}^{\text{H}} G_{\text{cL-d}}^{\text{H}}} \frac{L_{\text{out-q}} L_{\text{out-d}}}{(1+L_{\text{out-q}})(1+L_{\text{out-d}})}}$$

$$+ G_{\text{cL-qd}}^{\text{H}} \frac{-\frac{L_{\text{out-q}}}{G_{\text{cL-q}}^{\text{H}} R_{\text{eq-q}}} \left(\frac{L_{\text{out-q}}}{1+L_{\text{out-q}}} - 1 \right)}{1 - \frac{G_{\text{cL-dq}}^{\text{H}} G_{\text{cL-qd}}^{\text{H}}}{G_{\text{cL-q}}^{\text{H}} G_{\text{cL-d}}^{\text{H}}} \frac{L_{\text{out-q}} L_{\text{out-d}}}{(1+L_{\text{out-q}}(1+L_{\text{out-d}})}}. \quad \text{(C.12)}$$

The q-channel inverter-side inductor current transfer functions, when only the output-current loops are closed, can be given by

$$\hat{i}_{\text{iL1q}} = G_{\text{ioL-q}}^{\text{out}} \hat{i}_{\text{in}} + G_{\text{crL-dq}}^{\text{out}} \hat{u}_{\text{od}} - Y_{\text{L-q}}^{\text{out}} \hat{u}_{\text{oq}} + G_{\text{cL-dq}}^{\text{out}} \hat{u}_{\text{iL1d}}^{\text{ref}} + G_{\text{cL-q}}^{\text{out}} \hat{u}_{\text{iL1q}}^{\text{ref}}, \quad \text{(C.13)}$$

where

$$G_{\text{ioL-q}}^{\text{out}} = G_{\text{ioL-q}}^{\text{H}} + G_{\text{cL-dq}}^{\text{H}} \frac{-\frac{L_{\text{out-d}}}{G_{\text{cL-d}}^{\text{H}}} \left(\frac{G_{\text{ioL-d}}^{\text{H}}}{1+L_{\text{out-d}}} - \frac{G_{\text{ioL-q}}^{\text{H}}}{G_{\text{cL-q}}^{\text{H}}} \frac{G_{\text{cL-qd}}^{\text{H}}}{1+L_{\text{out-d}}} \frac{L_{\text{out-q}}}{1+L_{\text{out-q}}} \right)}{1 - \frac{G_{\text{cL-dq}} G_{\text{cL-qd}}}{G_{\text{cL-q}} G_{\text{cL-d}}} \frac{L_{\text{out-q}} L_{\text{out-d}}}{(1+L_{\text{out-q}})(1+L_{\text{out-d}})}}$$

$$+ G_{\text{cL-q}}^{\text{H}} \frac{-\frac{L_{\text{out-q}}}{G_{\text{cL-q}}^{\text{H}}} \left(\frac{G_{\text{ioL-q}}^{\text{H}}}{1+L_{\text{out-q}}} - \frac{G_{\text{ioL-d}}^{\text{H}}}{G_{\text{cL-d}}^{\text{H}}} \frac{G_{\text{cL-dq}}^{\text{H}}}{1+L_{\text{out-q}}} \frac{L_{\text{out-d}}}{1+L_{\text{out-d}}} \right)}{1 - \frac{G_{\text{cL-dq}}^{\text{H}} G_{\text{cL-qd}}^{\text{H}}}{G_{\text{cL-q}}^{\text{H}} G_{\text{cL-d}}^{\text{H}}} \frac{L_{\text{out-q}} L_{\text{out-d}}}{(1+L_{\text{out-q}})(1+L_{\text{out-d}})}}, \quad \text{(C.14)}$$

$$G_{\text{crL-dq}}^{\text{out}} = G_{\text{crL-dq}}^{\text{H}} + G_{\text{cL-dq}}^{\text{H}} \frac{-\frac{L_{\text{out-d}}}{G_{\text{cL-d}}^{\text{H}}} \left(-\frac{Y_{\text{L-d}}^{\text{H}}}{1+L_{\text{out-d}}} - \frac{G_{\text{cL-qd}}^{\text{H}}}{1+L_{\text{out-d}}} \frac{G_{\text{crL-dq}}^{\text{H}}}{G_{\text{cL-q}}^{\text{H}}} \frac{L_{\text{out-q}}}{1+L_{\text{out-q}}} \right)}{1 - \frac{G_{\text{cL-dq}}^{\text{H}} G_{\text{cL-qd}}^{\text{H}}}{G_{\text{cL-q}}^{\text{H}} G_{\text{cL-d}}^{\text{H}}} \frac{L_{\text{out-q}} L_{\text{out-d}}}{(1+L_{\text{out-q}})(1+L_{\text{out-d}})}}$$

$$+ G_{\text{cL-q}}^{\text{H}} \frac{-\frac{L_{\text{out-q}}}{G_{\text{cL-q}}^{\text{H}}} \left(\frac{G_{\text{crL-dq}}^{\text{H}}}{1+L_{\text{out-q}}} - \frac{G_{\text{cL-dq}}^{\text{H}}}{1+L_{\text{out-q}}} \frac{Y_{\text{L-d}}^{\text{H}}}{G_{\text{cL-d}}^{\text{H}}} \frac{L_{\text{out-d}}}{1+L_{\text{out-d}}} \right)}{1 - \frac{G_{\text{cL-dq}}^{\text{H}} G_{\text{cL-qd}}^{\text{H}}}{G_{\text{cL-q}}^{\text{H}} G_{\text{cL-d}}^{\text{H}}} \frac{L_{\text{out-q}} L_{\text{out-d}}}{(1+L_{\text{out-q}})(1+L_{\text{out-d}})}}, \quad \text{(C.15)}$$

$$
\begin{aligned}
Y_{\text{L-q}}^{\text{out}} = Y_{\text{L-q}}^{\text{H}} &- G_{\text{cL-dq}}^{\text{H}} \frac{-\frac{L_{\text{out-d}}}{G_{\text{cL-d}}^{\text{H}}}\left(\frac{G_{\text{crL-qd}}^{\text{H}}}{1+L_{\text{out-d}}} + \frac{G_{\text{cL-qd}}^{\text{H}}}{1+L_{\text{out-d}}}\frac{Y_{\text{L-q}}^{\text{H}}}{G_{\text{cL-q}}^{\text{H}}}\frac{L_{\text{out-q}}}{1+L_{\text{out-q}}}\right)}{1 - \frac{G_{\text{cL-dq}}^{\text{H}}G_{\text{cL-qd}}^{\text{H}}}{G_{\text{cL-q}}^{\text{H}}G_{\text{cL-d}}^{\text{H}}}\frac{L_{\text{out-q}}L_{\text{out-d}}}{(1+L_{\text{out-q}})(1+L_{\text{out-d}})}} \\
&- G_{\text{cL-dq}}^{\text{H}} \frac{D_{\text{q}}G_{\text{PLL}} - \frac{L_{\text{out-d}}}{G_{\text{cL-d}}^{\text{H}}}\left[\frac{D_{\text{q}}G_{\text{cL-d}}^{\text{H}}G_{\text{PLL}}}{1+L_{\text{out-d}}} + \frac{G_{\text{cL-qd}}^{\text{H}}}{1+L_{\text{out-d}}}\left(\frac{I_{\text{L1d}}G_{\text{PLL}}}{G_{\text{cL-q}}^{\text{H}}}\frac{L_{\text{out-q}}}{1+L_{\text{out-q}}} + \frac{D_{\text{d}}G_{\text{PLL}}}{1+L_{\text{out-q}}}\right)\right]}{1 - \frac{G_{\text{cL-dq}}^{\text{H}}G_{\text{cL-qd}}^{\text{H}}}{G_{\text{cL-q}}^{\text{H}}G_{\text{cL-d}}^{\text{H}}}\frac{L_{\text{out-q}}L_{\text{out-d}}}{(1+L_{\text{out-q}})(1+L_{\text{out-d}})}} \\
&- G_{\text{cL-q}}^{\text{H}} \frac{-\frac{L_{\text{out-q}}}{G_{\text{cL-q}}^{\text{H}}}\left(-\frac{Y_{\text{L-q}}^{\text{H}}}{1+L_{\text{out-q}}} - \frac{G_{\text{cL-dq}}^{\text{H}}}{1+L_{\text{out-q}}}\frac{G_{\text{crL-qd}}^{\text{H}}}{G_{\text{cL-d}}^{\text{H}}}\frac{L_{\text{out-d}}}{1+L_{\text{out-d}}}\right)}{1 - \frac{G_{\text{cL-dq}}^{\text{H}}G_{\text{cL-qd}}^{\text{H}}}{G_{\text{cL-q}}^{\text{H}}G_{\text{cL-d}}^{\text{H}}}\frac{L_{\text{out-q}}L_{\text{out-d}}}{(1+L_{\text{out-q}})(1+L_{\text{out-d}})}} \\
&- G_{\text{cL-q}}^{\text{H}}\left\{ \frac{D_{\text{d}}G_{\text{PLL}} + \frac{I_{\text{L1d}}G_{\text{PLL}}}{G_{\text{cL-q}}^{\text{H}}}L_{\text{out-q}}}{1 - \frac{G_{\text{cL-dq}}^{\text{H}}G_{\text{cL-qd}}^{\text{H}}}{G_{\text{cL-q}}^{\text{H}}G_{\text{cL-d}}^{\text{H}}}\frac{L_{\text{out-q}}L_{\text{out-d}}}{(1+L_{\text{out-q}})(1+L_{\text{out-d}})}} \right. \\
&\left. - \frac{\frac{L_{\text{out-q}}}{G_{\text{cL-q}}^{\text{H}}}\left[\frac{D_{\text{d}}G_{\text{cL-q}}^{\text{H}}G_{\text{PLL}}}{1+L_{\text{out-q}}} + I_{\text{L1d}}G_{\text{PLL}}\frac{L_{\text{out-q}}}{1+L_{\text{out-q}}} + \frac{G_{\text{cL-dq}}^{\text{H}}}{1+L_{\text{out-q}}}\frac{D_{\text{q}}G_{\text{PLL}}}{1+L_{\text{out-d}}}\right]}{1 - \frac{G_{\text{cL-dq}}^{\text{H}}G_{\text{cL-qd}}^{\text{H}}}{G_{\text{cL-q}}^{\text{H}}G_{\text{cL-d}}^{\text{H}}}\frac{L_{\text{out-q}}L_{\text{out-d}}}{(1+L_{\text{out-q}})(1+L_{\text{out-d}})}} \right\}, \quad (C.16)
\end{aligned}
$$

$$
\begin{aligned}
G_{\text{cL-dq}}^{\text{out}} = G_{\text{cL-dq}}^{\text{H}} &\frac{-\frac{L_{\text{out-d}}}{G_{\text{cL-d}}^{\text{H}}R_{\text{eq-d}}}\left(\frac{L_{\text{out-d}}}{1+L_{\text{out-d}}} - 1\right)}{1 - \frac{G_{\text{cL-dq}}^{\text{H}}G_{\text{cL-qd}}^{\text{H}}}{G_{\text{cL-q}}^{\text{H}}G_{\text{cL-d}}^{\text{H}}}\frac{L_{\text{out-q}}L_{\text{out-d}}}{(1+L_{\text{out-q}})(1+L_{\text{out-d}})}} \\
&+ G_{\text{cL-q}}^{\text{H}}\frac{-\frac{G_{\text{cL-dq}}^{\text{H}}}{R_{\text{eq-d}}G_{\text{cL-q}}^{\text{H}}}\frac{L_{\text{out-q}}}{1+L_{\text{out-q}}}\frac{L_{\text{out-d}}}{1+L_{\text{out-d}}}}{1 - \frac{G_{\text{cL-dq}}^{\text{H}}G_{\text{cL-qd}}^{\text{H}}}{G_{\text{cL-q}}^{\text{H}}G_{\text{cL-d}}^{\text{H}}}\frac{L_{\text{out-q}}L_{\text{out-d}}}{(1+L_{\text{out-q}})(1+L_{\text{out-d}})}}, \quad (C.17)
\end{aligned}
$$

$$
\begin{aligned}
G_{\text{cL-q}}^{\text{out}} = G_{\text{cL-dq}}^{\text{H}} &\frac{-\frac{G_{\text{cL-qd}}^{\text{H}}}{G_{\text{cL-d}}^{\text{H}}G_{\text{cL-q}}^{\text{H}}R_{\text{eq-d}}}\frac{L_{\text{out-d}}}{1+L_{\text{out-d}}}\frac{L_{\text{out-q}}}{1+L_{\text{out-q}}}}{1 - \frac{G_{\text{cL-dq}}^{\text{H}}G_{\text{cL-qd}}^{\text{H}}}{G_{\text{cL-q}}^{\text{H}}G_{\text{cL-d}}^{\text{H}}}\frac{L_{\text{out-q}}L_{\text{out-d}}}{(1+L_{\text{out-q}})(1+L_{\text{out-d}})}} \\
&+ G_{\text{cL-q}}^{\text{H}}\frac{-\frac{L_{\text{out-q}}}{G_{\text{cL-q}}^{\text{H}}R_{\text{eq-q}}}\left(\frac{L_{\text{out-q}}}{1+L_{\text{out-q}}} - 1\right)}{1 - \frac{G_{\text{cL-dq}}^{\text{H}}G_{\text{cL-qd}}^{\text{H}}}{G_{\text{cL-q}}^{\text{H}}G_{\text{cL-d}}^{\text{H}}}\frac{L_{\text{out-q}}L_{\text{out-d}}}{(1+L_{\text{out-q}}(1+L_{\text{out-d}})}}. \quad (C.18)
\end{aligned}
$$

The grid-side d-channel inductor current (i.e., the output current) can be given by

$$
\hat{i}_{\text{od}} = G_{\text{io-d}}^{\text{out}}\hat{i}_{\text{in}} - Y_{\text{o-d}}^{\text{out}}\hat{u}_{\text{od}} + G_{\text{cr-qd}}^{\text{out}}\hat{u}_{\text{oq}} + G_{\text{co-d}}^{\text{out}}\hat{u}_{\text{iL1d}}^{\text{ref}} + G_{\text{co-qd}}^{\text{out}}\hat{u}_{\text{iL1q}}^{\text{ref}}, \quad (C.19)
$$

where

$$G_{\text{ioL-d}}^{\text{out}} = G_{\text{io-d}}^{\text{H}} + \frac{-L_{\text{out-d}}\frac{G_{\text{co-d}}^{\text{H}}}{G_{\text{cL-d}}^{\text{H}}}\left(\frac{G_{\text{ioL-d}}^{\text{H}}}{1+L_{\text{out-d}}} - \frac{G_{\text{ioL-q}}^{\text{H}}}{G_{\text{cL-q}}^{\text{H}}}\frac{G_{\text{cL-qd}}^{\text{H}}}{1+L_{\text{out-d}}}\frac{L_{\text{out-q}}}{1+L_{\text{out-q}}}\right)}{1 - \frac{G_{\text{cL-dq}}G_{\text{cL-qd}}}{G_{\text{cL-q}}G_{\text{cL-d}}}\frac{L_{\text{out-q}}L_{\text{out-d}}}{(1+L_{\text{out-q}})(1+L_{\text{out-d}})}}$$

$$+ \frac{-L_{\text{out-q}}\frac{G_{\text{co-qd}}}{G_{\text{cL-q}}}\left(\frac{G_{\text{ioL-q}}^{\text{H}}}{1+L_{\text{out-q}}} - \frac{G_{\text{ioL-d}}^{\text{H}}}{G_{\text{cL-d}}^{\text{H}}}\frac{G_{\text{cL-dq}}^{\text{H}}}{1+L_{\text{out-q}}}\frac{L_{\text{out-d}}}{1+L_{\text{out-d}}}\right)}{1 - \frac{G_{\text{cL-dq}}^{\text{H}}G_{\text{cL-qd}}^{\text{H}}}{G_{\text{cL-q}}^{\text{H}}G_{\text{cL-d}}^{\text{H}}}\frac{L_{\text{out-q}}L_{\text{out-d}}}{(1+L_{\text{out-q}})(1+L_{\text{out-d}})}}, \quad \text{(C.20)}$$

$$Y_{\text{o-d}}^{\text{out}} = Y_{\text{o-d}}^{\text{H}} - \frac{-L_{\text{out-d}}\frac{G_{\text{co-d}}^{\text{H}}}{G_{\text{cL-d}}^{\text{H}}}\left(-\frac{Y_{\text{L-d}}^{\text{H}}}{1+L_{\text{out-d}}} - \frac{G_{\text{crL-dq}}^{\text{H}}}{G_{\text{cL-q}}^{\text{H}}}\frac{G_{\text{cL-qd}}^{\text{H}}}{1+L_{\text{out-d}}}\frac{L_{\text{out-q}}}{1+L_{\text{out-q}}}\right)}{1 - \frac{G_{\text{cL-dq}}^{\text{H}}G_{\text{cL-qd}}^{\text{H}}}{G_{\text{cL-q}}^{\text{H}}G_{\text{cL-d}}^{\text{H}}}\frac{L_{\text{out-q}}L_{\text{out-d}}}{(1+L_{\text{out-q}})(1+L_{\text{out-d}})}}$$

$$- \frac{-L_{\text{out-q}}\frac{G_{\text{co-qd}}}{G_{\text{cL-q}}}\left(\frac{G_{\text{crL-dq}}^{\text{H}}}{1+L_{\text{out-q}}} + \frac{Y_{\text{L-d}}^{\text{H}}}{G_{\text{cL-d}}^{\text{H}}}\frac{G_{\text{cL-dq}}^{\text{H}}}{1+L_{\text{out-q}}}\frac{L_{\text{out-d}}}{1+L_{\text{out-d}}}\right)}{1 - \frac{G_{\text{cL-dq}}^{\text{H}}G_{\text{cL-qd}}^{\text{H}}}{G_{\text{cL-q}}^{\text{H}}G_{\text{cL-d}}^{\text{H}}}\frac{L_{\text{out-q}}L_{\text{out-d}}}{(1+L_{\text{out-q}})(1+L_{\text{out-d}})}}, \quad \text{(C.21)}$$

$$G_{\text{cr-qd}}^{\text{out}} = G_{\text{cr-qd}}^{\text{H}} + G_{\text{co-d}}^{\text{H}}\frac{-\frac{L_{\text{out-d}}}{G_{\text{cL-d}}^{\text{H}}}\left(\frac{G_{\text{crL-qd}}^{\text{H}}}{1+L_{\text{out-d}}} + \frac{G_{\text{cL-qd}}^{\text{H}}}{1+L_{\text{out-d}}}\frac{Y_{\text{L-q}}^{\text{H}}}{G_{\text{cL-q}}^{\text{H}}}\frac{L_{\text{out-q}}}{1+L_{\text{out-q}}}\right)}{1 - \frac{G_{\text{cL-dq}}^{\text{H}}G_{\text{cL-qd}}^{\text{H}}}{G_{\text{cL-q}}^{\text{H}}G_{\text{cL-d}}^{\text{H}}}\frac{L_{\text{out-q}}L_{\text{out-d}}}{(1+L_{\text{out-q}})(1+L_{\text{out-d}})}}$$

$$+ G_{\text{co-d}}^{\text{H}}\frac{D_{\text{q}}G_{\text{PLL}} - \frac{L_{\text{out-d}}}{G_{\text{cL-d}}^{\text{H}}}\left[\frac{D_{\text{q}}G_{\text{cL-d}}^{\text{H}}G_{\text{PLL}}}{1+L_{\text{out-d}}} + \frac{G_{\text{cL-qd}}^{\text{H}}}{1+L_{\text{out-d}}}\left(\frac{I_{\text{L1d}}G_{\text{PLL}}}{G_{\text{cL-q}}^{\text{H}}}\frac{L_{\text{out-q}}}{1+L_{\text{out-q}}} + \frac{D_{\text{d}}G_{\text{PLL}}}{1+L_{\text{out-q}}}\right)\right]}{1 - \frac{G_{\text{cL-dq}}^{\text{H}}G_{\text{cL-qd}}^{\text{H}}}{G_{\text{cL-q}}^{\text{H}}G_{\text{cL-d}}^{\text{H}}}\frac{L_{\text{out-q}}L_{\text{out-d}}}{(1+L_{\text{out-q}})(1+L_{\text{out-d}})}}$$

$$+ G_{\text{co-qd}}^{\text{H}}\frac{-\frac{L_{\text{out-q}}}{G_{\text{cL-q}}^{\text{H}}}\left(-\frac{Y_{\text{L-q}}^{\text{H}}}{1+L_{\text{out-q}}} - \frac{G_{\text{cL-dq}}^{\text{H}}}{1+L_{\text{out-q}}}\frac{G_{\text{crL-qd}}^{\text{H}}}{G_{\text{cL-d}}^{\text{H}}}\frac{L_{\text{out-d}}}{1+L_{\text{out-d}}}\right)}{1 - \frac{G_{\text{cL-dq}}^{\text{H}}G_{\text{cL-qd}}^{\text{H}}}{G_{\text{cL-q}}^{\text{H}}G_{\text{cL-d}}^{\text{H}}}\frac{L_{\text{out-q}}L_{\text{out-d}}}{(1+L_{\text{out-q}})(1+L_{\text{out-d}})}}$$

$$+ G_{\text{co-qd}}^{\text{H}}\left\{\frac{D_{\text{d}}G_{\text{PLL}} + \frac{I_{\text{L1d}}G_{\text{PLL}}}{G_{\text{cL-q}}^{\text{H}}}L_{\text{out-q}}}{1 - \frac{G_{\text{cL-dq}}^{\text{H}}G_{\text{cL-qd}}^{\text{H}}}{G_{\text{cL-q}}^{\text{H}}G_{\text{cL-d}}^{\text{H}}}\frac{L_{\text{out-q}}L_{\text{out-d}}}{(1+L_{\text{out-q}})(1+L_{\text{out-d}})}} \right.$$

$$\left. - \frac{\frac{L_{\text{out-q}}}{G_{\text{cL-q}}^{\text{H}}}\left[\frac{D_{\text{d}}G_{\text{cL-q}}^{\text{H}}G_{\text{PLL}}}{1+L_{\text{out-q}}} + I_{\text{L1d}}G_{\text{PLL}}\frac{L_{\text{out-q}}}{1+L_{\text{out-q}}} + \frac{G_{\text{cL-dq}}^{\text{H}}}{1+L_{\text{out-q}}}\frac{D_{\text{q}}G_{\text{PLL}}}{1+L_{\text{out-d}}}\right]}{1 - \frac{G_{\text{cL-dq}}^{\text{H}}G_{\text{cL-qd}}^{\text{H}}}{G_{\text{cL-q}}^{\text{H}}G_{\text{cL-d}}^{\text{H}}}\frac{L_{\text{out-q}}L_{\text{out-d}}}{(1+L_{\text{out-q}})(1+L_{\text{out-d}})}}\right\}, \quad \text{(C.22)}$$

$$G_{\text{co-d}}^{\text{out}} = G_{\text{co-d}}^{\text{H}} \frac{-\frac{L_{\text{out-d}}}{G_{\text{cL-d}}^{\text{H}} R_{\text{eq-d}}} \left(\frac{L_{\text{out-d}}}{1+L_{\text{out-d}}} - 1 \right)}{1 - \frac{G_{\text{cL-dq}}^{\text{H}} G_{\text{cL-qd}}^{\text{H}}}{G_{\text{cL-q}}^{\text{H}} G_{\text{cL-d}}^{\text{H}}} \frac{L_{\text{out-q}} L_{\text{out-d}}}{(1+L_{\text{out-q}})(1+L_{\text{out-d}})}}$$

$$+ G_{\text{co-qd}}^{\text{H}} \frac{-\frac{G_{\text{cL-dq}}^{\text{H}}}{R_{\text{eq-d}} G_{\text{cL-q}}^{\text{H}}} \frac{L_{\text{out-q}}}{1+L_{\text{out-q}}} \frac{L_{\text{out-d}}}{1+L_{\text{out-d}}}}{1 - \frac{G_{\text{cL-dq}}^{\text{H}} G_{\text{cL-qd}}^{\text{H}}}{G_{\text{cL-q}}^{\text{H}} G_{\text{cL-d}}^{\text{H}}} \frac{L_{\text{out-q}} L_{\text{out-d}}}{(1+L_{\text{out-q}})(1+L_{\text{out-d}})}}, \quad \text{(C.23)}$$

$$G_{\text{co-qd}}^{\text{out}} = G_{\text{co-d}}^{\text{H}} \frac{-\frac{G_{\text{cL-qd}}^{\text{H}}}{G_{\text{cL-d}}^{\text{H}} G_{\text{cL-q}}^{\text{H}} R_{\text{eq-d}}} \frac{L_{\text{out-d}}}{1+L_{\text{out-d}}} \frac{L_{\text{out-q}}}{1+L_{\text{out-q}}}}{1 - \frac{G_{\text{cL-dq}}^{\text{H}} G_{\text{cL-qd}}^{\text{H}}}{G_{\text{cL-q}}^{\text{H}} G_{\text{cL-d}}^{\text{H}}} \frac{L_{\text{out-q}} L_{\text{out-d}}}{(1+L_{\text{out-q}})(1+L_{\text{out-d}})}}$$

$$+ G_{\text{co-qd}}^{\text{H}} \frac{-\frac{L_{\text{out-q}}}{G_{\text{cL-q}}^{\text{H}} R_{\text{eq-q}}} \left(\frac{L_{\text{out-q}}}{1+L_{\text{out-q}}} - 1 \right)}{1 - \frac{G_{\text{cL-dq}}^{\text{H}} G_{\text{cL-qd}}^{\text{H}}}{G_{\text{cL-q}}^{\text{H}} G_{\text{cL-d}}^{\text{H}}} \frac{L_{\text{out-q}} L_{\text{out-d}}}{(1+L_{\text{out-q}}(1+L_{\text{out-d}})}}. \quad \text{(C.24)}$$

Finally, the q-channel output current can be given by

$$\hat{i}_{\text{oq}} = G_{\text{io-q}}^{\text{out}} \hat{i}_{\text{in}} + G_{\text{cr-dq}}^{\text{out}} \hat{u}_{\text{od}} - Y_{\text{o-q}}^{\text{out}} \hat{u}_{\text{oq}} + G_{\text{co-dq}}^{\text{out}} \hat{u}_{\text{iL1d}}^{\text{ref}} + G_{\text{co-q}}^{\text{out}} \hat{u}_{\text{iL1q}}^{\text{ref}}, \quad \text{(C.25)}$$

where

$$G_{\text{io-q}}^{\text{out}} = G_{\text{io-q}}^{\text{H}} + G_{\text{co-dq}}^{\text{H}} \frac{-\frac{L_{\text{out-d}}}{G_{\text{cL-d}}^{\text{H}}} \left(\frac{G_{\text{ioL-d}}^{\text{H}}}{1+L_{\text{out-d}}} - \frac{G_{\text{ioL-q}}^{\text{H}}}{G_{\text{cL-q}}^{\text{H}}} \frac{G_{\text{cL-qd}}^{\text{H}}}{1+L_{\text{out-d}}} \frac{L_{\text{out-q}}}{1+L_{\text{out-q}}} \right)}{1 - \frac{G_{\text{cL-dq}} G_{\text{cL-qd}}}{G_{\text{cL-q}} G_{\text{cL-d}}} \frac{L_{\text{out-q}} L_{\text{out-d}}}{(1+L_{\text{out-q}})(1+L_{\text{out-d}})}}$$

$$+ G_{\text{co-q}}^{\text{H}} \frac{-\frac{L_{\text{out-q}}}{G_{\text{cL-q}}^{\text{H}}} \left(\frac{G_{\text{ioL-q}}^{\text{H}}}{1+L_{\text{out-q}}} - \frac{G_{\text{ioL-d}}^{\text{H}}}{G_{\text{cL-d}}^{\text{H}}} \frac{G_{\text{cL-dq}}^{\text{H}}}{1+L_{\text{out-q}}} \frac{L_{\text{out-d}}}{1+L_{\text{out-d}}} \right)}{1 - \frac{G_{\text{cL-dq}}^{\text{H}} G_{\text{cL-qd}}^{\text{H}}}{G_{\text{cL-q}}^{\text{H}} G_{\text{cL-d}}^{\text{H}}} \frac{L_{\text{out-q}} L_{\text{out-d}}}{(1+L_{\text{out-q}})(1+L_{\text{out-d}})}}, \quad \text{(C.26)}$$

$$G_{\text{cr-dq}}^{\text{out}} = G_{\text{cr-dq}}^{\text{H}} + G_{\text{co-dq}}^{\text{H}} \frac{-\frac{L_{\text{out-d}}}{G_{\text{cL-d}}^{\text{H}}} \left(-\frac{Y_{\text{L-d}}^{\text{H}}}{1+L_{\text{out-d}}} - \frac{G_{\text{cL-qd}}^{\text{H}}}{1+L_{\text{out-d}}} \frac{G_{\text{crL-dq}}^{\text{H}}}{G_{\text{cL-q}}^{\text{H}}} \frac{L_{\text{out-q}}}{1+L_{\text{out-q}}} \right)}{1 - \frac{G_{\text{cL-dq}}^{\text{H}} G_{\text{cL-qd}}^{\text{H}}}{G_{\text{cL-q}}^{\text{H}} G_{\text{cL-d}}^{\text{H}}} \frac{L_{\text{out-q}} L_{\text{out-d}}}{(1+L_{\text{out-q}})(1+L_{\text{out-d}})}}$$

$$+ G_{\text{co-q}}^{\text{H}} \frac{-\frac{L_{\text{out-q}}}{G_{\text{cL-q}}^{\text{H}}} \left(\frac{G_{\text{crL-dq}}^{\text{H}}}{1+L_{\text{out-q}}} - \frac{G_{\text{cL-dq}}^{\text{H}}}{1+L_{\text{out-q}}} \frac{Y_{\text{L-d}}^{\text{H}}}{G_{\text{cL-d}}^{\text{H}}} \frac{L_{\text{out-d}}}{1+L_{\text{out-d}}} \right)}{1 - \frac{G_{\text{cL-dq}}^{\text{H}} G_{\text{cL-qd}}^{\text{H}}}{G_{\text{cL-q}}^{\text{H}} G_{\text{cL-d}}^{\text{H}}} \frac{L_{\text{out-q}} L_{\text{out-d}}}{(1+L_{\text{out-q}})(1+L_{\text{out-d}})}}, \quad \text{(C.27)}$$

$$Y_{\text{o-q}}^{\text{out}} = Y_{\text{o-q}}^{\text{H}} - G_{\text{co-dq}}^{\text{H}} \frac{-\frac{L_{\text{out-d}}}{G_{\text{cL-d}}^{\text{H}}} \left(\frac{G_{\text{crL-qd}}^{\text{H}}}{1+L_{\text{out-d}}} + \frac{G_{\text{cL-qd}}^{\text{H}}}{1+L_{\text{out-d}}} \frac{Y_{\text{L-q}}^{\text{H}}}{G_{\text{cL-q}}^{\text{H}}} \frac{L_{\text{out-q}}}{1+L_{\text{out-q}}} \right)}{1 - \frac{G_{\text{cL-dq}}^{\text{H}} G_{\text{cL-qd}}^{\text{H}}}{G_{\text{cL-q}}^{\text{H}} G_{\text{cL-d}}^{\text{H}}} \frac{L_{\text{out-q}} L_{\text{out-d}}}{(1+L_{\text{out-q}})(1+L_{\text{out-d}})}}$$

$$- G_{\text{co-dq}}^{\text{H}} \frac{D_{\text{q}} G_{\text{PLL}} - \frac{L_{\text{out-d}}}{G_{\text{cL-d}}^{\text{H}}} \left[\frac{D_{\text{q}} G_{\text{cL-d}}^{\text{H}} G_{\text{PLL}}}{1+L_{\text{out-d}}} + \frac{G_{\text{cL-qd}}^{\text{H}}}{1+L_{\text{out-d}}} \left(\frac{I_{\text{L1d}} G_{\text{PLL}}}{G_{\text{cL-q}}^{\text{H}}} \frac{L_{\text{out-q}}}{1+L_{\text{out-q}}} + \frac{D_{\text{d}} G_{\text{PLL}}}{1+L_{\text{out-q}}} \right) \right]}{1 - \frac{G_{\text{cL-dq}}^{\text{H}} G_{\text{cL-qd}}^{\text{H}}}{G_{\text{cL-q}}^{\text{H}} G_{\text{cL-d}}^{\text{H}}} \frac{L_{\text{out-q}} L_{\text{out-d}}}{(1+L_{\text{out-q}})(1+L_{\text{out-d}})}}$$

$$- G_{\text{co-q}}^{\text{H}} \frac{-\frac{L_{\text{out-q}}}{G_{\text{cL-q}}^{\text{H}}} \left(-\frac{Y_{\text{L-q}}^{\text{H}}}{1+L_{\text{out-q}}} - \frac{G_{\text{cL-dq}}^{\text{H}}}{1+L_{\text{out-q}}} \frac{G_{\text{crL-qd}}^{\text{H}}}{G_{\text{cL-d}}^{\text{H}}} \frac{L_{\text{out-d}}}{1+L_{\text{out-d}}} \right)}{1 - \frac{G_{\text{cL-dq}}^{\text{H}} G_{\text{cL-qd}}^{\text{H}}}{G_{\text{cL-q}}^{\text{H}} G_{\text{cL-d}}^{\text{H}}} \frac{L_{\text{out-q}} L_{\text{out-d}}}{(1+L_{\text{out-q}})(1+L_{\text{out-d}})}}$$

$$- G_{\text{co-q}}^{\text{H}} \Bigg\{ \frac{D_{\text{d}} G_{\text{PLL}} + \frac{I_{\text{L1d}} G_{\text{PLL}}}{G_{\text{cL-q}}^{\text{H}}} L_{\text{out-q}}}{1 - \frac{G_{\text{cL-dq}}^{\text{H}} G_{\text{cL-qd}}^{\text{H}}}{G_{\text{cL-q}}^{\text{H}} G_{\text{cL-d}}^{\text{H}}} \frac{L_{\text{out-q}} L_{\text{out-d}}}{(1+L_{\text{out-q}})(1+L_{\text{out-d}})}}$$

$$- \frac{\frac{L_{\text{out-q}}}{G_{\text{cL-q}}^{\text{H}}} \left[\frac{D_{\text{d}} G_{\text{cL-q}}^{\text{H}} G_{\text{PLL}}}{1+L_{\text{out-q}}} + I_{\text{L1d}} G_{\text{PLL}} \frac{L_{\text{out-q}}}{1+L_{\text{out-q}}} + \frac{G_{\text{cL-dq}}^{\text{H}}}{1+L_{\text{out-q}}} \frac{D_{\text{q}} G_{\text{PLL}}}{1+L_{\text{out-d}}} \right]}{1 - \frac{G_{\text{cL-dq}}^{\text{H}} G_{\text{cL-qd}}^{\text{H}}}{G_{\text{cL-q}}^{\text{H}} G_{\text{cL-d}}^{\text{H}}} \frac{L_{\text{out-q}} L_{\text{out-d}}}{(1+L_{\text{out-q}})(1+L_{\text{out-d}})}} \Bigg\}, \quad (C.28)$$

$$G_{\text{co-dq}}^{\text{out}} = G_{\text{co-dq}}^{\text{H}} \frac{-\frac{L_{\text{out-d}}}{G_{\text{cL-d}}^{\text{H}} R_{\text{eq-d}}} \left(\frac{L_{\text{out-d}}}{1+L_{\text{out-d}}} - 1 \right)}{1 - \frac{G_{\text{cL-dq}}^{\text{H}} G_{\text{cL-qd}}^{\text{H}}}{G_{\text{cL-q}}^{\text{H}} G_{\text{cL-d}}^{\text{H}}} \frac{L_{\text{out-q}} L_{\text{out-d}}}{(1+L_{\text{out-q}})(1+L_{\text{out-d}})}}$$

$$+ G_{\text{co-q}}^{\text{H}} \frac{-\frac{G_{\text{cL-dq}}^{\text{H}}}{R_{\text{eq-d}} G_{\text{cL-q}}^{\text{H}}} \frac{L_{\text{out-q}}}{1+L_{\text{out-q}}} \frac{L_{\text{out-d}}}{1+L_{\text{out-d}}}}{1 - \frac{G_{\text{cL-dq}}^{\text{H}} G_{\text{cL-qd}}^{\text{H}}}{G_{\text{cL-q}}^{\text{H}} G_{\text{cL-d}}^{\text{H}}} \frac{L_{\text{out-q}} L_{\text{out-d}}}{(1+L_{\text{out-q}})(1+L_{\text{out-d}})}}, \quad (C.29)$$

$$G_{\text{co-q}}^{\text{out}} = G_{\text{co-dq}}^{\text{H}} \frac{-\frac{G_{\text{cL-qd}}^{\text{H}}}{G_{\text{cL-d}}^{\text{H}} G_{\text{cL-q}}^{\text{H}} R_{\text{eq-d}}} \frac{L_{\text{out-d}}}{1+L_{\text{out-d}}} \frac{L_{\text{out-q}}}{1+L_{\text{out-q}}}}{1 - \frac{G_{\text{cL-dq}}^{\text{H}} G_{\text{cL-qd}}^{\text{H}}}{G_{\text{cL-q}}^{\text{H}} G_{\text{cL-d}}^{\text{H}}} \frac{L_{\text{out-q}} L_{\text{out-d}}}{(1+L_{\text{out-q}})(1+L_{\text{out-d}})}}$$

$$+ G_{\text{co-q}}^{\text{H}} \frac{-\frac{L_{\text{out-q}}}{G_{\text{cL-q}}^{\text{H}} R_{\text{eq-q}}} \left(\frac{L_{\text{out-q}}}{1+L_{\text{out-q}}} - 1 \right)}{1 - \frac{G_{\text{cL-dq}}^{\text{H}} G_{\text{cL-qd}}^{\text{H}}}{G_{\text{cL-q}}^{\text{H}} G_{\text{cL-d}}^{\text{H}}} \frac{L_{\text{out-q}} L_{\text{out-d}}}{(1+L_{\text{out-q}}(1+L_{\text{out-d}})}}. \quad (C.30)$$